Title
A Robust non-Oxidative Glycolysis in a Model Organism for Efficient Biochemical Production

Author
Jaeger, Alec

Publication Date
2020

Peer reviewed|Thesis/dissertation

UNIVERSITY OF CALIFORNIA

Los Angeles

A Robust non-Oxidative Glycolysis in a Model Organism for Efficient Biochemical Production

A dissertation submitted in partial satisfaction of the requirements for the degree of Doctor of Philosophy in Chemical Engineering

by

Alec James Jaeger

2020

ABSTRACT OF THE DISSERTATION

A Robust non-Oxidative Glycolysis

in a Model Organism for

Efficient Biochemical Production

by

Alec James Jaeger

Doctor of Philosophy in Chemical Engineering

University of California, Los Angeles, 2020

Professor James C. Liao, Chair

Global climate change, caused by the emission of greenhouse gas (GHG) to the atmosphere, is one of the key challenges facing humanity in the coming decades. Carbon dioxide (CO_2) is one of the leading sources of overall GHG emission, and it is released to the environment in large quantities by the burning of petroleum or other fossil fuels as liquid fuel. Sustainable alternatives to fossil fuels can be produced from biomass using microbial whole-cell catalysis. Since biomass fixes atmospheric CO_2, burning these biomass-derived fuels as energy sources reduces the net emission of carbon to the environment. However, current biofuel processes often struggle to compete economically with fossil fuels. A key contributing factor to this problem is the

inefficient utilization of feedstock carbon in biomass. Since microbes use conserved metabolic pathways to catabolize carbohydrate feedstocks, inherent limitations in these pathways often cannot be avoided. Moreover, these pathways evolved in nature to prioritize growth rather than production considerations. A notable example of this is the carbon loss when forming two-carbon (C2) metabolites, such as acetyl-CoA. C2 metabolites are precursors to many industrial products, including important biofuels such as ethanol and butanol. Essentially all organisms degrade sugar to pyruvate, a three-carbon (C3) metabolite using the conserved glycolytic pathways. To produce C2, pyruvate is decarboxylated to produce one C2 equivalent and one CO_2, thus wasting a third of input carbon and effectively limiting the maximum carbon yield of C2-derived products to 67%. This carbon loss imposes a significant economic constraint on biorefining. While no natural pathway can bypass pyruvate formation, a synthetic non-oxidative glycolysis (NOG) was recently developed that directly degrades sugar phosphates into stoichiometric amounts of C2 equivalents. Here, we first constructed a strain of *E. coli*, a model microbial organism, which uses NOG for sugar catabolism rather than glycolysis. This was achieved by a combination of rational design and evolution. By coupling the pathway to growth, we were able to use evolution to develop a robust pathway and fine tune the relative activity of pathway enzymes. The resulting strain grew at a comparable rate to wild-type *E. coli* and could produce acetate, a C2-derived product, at yield exceeding the theoretical maximum using glycolysis. Since it uses NOG for sugar catabolism, this strain has fundamentally rewired metabolism, as it generates C2 metabolites before C3 metabolites. C3 metabolites are generated from C2 using carbon scavenging pathways. Thus, we believe this strain has considerable potential as a host for the production of C2-derived products. Following evolution of the NOG strain, the chromosome was sequenced to elucidate mutations acquired through evolution. The

effect of several of these mutations was also investigated here. We found that a transposon insertion inactivating PtsG, a component of the glucose-specific phosphotransferase system, was essential to the NOG strain's ability to grow in minimal media. When *ptsG* is deleted, the catabolic activator protein (CAP) is able to upregulate many genes, which is likely necessary for the NOG-dependent growth phenotype. Another transposon insertion in alternative sigma factor *rpoS* contributed to growth in the NOG strain, likely through the upregulation of enzymes that benefit NOG growth, such as the TCA cycle. We also evaluated mutations where the cell had fine-tuned the activity of pathway enzymes. A mutation knocking down activity in key NOG enzyme phosphoketolase (F/Xpk) was found to be beneficial for growth by potentially alleviating a kinetic trap in the NOG cycle. However, fixing a promotor truncation that had knocked down activity of Pck, a key gluconeogenic enzyme, actually improved growth rate in glucose media by about 15%. Since the mutation occurred before NOG growth was developed, it was reasoned that changing intracellular conditions after the adaptation to NOG-based growth caused an increase in Pck activity to be beneficial. We also explored using the NOG strain for the production of ethanol, a C2-derived liquid fuel. Since ethanol is more reduced than acetate, it cannot be generated without the supply of external reducing power using NOG. Using formate as the electron donor, we were able to improve ethanol yield from 0.26 to 0.82 through the addition of formate in anaerobic production. Further improvements in ethanol yield were limited by the cells ability to produce ATP to maintain sugar phosphorylation. Since the cell is dependent on acetate production to make ATP anaerobically, ethanol production will need to be integrated with respiration, which can convert excess reducing power into ATP using oxygen as an electron acceptor. Finally, we offer strategies for establishing robust, high yield ethanol production using the NOG strain in microaerobic conditions.

The dissertation of Alec James Jaeger is approved.

Yi Tang

Gregory Payne

James Liao, Committee Chair

University of California, Los Angeles

2020

DEDICATION

To my loving family for all their incredible support

TABLE OF CONTENTS

ACKNOWLEDGEMENTS

I would like to thank my advisor Professor James Liao for his guidance on the project and the opportunity to perform research in his lab. I would like to thank everyone in Liao Lab for comradery and robust scientific discussions. In particular, I would like to thank Dr. Paul Lin, my good friend and collaborator on this project. I would also like to extend my gratitude to Stephanie Gao, my laboratory assistant for all her hard work.

This work was supported by the Department of Energy award DE-SC0012384.

Chapter 3 is a version of Lin, P. P.*, Jaeger, A. J.* (*co-first authors), Wu, T. Y., Xu, S. C., Lee, A. S., Gao, F., Chen, P.W., & Liao, J. C. (2018). Construction and evolution of an Escherichia coli strain relying on nonoxidative glycolysis for sugar catabolism. *PNAS*, *115*(14), 3538-3546. Lin, P.P. and Jaeger, A.J. designed and performed experiments and contributed equally to the manuscript. Wu, T.W., Xu, S.C., Lee, A.S., Gao, F., and Chen, P.W. assisted with experiments. Liao, J.C. was the project director.

VITA

Education

- B.S. in chemical engineering from the Georgia Institute of Technology

Publication

- Lin, P. P.*, Jaeger, A. J.* (*co-first authors), Wu, T. Y., Xu, S. C., Lee, A. S., Gao, F., Chen, P.W., & Liao, J. C. (2018). Construction and evolution of an Escherichia coli strain relying on nonoxidative glycolysis for sugar catabolism. *PNAS, 115*(14), 3538-3546.

1 Introduction

1.1 Background

Rising atmospheric levels of greenhouse gases such as CO_2 is a major contributor to global climate change. A significant amount of greenhouse gas emission occurs due to the burning of unrenewable fossil fuels as liquid fuel. Since carbon sequestration into fossil fuel occurs over very large time scales, burning fossil fuel causes a significant net increase of carbon into the environment. This problem is exacerbated by increasing worldwide demand for low-cost sources of energy. As an alternative, sustainable liquid fuel is capable of being produced by microbial fermentation from biomass feedstocks. Such feedstocks, including algae switchgrass, and agricultural byproducts, are considerably more renewable than fossil fuel because biomass fixes atmospheric CO_2, thus significantly reducing net CO_2 emission. However, high production costs for bio-based fuels have limited their ability to effectively replace fossil fuels as cheap, widely available sources of energy. Since feedstock is a major component of the total capital cost for bio-based fuels, this proposal seeks to apply an organism using synthetic non-oxidative glycolysis (NOG) for carbohydrate catabolism to the production of liquid fuel. NOG-based metabolism conserves carbon when forming important industrial biofuels, including ethanol and butanol, thereby increasing the maximum carbon yield of these products 50% relative to natural organisms. Therefore, NOG could potentially improve the scalability of bio-based fuels by making them more economically viable through the reduction of feedstock cost.

1.2 Overview

The non-oxidative glycolysis (NOG) pathway is a synthetic sugar catabolism pathway and does not exist in nature. Chapter 2 will outline carbon loss in endogenous metabolism and will discuss the construction of the NOG pathway. To broadly apply NOG as a pathway for biochemical production, it is necessary to establish it as the sole pathway for carbon catabolism in a microbial organism that is a versatile biocatalyst. Moreover, linking NOG to growth should allow for the development of a robust pathway through growth selection. Chapter 3 will discuss the development of an *E. coli* strain that uses NOG for carbon catabolism, following the removal of endogenous catabolism pathways, by a combination of rational design and evolution. The resulting NOG-dependent *E. coli* strain's global metabolism is fundamentally distinct from naturally occurring organisms. Thus, characterization of several mutations in this NOG strain will be discussed in Chapter 4, as well as potential strategies to improve the rate of NOG-based growth. While previously NOG has been demonstrated for the efficient production of acetate at yields exceeding the theoretical maximum with glycolysis, Chapter 5 will summarize extending production in the NOG strain to the more valuable, reduced product ethanol, which can be used as liquid fuel. In this chapter, the feasibility of producing reduced products using NOG was verified. Finally, Chapter 6 will summarize future work for NOG-based production of alcohol, offer strategies for achieving the production of alcohol at near theoretical yield, as well as discuss the potential economic benefit of NOG-based production of ethanol.

2 Model organisms as hosts for biochemical production are limited by carbon loss

The utilization of microorganisms as whole-cell catalysts is a promising methodology for renewable chemical production. Rapid advances in genomics have greatly expanded our understanding and ability to manipulate model organisms such as *E. coli* and yeast to greatly improve their versatility. However, even with these advances, numerous challenges still exist. A key limitation in using living organisms as catalysts is the fact that nature has evolved metabolic pathways to optimize growth rather than production considerations such as product yield. Inherent carbon loss in endogenous metabolism imposes a major economic constraint on biorefining through increased feedstock costs. One of the most notable sources of carbon loss in metabolism occurs from the decarboxylation of pyruvate. Essentially all organisms use a variation of the conserved glycolytic pathways to degrade sugar into the three-carbon (C3) metabolite pyruvate without carbon loss. To generate two-carbon (C2) metabolites such as acetyl-CoA, pyruvate is decarboxylated, releasing one carbon equivalent as CO_2. Since C2 metabolites are precursors to many industrial products, this carbon loss is especially problematic, as the maximum carbon yield of these products is limited to 67%. While no native pathways can directly generate C2 at stoichiometric yield from sugar, a synthetic non-oxidative glycolysis (NOG) was designed that can degrade sugar phosphates into C2 equivalents without carbon loss. Implementing NOG-based production of C2-derived products can provide a tremendous economic benefit and make renewable whole-cell catalysis more competitive with fossil fuels.

2.1 Model organisms as hosts for sustainable chemical production

The genetic tractability of model microbial organisms such as *E. coli* and yeast makes them highly attractive platforms for chemical production in whole-cell catalysis.[1,2,3] While microbes have been harnessed by humanity for the production of desirable fermentation products for thousands of years, significant growth in the fields of synthetic biology and metabolic engineering have greatly expanded the ability of these organisms to be versatile and robust biocatalysts. A key advantage of microbial chemical production is sustainability. These organisms utilize biomass, which fixes carbon from the atmosphere, as feedstock and thus closes the carbon cycle. This is an extremely important consideration in an era of rising CO_2 levels.[4] Sustainability makes microbial catalysts attractive alternatives to traditional chemical processes that use nonrenewable fossil fuels as feedstock, such as petroleum. *E. coli* and yeast have been engineered for the production of liquid fuels, including ethanol,[5] butanol[6-8] and isobutanol,[9-10] as well as chemical feedstocks for polymer production, such as 1,3 propanediol,[11]1,2 propanediol,[12] and 1,4 butanediol.[13] These organisms are also good hosts for the production amino acids,[14-15] isoprenoids,[16-19] and numerous other natural products. However, despite numerous metabolic engineering strategies to improve yields, productivities, and titers, these processes still struggle to compete economically with those that utilize fossil fuels as feedstock. This section will overview a major constraint on the economics of biorefineries: inherent carbon inefficiency in endogenous metabolic pathways. Lost carbon causes many potential bioproducts to be produced at suboptimal yields and thereby limits the profitability of these processes through increased feedstock costs. Strategies for overcoming this inherent carbon loss using synthetic biology will be discussed.

2.2 Carbon loss in endogenous metabolism represents major limitation for biorefining

In living cells, sugars can be converted into various products using a series of metabolic reactions catalyzed by enzymes. The method by which microbes consume sugar to produce valuable products has long fascinated humanity. In the nineteenth century, Louis Pasteur discovered biomass yields on glucose were higher in aerobic conditions than anerobic conditions, while fermentation rates were reduced.[20] Decades of research later, all enzymatic steps comprising the Embden-Meyerhof-Parnas (EMP) pathway, the most common variation of glycolysis, were elucidated.[21] Glycolysis partially oxidizes sugar, generating the three-carbon (C3) metabolite pyruvate. In the process, ATP and NADH are also produced for biosynthetic purposes. Acetyl-CoA, a two-carbon molecule (C2), is another important metabolite. To produce acetyl-CoA, pyruvate is decarboxylated, splitting one molecule of C3 into one molecule of C2 and one molecule of carbon dioxide (CO_2). Since essentially all organisms use glycolysis for sugar catabolism, pyruvate and acetyl-CoA are always produced in this manner from sugar, with C3 generated before C2. Carbon loss forming C2 metabolites is a major challenge for biorefining, since many important industrial bioproducts, including alcohol, fatty acids, and isoprenoids are all generated from C2 precursors.[5,6,17,22] The maximum achievable carbon yield of these products is thus only 67%, limiting the efficiency of feedstock utilization, as well as increasing emissions of the harmful greenhouse gas CO_2. An overview of the EMP pathway and associated carbon loss is shown in Figure 2-1. This carbon loss is especially problematic in the production of C2-derived liquid fuels such as ethanol and butanol, where feedstock price is a substantial fraction of the overall capital cost and these processes must compete with low-price liquid fuels such as petroleum.[23]

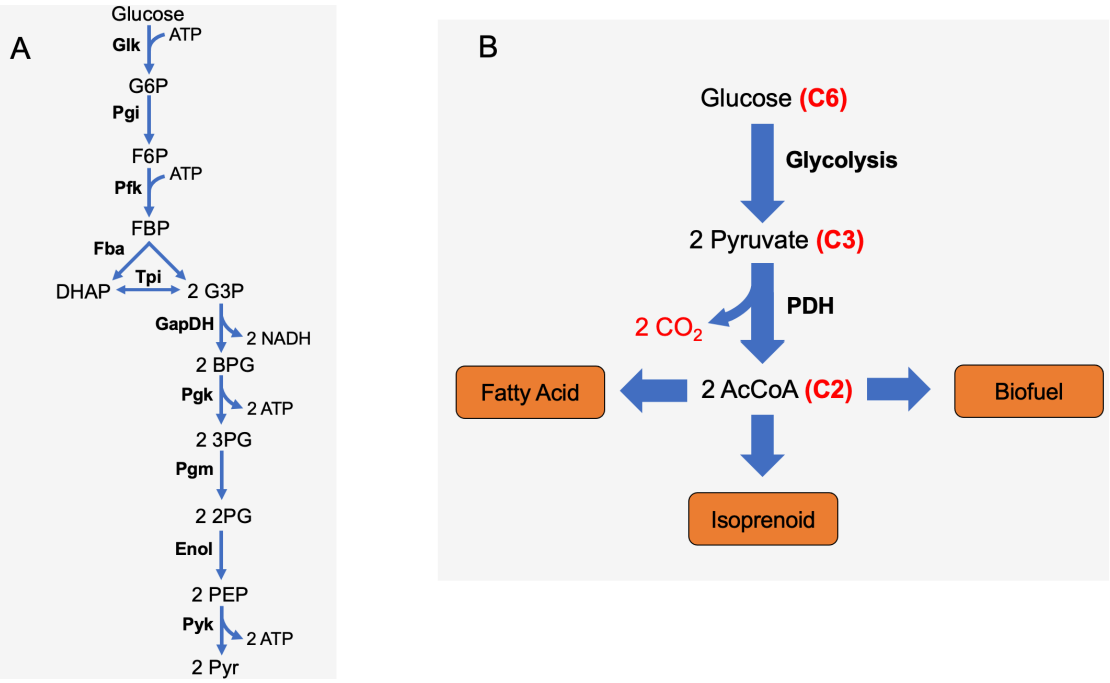

Figure 2-1: Overview of EMP glycolysis. (A) The EMP pathway partially oxidizes glucose into two pyruvate equivalents generating 2 ATP and 2 NADH. (B) Decarboxylation of pyruvate releases one third of input carbon as CO_2 when forming C2 metabolites. Since C2 metabolites are precursors to numerous bioproducts, including biofuel, isoprenoids and fatty acid, this carbon loss represents a major source of carbon loss in biorefining. Glk (glucokinase), Pgi (phosphoglucoisomerase), Pfk (phosphofructokinase), Fba (fructose bisphosphate aldolase), Tpi (triose phosphate isomerase), GapDH (glyceraldehyde 3-phosphate dehydrogenase), Pgk (phosphoglycerate kinase), Pgm (phosphoglycerate mutase), Enol (enolase), Pyk (pyruvate kinase), G6P (glucose 6-phosphate), F6P (fructose 6-phosphate), FBP (fructose 1,6-bisphosphate), DHAP (dihydroxyacetone phosphate), G3P (glyceraldehyde 3-phosphate), BPG (1,3-biphosphoglycerate) 3PG (3-phosphoglycerate), 2PG (2-phosphoglycerate), PEP (phosphoenolpyruvate), Pyr (pyruvate).

2.3 Reincorporation of CO_2 through carbon fixation pathways is challenging

Strategies to address the problem of carbon loss from pyruvate decarboxylation in *E. coli* include reincorporating CO_2 back into metabolism using a carbon fixation pathway. *E. coli* and yeast are heterotrophs and do not naturally fix CO_2. Unfortunately, native CO_2 fixing organisms have limitations as biocatalysts due to the relative lack of available genetic tools. Therefore, to avoid carbon loss, there has been a push to implement heterologous carbon fixation pathways

into *E. coli* or yeast. The most important carbon fixation pathway in nature is the Calvin-Benson-Bassham (CBB) cycle.[24-25] Rubisco, the CO_2 fixing enzyme from the Calvin-Benson-Bassham (CBB) cycle has been successfully overexpressed in *E.* coli, and the entire CBB has been applied as a growth pathway in synthetic *E. coli* strains.[26-29] In addition, expression of Rubisco in *E. coli* has been shown to increase the yield of products above the theoretical maximum.[30] However, this approach is challenging since it requires the heterologous overexpression of a complex enzyme with notoriously slow kinetic properties and requires ATP and NAD(P)H investment to drive the CBB pathway. In CBB-dependent autotrophs, the light reactions are used to supply the necessary NAD(P)H and ATP for carbon fixation, but heterologous implementation of this system has proven challenging.[31] Since CO_2 reincorporation is difficult, it would be highly desirable if this carbon loss could be eliminated. However, there is no naturally existing pathway that can bypass pyruvate formation to directly generate stoichiometric yields of C2 metabolites.

2.4 NOG is a phosphoketolase-dependent carbon rearrangement cycle that enables complete carbon conservation when forming C2 metabolites

To address the problematic carbon loss during pyruvate formation, a synthetic sugar catabolism pathway was conceived that bypasses pyruvate generation to directly generate C2 metabolites from sugar at 100% yield.[32] This pathway, termed non-oxidative glycolysis (NOG), offers tremendous potential for improving the economic feasibility of many bioprocesses since acetyl-CoA derived products can be generated at carbon yields much higher than is possible using glycolytic metabolism. The key enzyme in NOG is phosphoketolase, which cleaves fructose-6 phosphate (designated as Fpk activity) or xylulose 5-phosphate (designated as Xpk activity) into acetyl-phosphate (AcP) and a corresponding sugar phosphate.[33-35] In nature, this

enzyme participates in the phosphoketolase pathway, an alternative catabolism pathway to the EMP.[36-37] In NOG, phosphoketolase was coupled with a carbon rearrangement cycle consisting of transaldolase (Tal), transketolase (Tkt), ribose-phosphate isomerase (Rpi), ribose-phosphate epimerase (Rpe), fructose-6 bisphosphotase (Fbp), triose-phosphate isomerase (Tpi), & fructose-bisphosphate aldolase (Fba), for a total of eight enzymes. Besides F/Xpk, the other enzymes are from the pentose phosphate pathway (PPP), the EMP, or gluconeogenesis. A complete NOG cycle can be achieved using Fpk activity only, Xpk activity only, as well as combined F/Xpk activity. The complete NOG cycle with F/Xpk activity is demonstrated in Figure 2-2. In this description, a single fructose-6 phosphate (F6P) molecule is converted to 3 AcP molecules. The AcP produced in NOG can either be converted to acetate by acetate kinase (Ack) for ATP production, or converted to biosynthetic precursor acetyl-CoA by phosphotransacetylase (Pta). However, unlike glycolysis, NOG does not produce or consume electrons, and does directly not produce ATP. Since quickly generating ATP and NADH for biosynthesis is likely more important for cell growth than forming C2 metabolites with 100% efficiency, it is not surprising the NOG cycle does not occur in nature, even though many organisms contain all the available enzymes.[38-40] In their manuscript, Bogorad *et. al* demonstrated NOG in *E. coli* by producing acetate, a C2 product, from xylose at yields exceeding the previous theoretical maximum. Since the strain from this study contained both NOG and glycolysis, a redox condition favoring NOG was used to force carbon through the desired pathway. This result generated considerable excitement, since NOG could be applied for the production of many C2 derived products at yields exceeding the previous theoretical maximum.

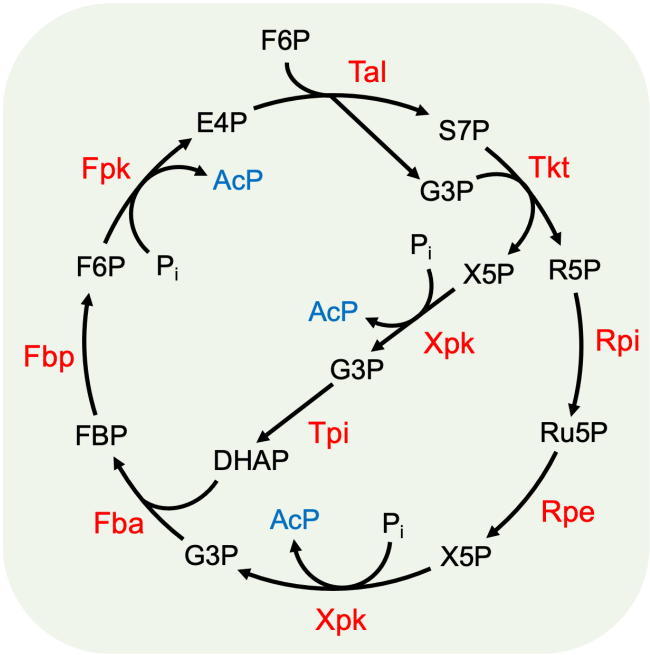

Figure 2-2: Overview of synthetic non-oxidative glycolysis (NOG). One F6P is degraded into 3 AcP without carbon loss. F6P (fructose 6-phosphate), S7P (sedoheptulose 7-phosphate), G3P (glyceraldehyde 3-phosphate), X5P xylulose 5-phosphate), R5P (ribose 5-phosphate), Ru5P (ribulose 5-phosphate), DHAP (dihydroxyacetone phosphate), FBP (fructose bisphosphate), E4P (erythrose 4-phosphate), AcP (acetyl-phosphate), P_i (inorganic phosphate). Fpk (F6P dependent phosphoketolase), Xpk (X5P dependent phosphoketolase), Tal (transaldolase), Tkt (transketolase), Rpi (ribose phosphate isomerase), Rpe (ribose phosphate epimerase), Fba (fructose bisphosphate aldolase), Fbp (fructose bisphosphotase).

2.5 Expanding NOG to the production of reduced products

While the development of NOG exhibited the production of acetate, a C2-derived product, at nearly theoretical yield on sugar,[32] the production of acetate is highly favorable in NOG-based metabolism since NOG since it is redox balanced. However, many important products derived from C2 are more reduced than acetate, including alcohol and fatty acid. Thus, external reducing power must be supplied to facilitate the production of reduced products using NOG.

Formate and hydrogen both represent potential external sources of reducing power. These substrates can be oxidized enzymatically and transfer electrons to cellular electron carriers. Formate is oxidized by formate dehydrogenase (Fdh) and hydrogen is oxidized by hydrogenase. Both formate and hydrogen can be produced renewable using electrolysis. Although formate is oxidized to CO_2, it can be regenerated back to CO_2 at high efficiency using an indium cathode fuel cell.[41-43] To easily integrate with downstream pathways, it is desirable to use enzymes that are soluble, oxygen-tolerant, and utilize NAD^+/NADH as a cofactor rather than more complex electron carriers. A well characterized Fdh enzyme from *Candida boidnii* fits these parameters.[44] Moreover, this enzyme has been functionally expressed in *E. coli* (NOG).[45-46]
Hydrogen can be obtained renewably from water electrolysis.[47] Hydrogenases are readily reversible but often use membrane-bound electron carriers or ferrodoxin as cofactors and are generally oxygen sensitive.[48-51] However, an oxygen-tolerant, soluble hydrogenase (SH) from *Cupriavidus necator* has been reported that utilizes NAD^+/NADH.[52-53] It has been functionally expressed in *E. coli* and has been applied for NADH regeneration purposes in *in vitro* systems, making it a promising candidate for hydrogen-based NOG chemical production.[54-56] If external reducing power can be utilized efficiently such that the input cost does not exceed the savings form conserved carbon feedstock, an NOG-based process for reduced products such as alcohol or fatty acid could have economic viability.

2.6 Conclusion

Microorganisms such as *E. coli* or yeast are attractive catalysts for chemical production due to their genetic versatility and ability to utilize sustainable feedstocks. Many industrially relevant chemicals are derived from C2 metabolites such as acetyl-CoA, and the carbon loss forming acetyl-CoA using glycolytic metabolism represents a major challenge in biorefining.

Since essentially all organisms are dependent on glycolysis to catabolize sugar, this carbon loss cannot be avoided using endogenous metabolism unless a carbon fixation pathway is implemented. The synthetic NOG pathway offers a solution to this problem, as pyruvate generation is bypassed to directly generate stoichiometric yields of C2 equivalents.[32] Although NOG was demonstrated *in vivo* using *E. coli,* this occurred under a strict condition in which carbon flux was forced through NOG rather than EMP to produce acetate, and could only be used with xylose due to the complex regulation and transport associated with glucose. Thus, it is highly desirable to replace glycolysis with NOG as the sole pathway for carbon catabolism in a model organism such as *E. coli*. Coupling the pathway to growth should also help establish a robust pathway through strain evolution. The resulting strain would favor NOG-based metabolism under all conditions and could be a potential host for the highly efficient production of many C2-derived products, including reduced products such as alcohol.

2.7 References

1. Pontrelli, S., Chiu, T. Y., Lan, E. I., Chen, F. Y. H., Chang, P., & Liao, J. C. (2018). Escherichia coli as a host for metabolic engineering. *Metabolic engineering*, *50*, 16-46.

2. Chen, X., Zhou, L., Tian, K., Kumar, A., Singh, S., Prior, B. A., & Wang, Z. (2013). Metabolic engineering of Escherichia coli: a sustainable industrial platform for bio-based chemical production. *Biotechnology advances*, *31*(8), 1200-1223.

3. Liu, L., Redden, H., & Alper, H. S. (2013). Frontiers of yeast metabolic engineering: diversifying beyond ethanol and Saccharomyces. *Current opinion in biotechnology*, *24*(6), 1023-1030.

4. Battin, T. J., Luyssaert, S., Kaplan, L. A., Aufdenkampe, A. K., Richter, A., & Tranvik, L. J. (2009). The boundless carbon cycle. *Nature Geoscience*, *2*(9), 598-600.

5. Ingram, L. O., Conway, T., Clark, D. P., Sewell, G. W., & Preston, J. F. (1987). Genetic engineering of ethanol production in Escherichia coli. *Applied and Environmental Microbiology*, *53*(10), 2420-2425.

6. Ingram, L. O., Conway, T., Clark, D. P., Sewell, G. W., & Preston, J. F. (1987). Genetic engineering of ethanol production in Escherichia coli. *Applied and Environmental Microbiology*, *53*(10), 2420-2425.

7. Generoso, W. C., Schadeweg, V., Oreb, M., & Boles, E. (2015). Metabolic engineering of Saccharomyces cerevisiae for production of butanol isomers. *Current opinion in biotechnology*, *33*, 1-7.

8. Atsumi, S., & Liao, J. C. (2008). Directed evolution of Methanococcus jannaschii citramalate synthase for biosynthesis of 1-propanol and 1-butanol by Escherichia coli. *Applied and environmental microbiology*, *74*(24), 7802-7808.

9. Atsumi, S., Hanai, T., & Liao, J. C. (2008). Non-fermentative pathways for synthesis of branched-chain higher alcohols as biofuels. *Nature*, *451*(7174), 86-89.

10. Avalos, J. L., Fink, G. R., & Stephanopoulos, G. (2013). Compartmentalization of metabolic pathways in yeast mitochondria improves the production of branched-chain alcohols. *Nature biotechnology*, *31*(4), 335-341.

11. Biebl, H., Menzel, K., Zeng, A. P., & Deckwer, W. D. (1999). Microbial production of 1, 3-propanediol. *Applied microbiology and biotechnology*, *52*(3), 289-297.

12. Clomburg, J. M., & Gonzalez, R. (2011). Metabolic engineering of Escherichia coli for the production of 1, 2-propanediol from glycerol. *Biotechnology and bioengineering*, *108*(4), 867-879.

13. Yim, H., Haselbeck, R., Niu, W., Pujol-Baxley, C., Burgard, A., Boldt, J., ... & Van Dien, S. (2011). Metabolic engineering of Escherichia coli for direct production of 1, 4-butanediol. *Nature chemical biology*, *7*(7), 445-452.

14. Lee, K. H., Park, J. H., Kim, T. Y., Kim, H. U., & Lee, S. Y. (2007). Systems metabolic engineering of Escherichia coli for L-threonine production. *Molecular systems biology*, *3*(1), 149.

15. Park, J. H., Lee, K. H., Kim, T. Y., & Lee, S. Y. (2007). Metabolic engineering of Escherichia coli for the production of L-valine based on transcriptome analysis and in silico gene knockout simulation. *Proceedings of the national academy of sciences*, *104*(19), 7797-7802.

16. Ajikumar, P. K., Xiao, W. H., Tyo, K. E., Wang, Y., Simeon, F., Leonard, E., ... & Stephanopoulos, G. (2010). Isoprenoid pathway optimization for Taxol precursor overproduction in Escherichia coli. *Science*, *330*(6000), 70-74.

17. Ajikumar, P. K., Xiao, W. H., Tyo, K. E., Wang, Y., Simeon, F., Leonard, E., ... & Stephanopoulos, G. (2010). Isoprenoid pathway optimization for Taxol precursor overproduction in Escherichia coli. *Science*, *330*(6000), 70-74.

18. Pitera, D. J., Paddon, C. J., Newman, J. D., & Keasling, J. D. (2007). Balancing a heterologous mevalonate pathway for improved isoprenoid production in Escherichia coli. *Metabolic engineering*, *9*(2), 193-207.

19. Meadows, A. L., Hawkins, K. M., Tsegaye, Y., Antipov, E., Kim, Y., Raetz, L., ... & Tsong, A. (2016). Rewriting yeast central carbon metabolism for industrial isoprenoid production. *Nature*, *537*(7622), 694-697.

20. Racker, E. (1980, February). From Pasteur to Mitchell: a hundred years of bioenergetics. In *Federation proceedings* (Vol. 39, No. 2, pp. 210-215).

21. Kresge, N., Simoni, R. D., & Hill, R. L. (2005). Otto Fritz Meyerhof and the elucidation of the glycolytic pathway. *Journal of Biological Chemistry*, *280*(4), e3-e3.

22. Machado, H. B., Dekishima, Y., Luo, H., Lan, E. I., & Liao, J. C. (2012). A selection platform for carbon chain elongation using the CoA-dependent pathway to produce linear higher alcohols. *Metabolic engineering*, *14*(5), 504-511.

23. Hamelinck, C. N., & Faaij, A. P. (2006). Outlook for advanced biofuels. *Energy policy*, *34*(17), 3268-3283.

24. Bassham, J. A. (1964). Kinetic studies of the photosynthetic carbon reduction cycle. *Annual Review of Plant Physiology*, *15*(1), 101-120.

25. Bar-Even, A., Noor, E., & Milo, R. (2012). A survey of carbon fixation pathways through a quantitative lens. *Journal of experimental botany*, *63*(6), 2325-2342.

26. Goloubinoff, P., Gatenby, A. A., & Lorimer, G. H. (1989). GroE heat-shock proteins promote assembly of foreign prokaryotic ribulose bisphosphate carboxylase oligomers in Escherichia coli. *Nature*, *337*(6202), 44-47.

27. Tabita, F. R., & Small, C. L. (1985). Expression and assembly of active cyanobacterial ribulose-1, 5-bisphosphate carboxylase/oxygenase in Escherichia coli containing stoichiometric amounts of large and small subunits. *Proceedings of the National Academy of Sciences*, *82*(18), 6100-6103.

28. Antonovsky, N., Gleizer, S., Noor, E., Zohar, Y., Herz, E., Barenholz, U., ... & Milo, R. (2016). Sugar synthesis from CO2 in Escherichia coli. *Cell*, *166*(1), 115-125.

29. Gleizer, S., Ben-Nissan, R., Bar-On, Y. M., Antonovsky, N., Noor, E., Zohar, Y., ... & Milo, R. (2019). Conversion of Escherichia coli to generate all biomass carbon from CO2. *Cell*, *179*(6), 1255-1263.

30. Tseng, I. T., Chen, Y. L., Chen, C. H., Shen, Z. X., Yang, C. H., & Li, S. Y. (2018). Exceeding the theoretical fermentation yield in mixotrophic Rubisco-based engineered Escherichia coli. *Metabolic engineering*, *47*, 445-452.

31. Claassens, N. J., Sousa, D. Z., dos Santos, V. A. M., de Vos, W. M., & van der Oost, J. (2016). Harnessing the power of microbial autotrophy. *Nature Reviews Microbiology*, *14*(11), 692-706.

32. Bogorad, I. W., Lin, T. S., & Liao, J. C. (2013). Synthetic non-oxidative glycolysis enables complete carbon conservation. *Nature*, *502*(7473), 693-697.

33. Meile, L., Rohr, L. M., Geissmann, T. A., Herensperger, M., & Teuber, M. (2001). Characterization of the D-xylulose 5-phosphate/D-fructose 6-phosphate phosphoketolase gene (xfp) from Bifidobacterium lactis. *Journal of bacteriology*, *183*(9), 2929-2936.

34. Grill, J. P., Crociani, J., & Ballongue, J. (1995). Characterization of fructose 6 phosphate phosphoketolases purified from Bifidobacterium species. *Current microbiology*, *31*(1), 49-54.

35. Yin, X., Chambers, J. R., Barlow, K., Park, A. S., & Wheatcroft, R. (2005). The gene encoding xylulose-5-phosphate/fructose-6-phosphate phosphoketolase (xfp) is conserved among Bifidobacterium species within a more variable region of the genome and both are useful for strain identification. *FEMS microbiology letters*, *246*(2), 251-257.

36. Sonderegger, M., Schümperli, M., & Sauer, U. (2004). Metabolic engineering of a phosphoketolase pathway for pentose catabolism in Saccharomyces cerevisiae. *Applied and environmental microbiology*, *70*(5), 2892-2897.

37. Årsköld, E., Lohmeier-Vogel, E., Cao, R., Roos, S., Rådström, P., & van Niel, E. W. (2008). Phosphoketolase pathway dominates in Lactobacillus reuteri ATCC 55730 containing dual pathways for glycolysis. *Journal of bacteriology*, *190*(1), 206-212.

38. Schramm, M., Klybas, V., & Racker, E. (1958). Phosphorolytic cleavage of fructose-6-phosphate by fructose-6-phosphate phosphoketolase from Acetobacter xylinum. *Journal of Biological Chemistry*, *233*(6), 1283-1288.

39. Fandi, K. G., Ghazali, H. M., Yazid, A. M., & Raha, A. R. (2001). Purification and N-terminal amino acid sequence of fructose-6-phosphate phosphoketolase from Bifidobacterium longum BB536. *Letters in applied microbiology*, *32*(4), 235-239.

40. Liu, L., Zhang, L., Tang, W., Gu, Y., Hua, Q., Yang, S., ... & Yang, C. (2012). Phosphoketolase pathway for xylose catabolism in Clostridium acetobutylicum revealed by 13C metabolic flux analysis. *Journal of bacteriology*, *194*(19), 5413-5422.

41. Ma, W., Xie, S., Zhang, X. G., Sun, F., Kang, J., Jiang, Z., ... & Wang, Y. (2019). Promoting electrocatalytic CO 2 reduction to formate via sulfur-boosting water activation on indium surfaces. *Nature communications*, *10*(1), 1-10.

42. Ikeda, S., Takagi, T., & Ito, K. (1987). Selective formation of formic acid, oxalic acid, and carbon monoxide by electrochemical reduction of carbon dioxide. *Bulletin of the Chemical Society of Japan*, *60*(7), 2517-2522.

43. Li, H., Opgenorth, P. H., Wernick, D. G., Rogers, S., Wu, T. Y., Higashide, W., ... & Liao, J. C. (2012). Integrated electromicrobial conversion of CO2 to higher alcohols. *Science*, *335*(6076), 1596-1596.

44. Schütte, H., Flossdorf, J., Sahm, H., & Kula, M. R. (1976). Purification and properties of formaldehyde dehydrogenase and formate dehydrogenase from Candida boidinii. *European Journal of Biochemistry*, *62*(1), 151-160.

45. Berrıos-Rivera, S. J., Bennett, G. N., & San, K. Y. (2002). Metabolic engineering of Escherichia coli: increase of NADH availability by overexpressing an NAD+-dependent formate dehydrogenase. *Metabolic engineering*, *4*(3), 217-229.

46. Shen, C. R., Lan, E. I., Dekishima, Y., Baez, A., Cho, K. M., & Liao, J. C. (2011). Driving forces enable high-titer anaerobic 1-butanol synthesis in Escherichia coli. *Applied and environmental microbiology*, *77*(9), 2905-2915.

47. Zeng, K., & Zhang, D. (2010). Recent progress in alkaline water electrolysis for hydrogen production and applications. *Progress in energy and combustion science*, *36*(3), 307-326.

48. Soboh, B., Linder, D., & Hedderich, R. (2004). A multisubunit membrane-bound [NiFe] hydrogenase and an NADH-dependent Fe-only hydrogenase in the fermenting bacterium Thermoanaerobacter tengcongensis. *Microbiology*, *150*(7), 2451-2463.

49. Kelly, C. L., Pinske, C., Murphy, B. J., Parkin, A., Armstrong, F., Palmer, T., & Sargent, F. (2015). Integration of an [FeFe]-hydrogenase into the anaerobic metabolism of Escherichia coli. *Biotechnology Reports*, *8*, 94-104.

50. Frey, M. (2002). Hydrogenases: hydrogen-activating enzymes. *ChemBioChem*, *3*(2-3), 153-160.

51. Fontecilla-Camps, J. C., Volbeda, A., Cavazza, C., & Nicolet, Y. (2007). Structure/function relationships of [NiFe]-and [FeFe]-hydrogenases. *Chemical reviews*, *107*(10), 4273-4303.

52. Burgdorf, T., Lenz, O., Buhrke, T., Van Der Linden, E., Jones, A. K., Albracht, S. P., & Friedrich, B. (2005). [NiFe]-hydrogenases of Ralstonia eutropha H16: modular enzymes for oxygen-tolerant biological hydrogen oxidation. *Journal of molecular microbiology and biotechnology*, *10*(2-4), 181-196.

53. Burgdorf, T., van der Linden, E., Bernhard, M., Yin, Q. Y., Back, J. W., Hartog, A. F., ... & Friedrich, B. (2005). The soluble NAD+-reducing [NiFe]-hydrogenase from Ralstonia eutropha H16 consists of six subunits and can be specifically activated by NADPH. *Journal of bacteriology*, *187*(9), 3122-3132.

54. Mertens, R., Greiner, L., van den Ban, E. C., Haaker, H. B., & Liese, A. (2003). Practical applications of hydrogenase I from Pyrococcus furiosus for NADPH generation and regeneration. *Journal of Molecular Catalysis B: Enzymatic*, *24*, 39-52.

55. Ratzka, J., Lauterbach, L., Lenz, O., & Ansorge-Schumacher, M. B. (2011). Systematic evaluation of the dihydrogen-oxidising and NAD+-reducing soluble [NiFe]-hydrogenase from Ralstonia eutropha H16 as a cofactor regeneration catalyst. *Biocatalysis and Biotransformation*, *29*(6), 246-252.

56. Ghosh, D., Bisaillon, A., & Hallenbeck, P. C. (2013). Increasing the metabolic capacity of Escherichia coli for hydrogen production through heterologous expression of the Ralstonia eutropha SH operon. *Biotechnology for biofuels*, *6*(1), 122.

3 Construction of *E. coli* for non-oxidative dependent growth

Essentially all organisms use a variation of glycolysis for sugar degradation. Glycolysis degrades sugar into three-carbon (C3) metabolites, which are then decarboxylated to form two-carbon (C2) metabolites, losing one carbon equivalent as CO_2. This carbon loss is problematic in biorefining, since many industrially relevant chemicals are derived from C2 metabolites. The recent development of synthetic non-oxidative glycolysis (NOG) generated considerable excitement since it directly generates stoichiometric amounts of C2 metabolites from sugar, allowing for the production of C2-derived products at 100% yields. To realize the potential of NOG, we replaced glycolysis with NOG as the sugar catabolism pathway in *E. coli*. NOG-based growth was established using a combination of rational design and evolution. This process required a fundamental rewiring of the cell's global metabolism. Rather than degrading sugar into C3 metabolites before producing C2 metabolites with carbon loss, this NOG strain first generates C2 metabolites, and C3 is later synthesized from C2. NOG-based growth was established through a combination of rational design and evolution. Isolated colonies grew at a comparable rate to wild-type *E. coli*, produced C2-derived products at yields exceeding the theoretical maximum with glycolysis, and catabolized sugar in a manner consistent with NOG. This NOG-dependent strain could be a promising host for production of C2-derived products.

3.1 Introduction

Glycolysis is the fundamental pathway for sugar catabolism.[1] While multiple variations of glycolysis exist, the most common glycolytic variation is known as the Embden-Meyerhof-Parnas (EMP) pathway.[2] The EMP pathway degrades one molecule of glucose, a hexose, into two three-carbon (C3) pyruvate molecules, as well as two molecules of ATP and two molecules

of NADH. Pyruvate can be used as a biosynthetic precursor for amino acid synthesis, or decarboxylated to form two-carbon metabolites (C2) such as acetyl-CoA. For each C2 molecule produced, one molecule of carbon dioxide is released to the environment. This carbon loss represents a major economic limitation in bioprocessing, since C2 metabolites are precursors to a wide variety of industrial products, including fatty acids,[3] alcohols,[4-6] isoprenoids,[7-9] and alkanes.[10-12] Since feedstock costs represent a substantial fraction of operating costs in bioprocesses using both conventional and cellulosic carbon sources, this carbon loss is especially problematic.[13] Since no naturally-occurring pathway can bypass C3 production to generate C2 at 100% yield, this carbon loss is unavoidable unless CO_2 is reincorporated through carbon fixation. Recently, a synthetic non-oxidative glycolysis was developed that combines phosphoketolase (Xpk) with a carbon rearrangement cycle to bypass pyruvate production and directly generate C2 without carbon loss.[14] Although NOG was demonstrated in *E.* coli to produce a C2-derived product at a yield above the previous theoretical maximum, this strain still relied on the EMP pathway for growth and only used the desired pathway when specific redox conditions favored NOG. Moreover, in this study NOG was not compatible with glucose, the world's most abundant sugar, due to regulation and dependence on the phosphotransferase (PTS) system.[15] Xpk is the key enzyme in NOG, and it degrades fructose 6-phosphate or xylulose 5-phospahte into acetyl-phosphate (AcP), a C2 metabolite, and the corresponding sugar phosphate.[16] Xpk is a component of the bifido shunt, a carbon catabolism pathway found in *Bifidobacterium*.[17] Although incorporating the bifido shunt or Xpk alongside the EMP can improve carbon yield of acetyl-CoA,[18-20] this strategy still relies on the EMP to generate C3 and cannot completely convert sugar into C2 equivalents without carbon loss. Thus, here we sought to implement NOG as the sole pathway for carbon catabolism in *E. coli*. Establishing NOG as a growth pathway was achieved

through a combination of rational design and evolution. By coupling the pathway to growth, we used evolutionary selection to establish a robust pathway. The resulting strain initially produces C2 from sugar using Xpk, then converts C2 into C3 using carbon scavenging pathways such as the glyoxylate shunt and gluconeogenesis. While NOG does not directly produce ATP or reducing power, the cell is able to generate them in the TCA cycle, allowing for aerobic growth. Strains isolated following evolution were able to produce C2-derived products at yields exceeding the theoretical maximum using glycolysis, and carbon-labeling confirmed the pattern in the resulting products was consistent with NOG-based metabolism. We believe the resulting strain could be a useful host for chemical production.

3.2 Materials and methods

3.2.1 Medium and cultivation

All *E. coli* strains were cultured by rotary shaking (250 rpm, New Brunswick Scientific) at 37 degrees. All media ingredients were purchased through Fisher Scientific unless otherwise noted. To maintain plasmids *E. coli* strains were grown in LB or SGC media containing appropriate antibiotics. Antibiotics were used at the concentrations as listed: 200 μg/L Carbenicillin, 50 μg/L kanamycin, 20 μg/L chloramphenicol, 50 μg/L spectinomycin. Minimal media contained 10 g/L glucose, 1x m9 salts, 0.2 mM $CaCl_2$, 2 mM $MgSO_4$, (Sigma Aldrich), 100 mM MOPS buffer, and vitamin mix (0.02 g/L pyridoxamine dihydrochloride (Sigma Aldrich), 4-aminobenzoic acid (Sigma Aldrich), 0.002 g/L biotin, 0.002 g/L B12 and 0.01 g/L thiamin). Sodium acetate (Sigma Aldrich) or cas amino acids was added as required as nutritional supplement.

3.2.2 Plasmid construction

Plasmids from this study are listed in Appendix II. PCR fragments for plasmid construction were amplified using Phire Hot Start II DNA polymerase (Thermo Scientific). PCR products were purified by a PCR purification kit (Zymo Research). *E. coli* XL1-B chemical competent cells were used for cloning. For plasmid construction, each fragment contained 20-30 bp overlapping sequences and were mixed at equimolar amounts. Plasmids were assembled using Gibson Assembly Master (NEB). Plasmids were verified by sequencing (Laragen, Culver City, CA).

3.2.3 Genome engineering

To construct the NOG strains, genes were deleted using the previously described Flp-Frt system or CRISPR-Cas9.[21-22] Successful edits were confirmed by colony PCR and sequencing (Laragen, Culver City, CA). Phosphoketolase was integrated into the genome using the Cre-*lox* system.[23] A strain list for this study is found in Appendix I.

3.2.4 Genome sequencing

Genomic DNA was extracted by Qiagen Gentra Puragene following the manufacturer's instructions. DNA sequencing was performed by the High Throughput Sequencing Core at Academia Sinica (Taipei, Taiwan).

3.2.5 NOG strain evolution

NOG6 was evolved in glucose minimal media plus 5 mM acetate. When the culture reached its maximum optical density, it was reinoculated into fresh media at OD_{600}= 0.1. NOG21 and

NOG26 were evolved by serial streaking on glucose minimal media plates. Fast growing colonies were selected for the next round of streaking.

3.2.6 Whole pathway assay to identify limiting enzymes

NOG strains were grown overnight glucose minimal media supplemented with acetate and were lysed with Bugbuster (Sigma Aldrich). Protein concentration was measured by Bradford assay. The assay generated AcP from F6P, and AcP was quantified as previously described.[14] The assay mixture contained 100 mM phosphate buffer (pH 7.5), 5 mM $MgCl_2$, 1 mM TPP and 40 mM F6P. 5 μg of purified NOG enzymes (Xpk, Rpe, Rpi, Tal, Tkt, Fbp, Tpi, and Fba) were added to 40 μg strain lysate to establish the positive control, and test samples contained one of the purified NOG enzymes removed.

3.2.7 Growth characterization

Strains were precultured in minimal media with 5 mM acetate for 16 hours. Strains were reinoculated into glucose minimal media at OD_{600}= 0.1. OD_{600} readings were measured using an Agilent 8453 UV-Vis spectrophotometer (Agilent Technologies).

3.2.8 Tal and Tkt bioprospecting

Multiple Tal and Tkt candidates were cloned with a N-terminal His-Tag as mentioned before.[24] Purified protein was obtained using the His-SpinProtein Miniprep kit (Zymo) following the manufacturers protocol. The Tkt assay contained 0.5-4 mM ribulose 5-phosphate, 50 mM phosphate buffer (pH 7.5), 5 mM $MgCl_2$ 2U Pgi, 2U Zwf, 2U Rpe, 2U Rpi, 2U Tal, and 5 μg Tkt. Tkt activity was quantified by detecting NADPH generation at OD_{340}. The extinction

coefficient for NADPH production was 6220 M^{-1} cm^{-1}. The Tal assay contained the same conditions except 2U Tkt and 5 μg Tal was used instead. Absorbances were taken using Agilent 8453 UV-Vis spectrophotometer (Agilent Technologies).

3.2.9 EMRA to evaluate pathway robustness

Ensemble modeling robustness analysis (EMRA) is a stochastic modeling technique to evaluate pathway robustness.[25] Unknown pathway parameters are randomly sampled within a reasonable range, creating an ensemble of 1000 different models with different values for unknown parameters. Here, the robustness in the TCA cycle and glyoxylate shunt was analyzed. The robustness was determined by the probability of a model within the ensemble would fail in response to enzyme perturbation (upregulation or downregulation). Failure occurs when the real component of the system's eigenvalues becomes positive.[26]

3.2.10 Fermentation and carbon tracing

Strains were grown in LB media plus 10 g/L glucose under aerobic conditions and were induced with 1 mM IPTG for 16 hr. Cells were washed once with the production media and resuspended anaerobically to OD_{600}= 20-25. Labeled glucose was used for the ^{13}C carbon tracing experiments.

3.2.11 GC-MS analysis

Acetate was identified at m/z of 60, 61 (m+1), and 62 (m+2) and formate was identified at m/z of 29, and 30 (m+1). Glucose labeled with ^{13}C at the 3,4 position was used. Thus, using glycolytic metabolism the ^{13}C should be incorporated into formate and not acetate, and should be incorporated into acetate using NOG-based metabolism. GC-MS data was quantified on an

Agilent 6890/5973 GC/MS. An HP-free fatty acid phase (FFAP) column was used for analysis. The inlet temperature was 250 °C. The initial oven temperature was 70 °C for 1 min, followed by a ramp of 20 °C/min up to a 2 min hold at 240 °C.

3.2.12 cAMP quantification

E. coli strains were grown in glucose minimal media with 1% cas amino acids and harvested at log phase. Samples were diluted in 0.1 M HCl (1:10). Intracellular and extracellular cAMP was measured using the Colorimetric cAMP Direct Immunoassay Kit (BioVision) according to the manufacturer's instructions.

3.2.13 Pck enzyme assay

E. coli strains for the Pck assay were grown in glucose minimal media containing 1% casamino acids. Cells were lysed using the Tissue Lyser II (Qiagen). Pck activity was measured using a coupled assay modified from the literature.[27] The reaction mixture contained 100 mM imidazole, 5 mM $MnCl_2$, 1 mM ADP, 40 mM PEP, 45 mM $NaHCO_3$, 0.2 mM NADH, and 5 U purified malate dehydrogenase. 20 μl lysate was added. Protein concentrations were measured using Bradford assay and Pck activity was quantified by detecting the change in absorbance at OD_{340}. The extinction coefficient for NADH was (6220 M^{-1} cm^{-1}). Absorbances were taken using Agilent 8453 UV-Vis spectrophotometer (Agilent Technologies).

3.2.14 Pta enzyme assay

E. coli strains for the Pta assay were grown in glucose minimal media containing 1% casamino acids. Cells were lysed using the Tissue Lyser II (Qiagen). Pta activity was detected using a

previously described method.[24] The reaction mixture contained 10 mM Tris-HCl buffer (pH=7.5), 0.2 mM NADH, 2 mM acetyl-phosphate, 1 mM CoA, and 30 μg purified PduP (*B. methalonicus*). 20 μl lysate was added. Protein concentrations were measured using Bradford assay. Pta activity was quantified by detecting the change in absorbance at OD_{340}. The extinction coefficient for NADH was (6220 M^{-1} cm^{-1}). Absorbances were taken using Agilent 8453 UV-Vis spectrophotometer (Agilent Technologies).

3.2.15 Isocitrate lyase assay

E. coli strains for the isocitrate lyase assay were grown in glucose minimal media containing 1% casamino acids. Cells were lysed using the Tissue Lyser II (Qiagen). The reaction mixture contained 25 mM MOPS, 5 mM $MgCl_2$, 1 mM EDTA, 4 mM phenylhydrazine HCL, 1 mM isocitrate, and 20 µL strain lysate. Glyoxylate formed by isocitrate lyase reacted to form phenylhydrazine glyoxylate, which was measured at 324 nm. Protein concentrations were measured using Bradford assay. The extinction coefficient for phenylhydrazine glyoxylate is (16.8 mM^{-1} cm^{-1}).

3.3 Results

3.3.1 Rationale of strain design

The EMP pathway degrades sugars such as glucose into pyruvate plus NADH and ATP. Pyruvate can be decarboxylated into acetyl-CoA along with the generation of additional NADH. Pyruvate, other intermediates in the EMP pathway, and acetyl-CoA are crucial biosynthetic precursors, and NADH/ATP are needed to drive biosynthetic pathways and support growth. In NOG, sugar is degraded to acetyl-CoA without carbon loss, but no ATP or NADH is generated.

Since one mol of ATP is required to phosphorylate one mol of sugar, the pathway requires ATP production by some other mechanism. Retaining carbon is beneficial for biorefining since carbon fixation in organisms such as *E. coli* is challenging. To generate valuable reduced products, electrons can be supplied externally, and can also be used to generate ATP using respiration. However, in order for NOG to support glucose growth, C3 biosynthetic precursors in lower glycolysis will need to be produced. Thus, we planned to use carbon scavenging pathways such as the glyoxylate shunt (GS) and gluconeogenesis. NAD(P)H in the GS shunt can also be used for ATP production in aerobic conditions, solving the ATP deficit when producing AcP using NOG. Since carbon scavenging pathways are repressed on glucose, we sought to combine rational design and evolution to implement NOG as a growth pathway. We planned to facilitate evolution by the expression of *mutD5*, which has been shown to increase the mutation rate in *E. coli* 37,000 fold in rich media and 480 fold in minimal media.[28]

3.3.2 Removal of endogenous glycolytic pathways

The first step in constructing *E. coli* for NOG growth is to remove the pathways it uses to grow on sugar, i.e. glycolysis and its variations, and other potential pathways that could lead to non-NOG dependent growth. Deleting the *gapA* gene, which codes for glyceraldehyde 3-phosphate dehydrogenase, has previously been shown to abolish glucose growth in *E. coli*.[29-30] Therefore, this gene was deleted from JCL16, a wild-type *E. coli* strain. Consistent with previous studies, the resulting strain could no longer grow on glucose minimal media. Instead, minimal media containing glycerol, succinate and amino acids (SGC) could restore the growth of the strain.[29] Although deleting *gapA* completely abolished growth, *E. coli* still contains pathways that can compensate for GapA by bypassing it to produce pyruvate from intermediates in upper

glycolysis. Presumably, they are unable to rescue glucose growth following the deletion of *gapA* because they are not sufficiently expressed, but they could potentially be upregulated through evolution. One such pathway is the methylglyoxal pathway.[31] In order to remove this pathway, *mgsA*, which codes for methylglyoxal synthase, was deleted. The resulting strain was designated PHL2. Following the construction of PHL2, we tested whether we could restore growth on glucose by the overexpression of Xpk, the only enzyme for NOG not already contained in *E. coli*. Therefore, the bifunctional *xpk* from *Bifidobacterium adolescentis*, was cloned onto a colE origin plasmid backbone under the P_1lacO_1 promotor, creating pPL157. However, the resulting strain, PHL2/pPL157, was unable to grow, likely due to insufficient expression of pathway enzymes and/or regulation of these enzymes. Next, evolution was applied to achieve glucose growth using serial dilutions. Strains were given an excess of glucose and small amount of SGC media sufficient to allow the cell to grow to a low OD_{600} (<0.3). In these conditions, cells that adapt to utilize glucose are able to reproduce more than those growing on SGC only and will quickly come to dominate the culture. Evolution was facilitated in some cultures through the presence of a strong mutator phenotype achieved through the overexpression of *mutD5*. While no glucose growth was observed in strains not overexpressing *mutD5* after two months evolutions, a strain containing the mutator phenotype developed glucose growth within two weeks. However, this strain's growth was found to not be dependent on Xpk since the removal of pPL157 did not abolish the growth phenotype in this strain. In order to have better protection against potential suppressor pathways, more knockouts in the strain were carried out. Erythrose 4-phosphate dehydrogenase (*gapB*), which is a possible gapA isozyme, was deleted.[32] To provide further insurance against other GapA isozymes, phosphoglycerate kinase (*pgk*), a second essential EMP gene, was deleted.[30] In addition, we deleted the Entner-Doudoroff pathway, another potential

GapA bypass.[33] To remove this pathway, glucose 6-phosphate dehydrogenase (*zwf)*, phosphogluconate dehydrogenase (*edd*), and Entner-Doudoroff aldolase (*eda*) were all deleted. The resulting strain, designated PHL7, did not develop growth in glucose media after 2 months evolution with *mutD5*, demonstrating that it did not readily develop suppressor pathways.

3.3.3 Further genome edits to alter endogenous regulation, remove potential futile cycles and integration of phosphoketolase

The scheme for developing NOG growth relies on the upregulation of carbon scavenging pathways, such as gluconeogenesis and the glyoxylate shunt, that are normally repressed on glucose.[34] While this repression could be alleviated by evolution, we sought to carry out further genome edits to directly address this problem. We deleted isocitrate lyase regulator (*iclR*), which represses the *aceBAK* operon containing components of the glyoxylate shunt.[35] Next, the promotor for the *pckA* gene, which codes for the gluconeogenic enzyme phosphoenolpyruvate carboxykinase, was replaced with the P_1lacO_1 promotor to alleviate transcriptional repression.[36-37] Pck represents a key step in the NOG growth schematic since it directly links lower glycolysis with the TCA cycle. Next, we deleted potential futile cycles that could be detrimental to NOG growth. First, *pfkA,* the major phosphofructokinase in *E. coli,*[38] was deleted since it could form a futile cycle with *fbp* that could drain ATP. Secondly, *poxB,* the gene coding for pyruvate oxidase was deleted, to prevent pyruvate loss back to C2. Finally, *B. adolescentis* phosphoketolase was integrated into the chromosome under the $P_Llac O_1$ promotor to better stabilize the phenotype during evolution. We found increased enzyme activities for isocitrate lyase and phosphoketolase in PHL13 (Figure S3-1). The resulting strain was designated PHL13. An overview of NOG growth and the strategy to develop it are shown in Figure 3-1 and Figure 3-2 respectively.

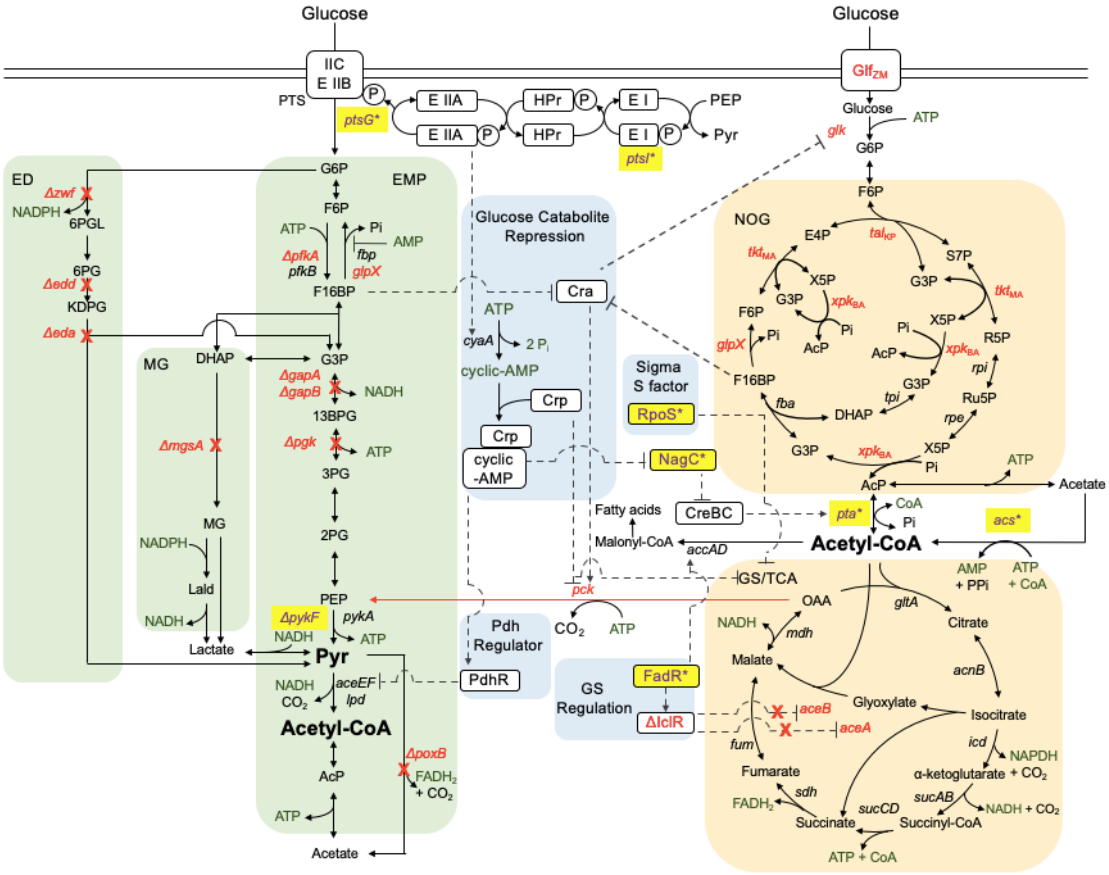

Figure 3-1 Overview of growth in the NOG strain. Red color represents genes overexpressed or deleted. Gray lines represent regulation. Purple color represents gene mutations or deletions through evolution. EMP, Embden–Meyerhof–Parnas; NOG, non-oxidative glycolysis; TCA, tricarboxylic acid cycle; GS, glyoxylate shunt; ED, Entner–Doudoroff; MG, methylglyoxal; Glf, glucose facilitator; Cra, Catabolite repressor activator; Crp, cAMP receptor protein; RpoS, RNA polymerase, sigma S; IclR, DNA-binding transcriptional repressor for GS; FadR, fatty acid metabolism regulator protein; PdhR, pyruvate dehydrogenase complex regulator; CreBC, Two-Component signal transduction system; NagC, DNA-binding transcriptional dual regulator;G6P, glucose 6-phosphate; F6P, fructose 6-phosphate; F16BP, fructose 1,6-bisphosphate; G3P, glyceraldehyde 3-phosphate; DHAP, dihydroxyacetone phosphate; 13BPG, 1,3-bisphosphoglycerate; 3PG, 3-phosphoglycerate; 2PG, 2-phosphoglycerate; PEP, phosphoenolpyruvate; Pyr, pyruvate; 6PGL, 6-phospho D-glucono-1,5-lactone; 6PG, gluconate 6-phosphate; KDPG, 2-keto-3-deoxy-6-phospho-gluconate; Lald, lactaldehyde; S7P, sedoheptulose 7-phosphate; X5P, xylulose 5-phosphate; R5P, ribose 5-phosphate; Ru5P, ribulose-5-phosphate; AcP, acetyl phosphate; E4P, erythrose 4-phosphate; OAA, oxaloacetate. *ptsG*, glucose-specific PTS enzyme IIBC component; *pfk*, 6-phosphofructokinase; *gapA*, glyceraldehyde-3-phosphate dehydrogenase; *gapB*, erythrose-4-phosphate dehydrogenase; *pgk*, phosphoglycerate kinase; *pyk*, pyruvate kinase; *aceEF*, pyruvate dehydrogenase subunits, *lpd*, lipoamide dehydrogenase; *zwf*, glucose-6-phosphate dehydrogenase, *edd*, phosphogluconate dehydratase; *eda*, KDPG aldolase; *mgsA*, methylglyoxal synthase; *xpk*, phosphoketolases; *glk,* glucokinase; *fba*; F16BP aldolase; *fbp*, fructose 1,6-bisphosphatase; *glpX*, type II fructose 1,6-bisphosphatase; *tkt*, transketolase; *tal*, transaldolase; *rpe*, ribulose-5-phosphate epimerase; *rpi*, ribose-5-phosphate isomerase; *pta*, phosphate acetyltransferase; *gltA*, citrate synthase; *acnB*, aconitate hydratase; *icd*, isocitrate dehydrogenase; *sdh*, succinate:quinone oxidoreductase; *fum*, fumarase; *mdh*, malate dehydrogenase; *aceA*, isocitrate lyase; *aceB*, malate synthase; *pck*, phosphoenolpyruvate carboxykinase; *cyaA*, adenylate cyclase; *acs*, acetyl-CoA synthase; *poxB*, pyruvate oxidase, *accAD*, acetyl-CoA carboxyltransferase subunit α and β. The subscript letters represent the source of the gene: BA, *Bifidobacterium adolescents*; ZM, *Zymomonas mobilis*; MB, *Methylomicrobium buryatense* 5GB1*;* KP, *Klebsiella pneumonia*.

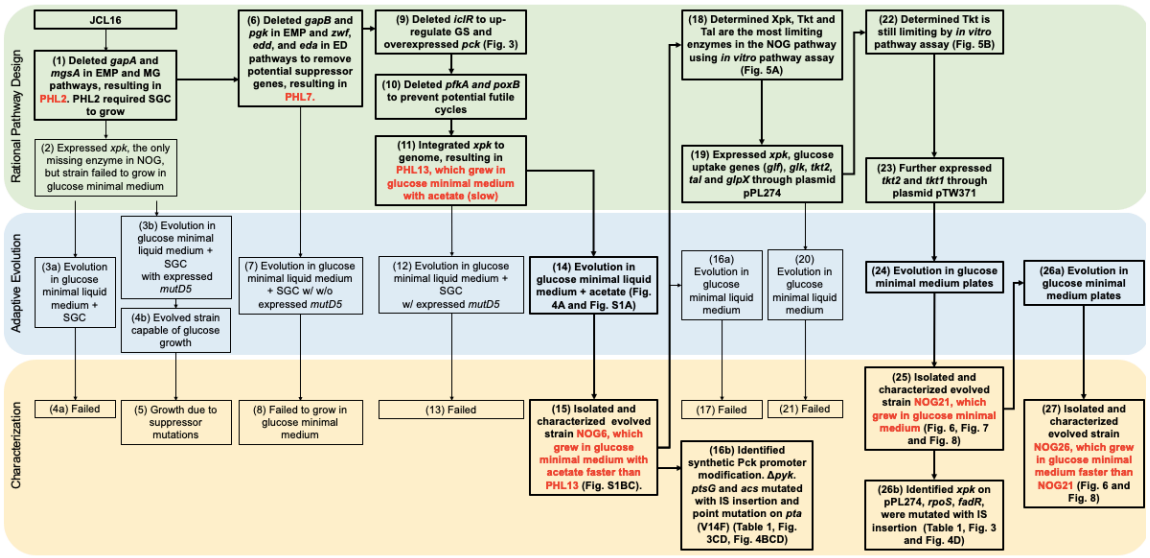

Figure 3-2: Logic of establishing NOG growth. Bold lines and text represent successful engineering. EMP, Embden–Meyerhof–Parnas; MG, methylglyoxal; ED, Entner–Doudoroff; NOG, non-oxidative glycolysis; GS, glyoxylate shunt; *gapA*, glyceraldehyde-3-phosphate dehydrogenase; *mgsA*, methylglyoxal synthase; *xpk*, phosphoketolases; *mutD5*, *E. coli* mutator; *gapB*, erythrose-4-phosphate dehydrogenase; *pgk*, phosphoglycerate kinase; *zwf*, glucose-6-phosphate dehydrogenase, *edd*, phosphogluconate dehydratase; *eda*, KDPG aldolase; *iclR*, DNA-binding transcriptional repressor for GS; *pfkA*, 6-phosphofructokinase A; *poxB*, pyruvate oxidase; *pck*, phosphoenolpyruvate carboxykinase; *pykF*, pyruvate kinase; *ptsG*, glucose-specific PTS enzyme IIBC component; *acs*, acetyl-CoA synthase; *tkt*, transketolase; *tal*, transaldolase; *glf*, glucose facilitator; *glk*, glucokinase; *glpX*, type II fructose 1,6-bisphosphatase; *rpoS*, RNA polymerase, sigma S; *fadR*, fatty acid metabolism regulator protein; AcP, acetyl phosphate. SGC is the M9 minimal salt medium with 50 mM glycerol, 50 mM succinate and 0.1% casamino acid. Gene locus number: *tkt1*, WP_017840137; *tkt2*, WP_017841573.

3.3.4 Evolution of PHL13 in minimal media with acetate to upregulate acetyl-CoA to pyruvate

Following the construction of PHL13, we sought to adapt it to NOG-based growth using evolution. Rather than using SGC only as the secondary carbon source, we now utilized acetate since it provided a better representation of the NOG growth scheme. To grow on acetate, *E. coli* converts acetate directly into acetyl-CoA using acetyl-CoA synthase (Acs), or the combination of acetate kinase (Ack) and phosphotransacetylase (Pta). Thus, this requires the same carbon scavenging pathways that would be needed for NOG growth.

Initially the PHL13 cultures grew very slowly on acetate, but after repeated dilutions in this media, we found that the cultures were able to grow to their maximum OD_{600} within 24 hr. Moreover, the maximum OD_{600} was found to be dependent on the amount of acetate supplied, indicating acetate was limiting for growth (Figure 3-3). We sought to continue evolution to wean the cells off acetate by selecting cells that could use NOG to increase their supply of C2.

We evolved several dozen cultures in parallel with and without *mutD5* expression but were unable to eliminate the requirement for acetate over several months of evolution. While the goal of implementing NOG growth was not achieved, we were able to adapt the cell to use its carbon scavenging pathways in the presence of glucose by demonstrating fast growth in glucose plus acetate. We isolated one such partially evolved strain, NOG6, for further use.

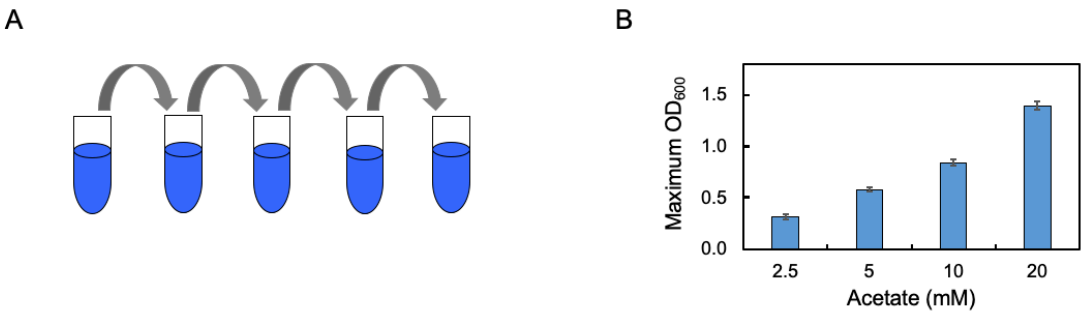

Figure 3-3: Evolution strategy and dependence on acetate for growth in NOG6 in glucose plus acetate media (A) Strategy of serial dilutions for evolution. Cultures were grown in m9 glucose media plus 5 mM acetate to allow limited acetate-based growth. Cultures that evolve to utilize glucose should quickly dominate the culture. (B) Final OD_{600} in NOG6 was dependent on the amount of acetate supplied in glucose plus acetate media. Evolution established robust glucose plus acetate growth but further evolution did not eliminate the requirement for acetate.

3.3.5 Rational design and establishment of NOG growth

Since evolution failed to establish NOG growth, we considered that the pathway may have been limited by the poor activity of some of its enzymes. Since most mutations are deleterious, it may be difficult to increase their activity by evolution. Therefore, we sought to identify potential limiting enzymes in the NOG cycle so they could be further expressed. To this end, we applied a whole-pathway assay to elucidate limiting enzymes in the NOG6 strain, the evolved strain with improved glucose plus acetate growth. To simulate the NOG cycle, we fed fructose 6-phosphate (F6P) to strain lysates and measured production of the output AcP. To establish a robust NOG cycle *in vitro*, we supplemented the NOG6 strain lysate with purified versions of all NOG enzymes. To check for enzyme limitation, we evaluated how the removal of a single purified enzyme affected AcP production relative to the control containing all enzymes. When limiting enzymes are removed from the enzyme mix, AcP yields would significantly decrease. This would indicate the AcP production is dependent on the activity of the purified enzyme, would identify the limiting enzyme as a candidate for further overexpression. When the pathway assay was performed on the NOG6 strain, we identified Xpk, Tkt, and Tal as the most limiting enzymes for AcP production (Figure 3-4). To address this limitation, *xpk, tkt,* and *tal* were further overexpressed on a plasmid. Rather than using the native *E. coli tal* & *tkt*, we cloned *tkt2* from *Methylomicrobium buryatense* and *tal* from *Klebsiella pneumoniae*. These enzymes were identified as highly active by bioprospecting (Figure S3-2). In addition to overexpressing limiting enzymes, we also sought to address other potential problems: Inefficient glucose transport and allosteric regulation of NOG enzymes. Since glucose transport/phosphorylation in *E. coli* relies on the phosphotransferase system,[15] which uses PEP as the phosphate donor, this system may not function well when glycolysis is removed. Thus, we overexpressed the glucose

facilitator *(glf)* gene from *Zymomonas mobilis*[39] and *E. coli*'s native glucokinase (*glk*) for PTS-independent transport and phosphorylation. Although *E. coli* already contains *glk,* its expression is reduced 50% on glucose.[40] To alleviate the allosteric inhibition of NOG enzyme Fbp by AMP and G6P,[41-42] we also overexpressed the gene coding for Fbp isozyme *glpX*. The resulting plasmid was designated pPL274. We tested NOG6/pPL274 for growth on glucose, but it was not able to grow without supplementation, even after 2 months evolution.

Even though limiting enzymes Xpk, Tkt, and Tal were overexpressed on pPL274, we considered that enzyme limitation might not have been completely solved. We repeated the pathway assay on NOG6/pPL274 and checked for limitation in Xpk, Tkt, and Tal (Figure 3-4). We found that Tkt was by far the most limiting enzyme for AcP production in NOG6/pPL274, as the removal of purified Tkt dropped AcP yields more than 50%. To fix this limitation, we transformed NOG6/pPL274 with pTW371, which contained a second copy of *tkt2* from *M. buryatense* as well as a copy of its isozyme *tkt1* from the same organism.

We found that after 8 days NOG6/pPL274/pTW371 grew weakly on glucose minimal media without any nutritional supplementation. Growth was improved by serial streaking, selecting for fast growing colonies on agar plates with m9 glucose media. After 1 month, a fast-growing colony was isolated and designated NOG21. NOG21 was evolved by serial streaking for an additional month, after which another evolved strain, NOG26 was isolated.

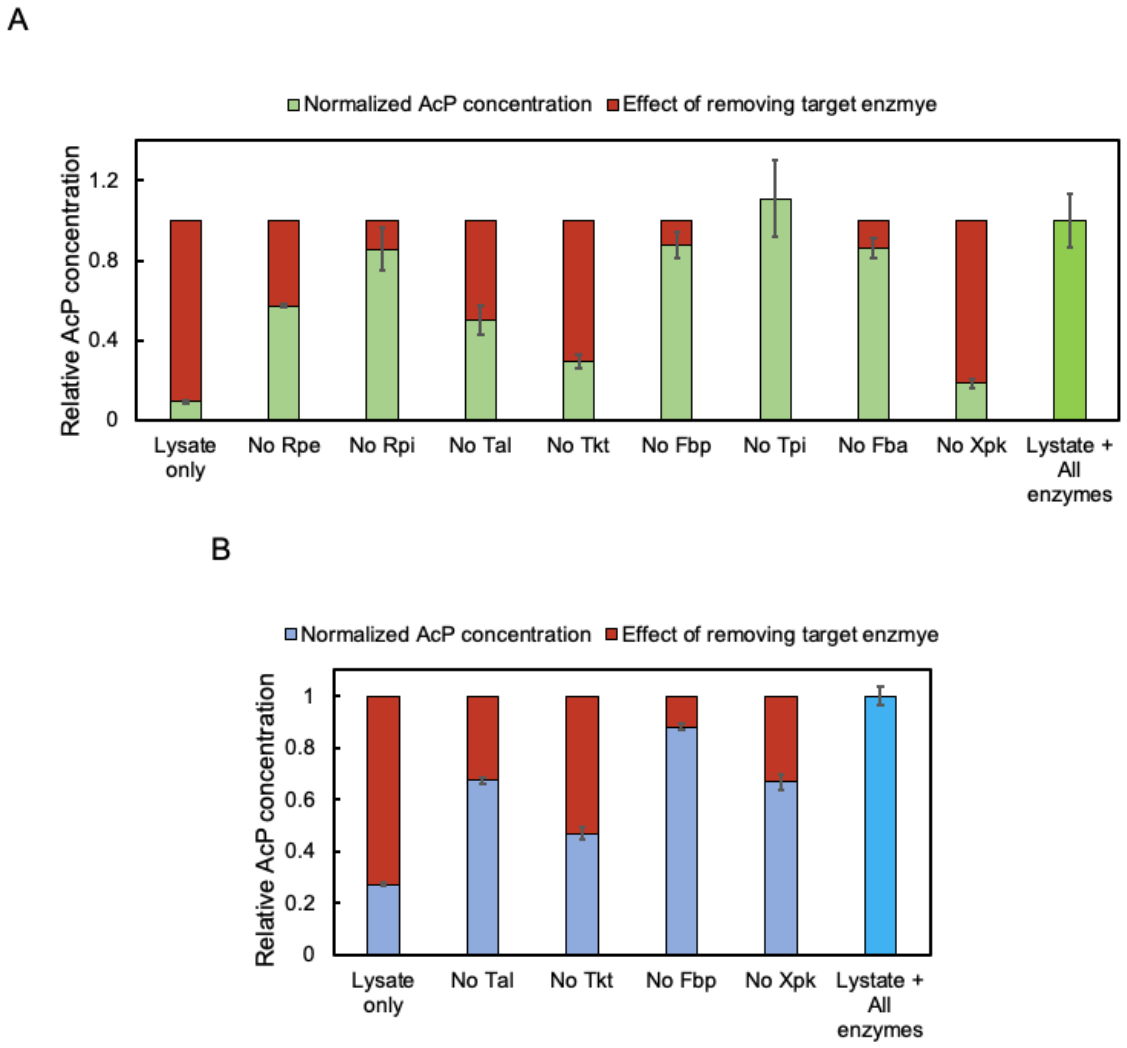

Figure 3-4: Pathway assay to elucidate limiting enzymes in NOG6 strain lysate. AcP yield was normalized to the positive control, which contained all enzymes (A) Effect of removing each purified NOG enzyme on AcP production in NOG6 strain lysate. Xpk, Tkt and Tal were the most limiting enzymes for AcP production. (B) Effect of removing each purified NOG enzyme on AcP production in NOG6/pPL274 lysate. Tkt was the most limiting enzyme for AcP production.

3.3.5 Growth characterization of NOG strains

The doubling time in glucose media of NOG21 and NOG26 were 4.8 and 3.6 hours respectively. This was between 2-3 fold higher than the doubling time of the wild type JCL16 (1.8 h) (Figure 3-5). Interestingly, we found that the *xpk* copy on pPL274 had become mutated during the evolution by transposon insertion. This likely caused all the Xpk activity in the strain to come

from the chromosomal copy of *xpk*. Although *xpk* was overexpressed when it was determined to be limiting for AcP production in vitro using the pathway assay, the Fpk component of Xpk activity is predicted to form a kinetic trap in NOG and decrease pathway robustness.[26] Thus, this mutation likely knocked down Xpk activity into the working range. The mutated plasmid was designated pPL274* to differentiate it from pPL274. Deleting the chromosomal copy of *xpk* from both NOG21 and NOG26 completely abolished glucose growth following the retransformation of pPL274* and pTW371. As expected, both NOG21 and NOG26 could not grow anaerobically.

3.3.6 Genome sequencing of NOG strain

The establishment of NOG-based growth in *E. coli* consisted of two major developments. First, the strain upregulated its carbon scavenging pathways despite catabolite repression to grow robustly in glucose plus acetate media. Next, the strain evolved to use NOG to grow on sugar media without needing nutritional supplementation. To evaluate what mutations contributed to growth, we conducted next-generation sequencing on strains isolated at the end of each development, NOG6 and NOG21. We compared the results to PHL13, the initial strain constructed prior to evolution. Relative to PHL13, NOG21 was found to have around 50 mutations total.

We discovered the *ptsG* gene acquired a transposon insertion which likely completely inactivated its functionality. This mutation was detected in both NOG6 and NOG21, so the mutation occurred while the strain was adapting to grow on glucose plus acetate. PtsG is a glucose-specific component of the PTS system, involved in phosphate transfer from PEP to glucose for glucose uptake and phosphorylation. An *E. coli* mutant strain lacking *ptsG* was found to have increased amounts of intracellular cyclic-AMP (cAMP).[43] We confirmed that intracellular levels

of cAMP in NOG6 and NOG21 were elevated. (Figure S3-3). cAMP binds the cyclic-AMP receptor protein (CRP) and is involved in the activation of many catabolic genes,[44] One such gene is *pdhR*, which transcriptionally represses the pyruvate dehydrogenase (PDH) complex.[45] PDH could be detrimental to NOG-based growth by converting pyruvate back to acetyl-CoA. Another potentially beneficial mutation that altered strain regulation occurred in *rpoS*, which encodes an alternative sigma factor σ^S and is involved the E. coli stress response.[46] *rpoS* was also inserted by a transposon, and this mutation was detected in NOG21 but not NOG6. Since it has been reported that RpoS downregulates the TCA cycle and glyoxylate shunt,[47] it is possible the upregulation of these genes benefited NOG growth.

Mutations affecting a kinetic trap between the TCA cycle and glyoxylate shunt were also observed in NOG6, suggesting balancing flux between these pathways is a key element of robust growth in glucose plus acetate media. The most notable of these mutations was a promotor truncation in the *pck* promotor. Our rational design including changing the Pck promotor to P_1*lac*O_1 to overcome transcriptional repression. However, following evolution on glucose plus acetate media, this promotor became mutated and as a result the activity of Pck was knocked down (Figure S3-4). Initially, this appeared contrary to our design that strong Pck would be beneficial for NOG growth. However, it was reasoned that if Pck activity was too strong, this could possibly drain TCA cycle intermediates if the activities of Pck and GltA, the entry point of the TCA cycle were not balanced. If TCA intermediates were drained, acetyl-CoA could no longer enter the TCA cycle, and biosynthetic precursor in lower glycolysis would no longer be provided. To further characterize this kinetic trap in Pck, Ensemble Modeling Robustness Analysis (EMRA)[26] was performed on the GS/TCA cycle in NOG-based growth. EMRA investigates how perturbations in relative activities of pathway enzymes affects pathway

robustness.[26] The EMRA analysis (Figure S3-5) predicted the kinetic trap in Pck, as robustness decreased when Pck activity was upregulated. Likewise, a kinetic trap was also predicted for the competing step, as robustness decreased when GltA activity or the rate of acetyl-CoA supply through Pta was upregulated. A point mutation in *pta* that knocked down the activity of this enzyme was also detected in NOG6 (Figure S3-4), demonstrating how the strain altered the relative activity of these enzymes to be in the working range. These results demonstrated the benefit of the glucose plus acetate evolution to balance relative enzyme activity. By selecting for fast growing cells, we were able to isolate a mutant that evolved a robust GS and gluconeogenesis to generate C3 from acetate in media containing glucose. Pta activity in PHL13 was likely increased vs. JCL16 due to an increase in its activator CreBC.[48] The increased cAMP levels in PHL13 (Figure S3-3) likely downregulated CreBC repressor NagC.[49-50]

3.3.7 C2 yield and carbon labeling in evolved NOG21 was consistent with NOG-based metabolism

In order to verify the evolved strains were using NOG to catabolize sugar tested their fermentative phenotypes and carbon labeling was performed. The fermentative phenotype of NOG21 and NOG26 was distinct from the wild type strain JCL16. NOG21 and NOG26 produced mostly acetate, while JCL16 produced mostly lactate. NOG21 converted glucose to acetate at a molar yield of about 2.4, significantly higher than the theoretical maximum using EMP (Figure 3-5), demonstrating the presence of the NOG pathway. Relative to NOG21, NOG26 had a slightly lower acetate yield but produced more lactate and succinate. As NOG26 grew faster than NOG21, these data suggested than NOG26 had further upregulated its TCA/GS.

Although these production results demonstrated the presence of NOG, further engineering is needed to eliminate byproducts in the TCA cycle to achieve higher carbon yields of C2 products. Carbon labeling was also used to verify the evolved strains were using NOG (Figure 3-6). Strains were fed 3,4 labeled glucose under anaerobic conditions and the carbon labeling in their products was evaluated. Using EMP-based metabolism, 3,4 labeled glucose should yield labeled formate from PflB decarboxylation and unlabeled acetate. Since NOG conserves carbon, unlabeled, single labeled, and double labeled acetate should be detected. The results were in line with expectations, as the wild type JCL16 produced labeled formate and no labeled acetate, while NOG21 produced labeled acetate but no labeled formate. Therefore, these results support that NOG21 uses the NOG pathway to catabolize sugars.

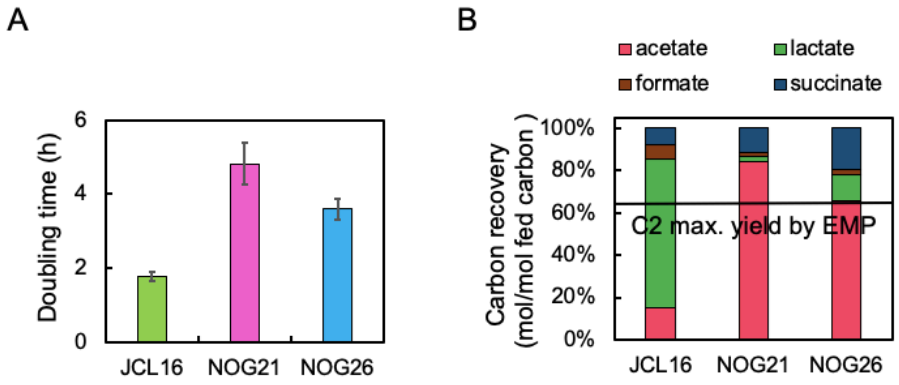

Figure 3-5: Characterization of evolved NOG strains phenotypes for growth and production (A) Doubling times in minimal glucose media in JCL16, NOG21, and NOG26 (B) Relative product yields in JCL16, NOG21, and NOG26. JCl16 produces mostly lactate, while NOG21 and NOG26 produce mostly acetate. NOG21 produces acetate at yields above the theoretical maximum using EMP. This demonstrates the evolved strains catabolize sugar using the NOG pathway.

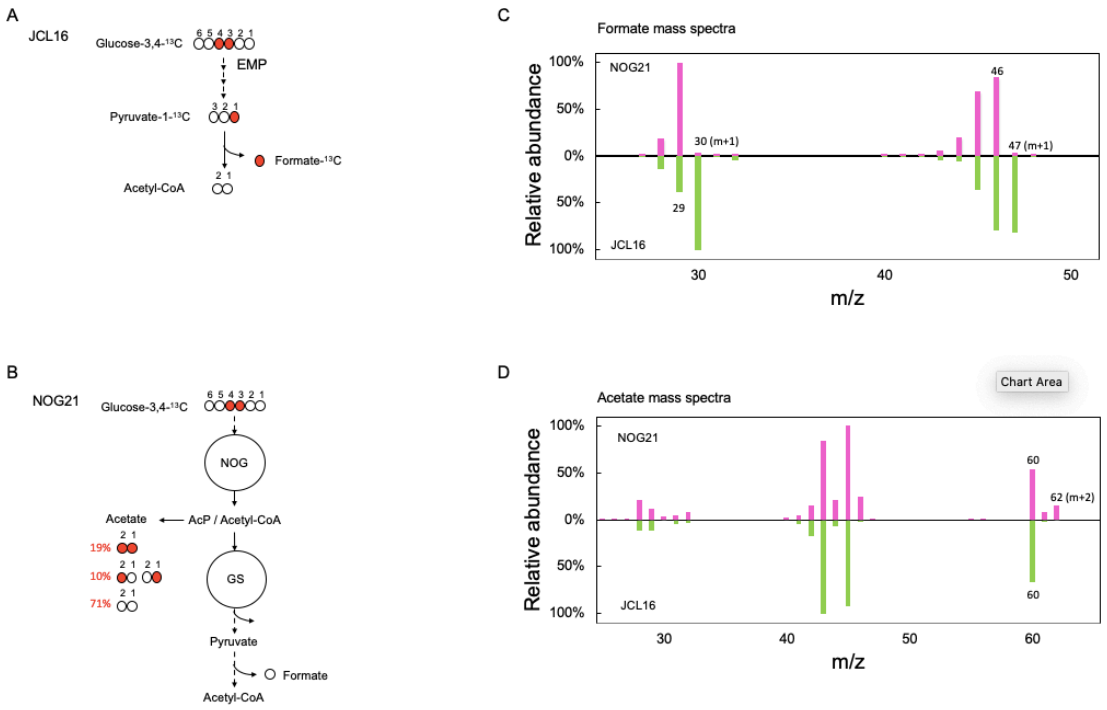

Figure 3-6: Carbon labeling in NOG21/pPL274*/pTW371. (A) Glucose labeled at the 3,4 position should be decarboxylated as formate or CO_2 in EMP metabolism. (B) Glucose labeled at the 3,4 position should be incorporated into unlabeled, single-labeled, or double-labeled acetate using NOG. (C) Carbon labeling of formate produced. JCL16 produced a significant amount of labeled formate, while no labeled formate as detected in NOG21. (D) Carbon labeling of acetate. JCL16 produced only unlabeled acetate, but NOG21 produced unlabeled, single-labeled and double-labeled acetate. These results are consistent with NOG21 using NOG-based metabolism.

3.4 Discussion and conclusions

Here, we constructed an *E. coli* strain utilizing non-oxidative glycolysis for carbon catabolism by combining rational design and large-scale evolution. Although many organisms contain all NOG enzymes,[51-54] the pathway likely never evolved naturally since efficient formation of C2 is less desirable than fast generation of ATP and NADH for growth. Following the adaptation to NOG, the resulting strain's metabolism is fundamentally different from glycolytic metabolism in that the cell synthesizes C2 metabolites before producing C3

metabolites. Coupling the pathway to growth allowed us to select for fast growing strains which evolved to develop a robust pathway. Rational design was applied to facilitate the cell's ability to evolve growth. We believe the strategy of coupling pathway robustness to growth could be an effective general tool to adapt organisms to synthetic pathways with desirable characteristics.

We verified the evolved strain was utilizing NOG by ensuring yields of C2 derived products and carbon labeling of products was consistent with NOG-based rather than glycolytic metabolism. Deleting chromosomal phosphoketolase, the key enzyme of NOG, was also found to remove growth in evolved strains NOG21 and NOG26. Sequencing of the evolved NOG21 strain revealed more than 50 mutations, affecting global regulation in the cell and helping to balance flux between competing pathways. Some of the mutations directly affected genes that were upregulated through rational design, such as Xpk and Pck, reducing the activity of these genes to balance potential kinetic traps. Since constructing the activities of these enzymes to be in the working range is likely quite difficult, relying on the cell to fine-tune relative activities through evolution proved to be an effective strategy to achieve robust growth.

Since the evolved strains were able to produce acetate, a C2-derived product, at yields exceeding the previous theoretical maximum, it is desirable to extend production to more valuable products such as alcohols, including ethanol and butanol, which can be used as liquid fuels. Since alcohols are more reduced than acetate, this will require an input of external reducing power. This can be achieved through the supply of formate and hydrogen, both of which can be generated renewably using electricity. While some organisms are capable of using hydrogen to reduce CO_2 into acetyl-CoA, these organisms are less well-characterized as *E. coli*.[55-56] Since NOG saves 50% of input carbon feedstock relative to EMP-based metabolism, the profitability for C2-derived products

can be greatly improved as long as the input cost of the reducing power does not exceed the savings from feedstock.

3.5 Appendices

3.5.1 Strain list

Strain	Genotype	Comments	Reference
BW25113	*rrnB*$_{T14}$ Δ*lacZ*$_{w116}$*hsdR514* Δ*araBAD*$_{AH33}$ Δ*rhaBAD*$_{LD78}$	Wild Type	
JCL16	BW25113/F'[*tra*D36 *proAB*$^{+}$ lacI^{q}ZΔM15(Tet^{r})]	Wild Type	
PHL2	JCL16 Δ*gapA::FRT* Δ*mgsA::FRT*	Grows on glycerol plus succinate	This Study
PHL7	JCL16 Δ*gapA::FRT* Δ*mgsA::FRT* Δ(*pgk gapB*)*::FRT* Δ*zwf::FRT* Δ(*edd eda*)*::*Kan^{r}	Grows on glycerol plus succinate	This Study
PHL13	JCL16 Δ*gapA::FRT* Δ*mgsA::FRT* Δ(*pgk gapB*)*::FRT* Δ*pfkA::FRT* Δ*iclR::FRT* Δ*poxB::cat* Δ*zwf::FRT* Δ(*edd eda*)*::*(P$_{L}$*lacO*$_{1}$*::f/xpk*$_{BA}$) ΔP$_{pck}$::P$_{L}$*lacO*$_{1}$	Grows on glycerol plus succinate	This Study
NOG6	Evolved from PHL13	Grows on glucose plus acetate media	This Study
NOG21	Evolved from NOG6	Grows on glucose with pPL274* and pTW371	This Study
NOG26	Evolved from NOG6	Grows on glucose with pPL274* and pTW371	This Study

3.5.2 Plasmid list

Plasmid	Description	Reference
pPL71	P*araB::mutD5* ColE *ori* Gen^r	This Study
pPL274	P$_L$*lacO*$_1$*::f/xpk*$_{BA}$ *glf*$_{ZM}$ *glk*$_{EC}$ tkt2$_{MB}$ *tal*$_{KP}$ *glpX*$_{EC}$ ColE *ori* Carb^r	This Study
pPL274*	P$_L$*lacO*$_1$*::f/xpk*$_{BA}$ (mutated by transposon insertion) *glf*$_{ZM}$ *glk*$_{EC}$ tkt2$_{MB}$ *tal*$_{KP}$ *glpX*$_{EC}$ ColE *ori* Carb^r	This Study
pTW371	P$_L$*lacO*$_1$*:: tkt2*$_{MB}$ *tkt1*$_{MB}$ CloDF13 *ori* Spec^r	This Study

3.5.3 Sequencing results of NOG6 and NOG21 relative to PHL13

Strain	Transposon insertion into coding regions (insertion point/total size)	Transposon insertion into non-coding region	Point mutation			Indel	Genome truncation
			Codon change	Synonymous mutation	non-coding region	Codon change	location[a]
PHL13 (relative to JCL16)	0	0	*paoA* (E130K) *glk* (D302N)	*yagF* (A445) *mlaE* (L99)	3	0	
NOG6 (relative to PHL13)	*htrE* (1695/2598), *dgt* (758/1518), *djlB* (974/1428) *ybhI* (931/1434), *pgaB* (1219/2019), *ptsG* (450/1434) *narH* (224/1539), *sieB* (224/1539), *ydcS* (487/489) *ydjX* (4/711), *yeaR* (123/360), *cutC* (559/747) *wbbK* (266/1119), *yfdS* (79/363), *dsdC* (85/936) *yffQ* (356/378), *araE* (52/1149), *gspO* (173/678) *gadW* (328/729), *xylG* (359/1542), *yiaT* (230/741) *acs* (1241/1959)	4	*pta* (V14F) *ptsI* (A376T)	0	1	*Frc* (184_185insG)	*lacO* on the synthetic Pck promoter[b] 1,747,769 - 1,773,895 (including *pykF* complete deletion)
NOG21 (relative to NOG6)	*mhpR* (381/384), *ybaE* (481/1701), *ybhD* (93/954) *fadR*(83/720), *dhaK* (129/1071), *ydbD* (1873/2307) *mall* (924/1029), *elaD* (763/1212), *yfjW* (925/1704) *ypjA*(68/4581), *ygaQ* (1067/2253), *hypD* (706/1122) *rpoS* (832/993), *yhaJ* (705/897), *mutM* (4/810) *xpk* (177/2478) on pPL274	10	*yciG* (N35K) *sad* (C423R) *dfp* (T21N)	*ycfT* (E180) *nupC* (A85) *yqeF* (A384)	3	*gluQ* (921_922insG) *nagC* (950_951insC) *nagC* (940_942delT)	301,541-302,628 316,465-326,263 3,730,690-3,751,638 4,304,834-4,306,399

[a] Location was based the sequence result of the *E. coli* MG1655 genome (NC_000913.2).
[b] Native Pck promoter was replaced by the synthetic P$_L$*lacO*$_1$ promoter in PHL13. After evolution, part of the P$_L$*lacO*$_1$ promoter region (23 bp) was deleted

3.5.4 Supplementary figures

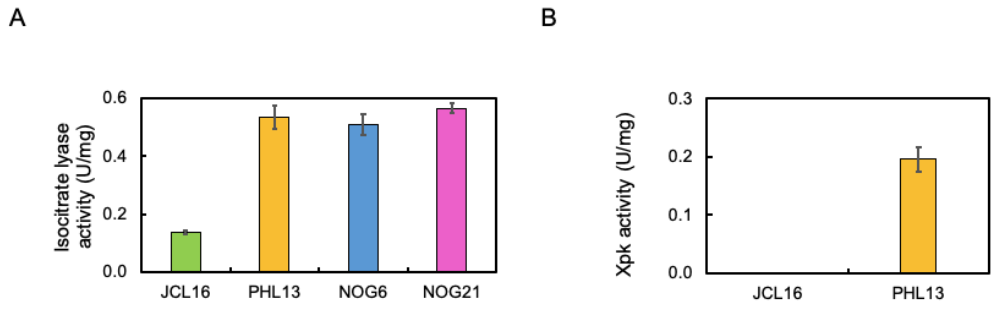

Figure S3-1: Enzyme assays following construction of PHL13 (A) Isocitrate lyase activity was upregulated following the deletion of *iclR* (B) Phosphoketolase (Xpk) activity following integration in PHL13

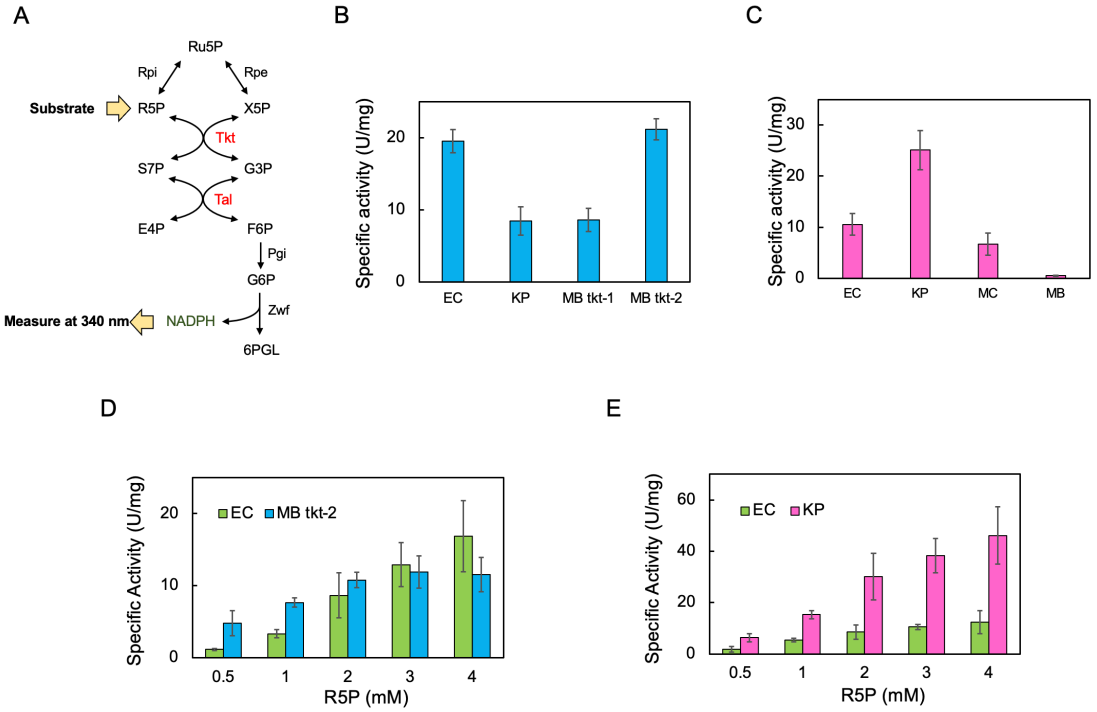

Figure S3-2: Bioprospecting of transaldolase (Tal) and transketolase (Tkt) from *E. coli*, *Methylomicrobium buryatense*, and *Klebsiella pneumoniae*. (A) Overview of coupled assay to measure Tkt or Tal activity. (B) Maximum specific activity of different transketolase variants. (C) Maximum specific activity of different transaldolase variants. (D) Specific activity of Tkt2 from *Methylomicrobium buryatense* (MB) and *E. coli* (EC) at different substrate concentrations. Tkt2 from *M. buryatense* had higher specific activity at lower concentration of substrate. (E) Specific activity of Tal from *Klebsiella pneumoniae* (KP) and *E. coli* (EC) at different concentrations of substrates. Tal from KP was more activity across all concentrations

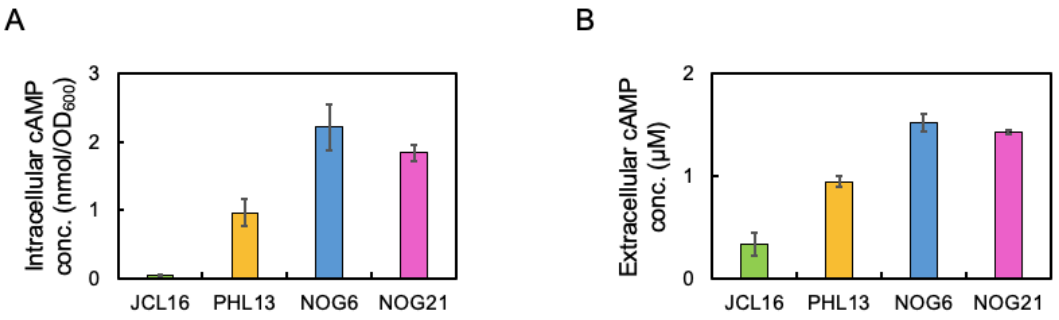

Figure S3-3: Measurement of cyclic-AMP (cAMP) during log phase in glucose plus 1% cas amino acid media (A) Intracellular cAMP levels in NOG6 and NOG21 were elevated twofold relative to PHL13 following the insertion mutation in *ptsG*. cAMP levels were likely elevated in PHL13 relative to JCL16 since the cell was not consuming glucose due to the knockout of glycolysis (B) Extracellular cAMP levels exhibited a similar trend as with intracellular cAMP

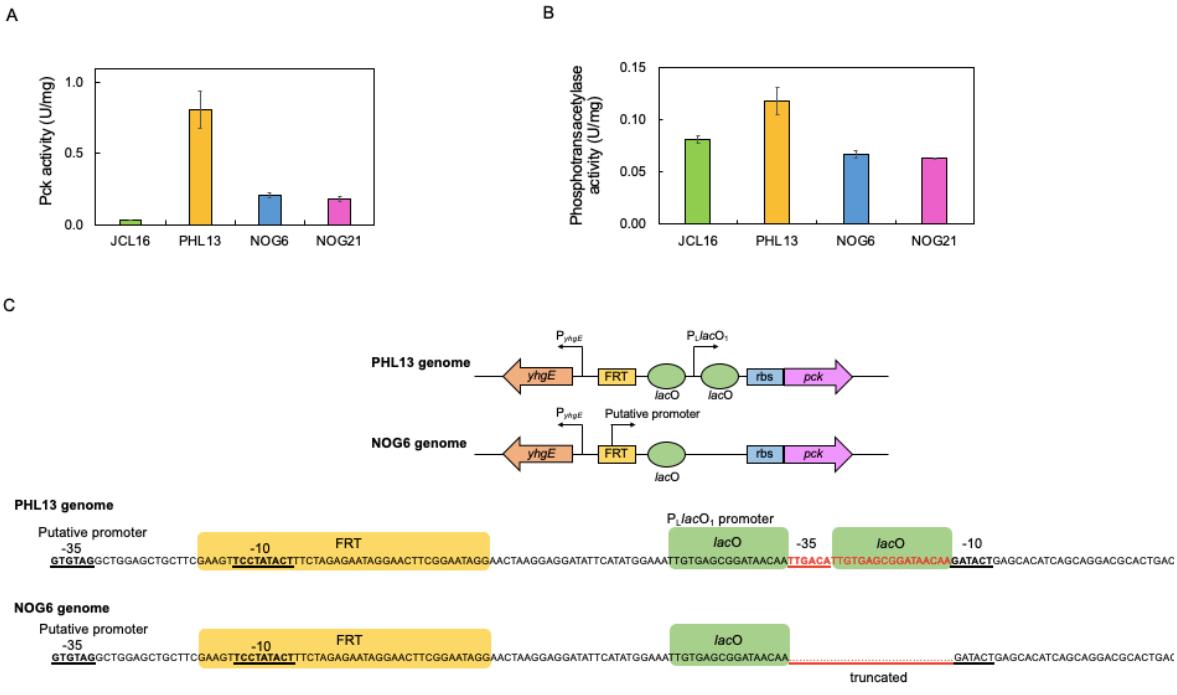

Figure S3-4: Mutations to balance Pck with the TCA cycle and glyoxylate shunt. (A) Pck activity in NOG6 and NOG21 lysates was knocked down relative to PHL13 following the Pck promotor truncation. (B) Pta activities in NOG6 and NOG21 lysates were knocked down following the point mutation in Pta. (C) Location of the promotor truncation. Transcription is predicted to occur from a putative promotor in the FRT site

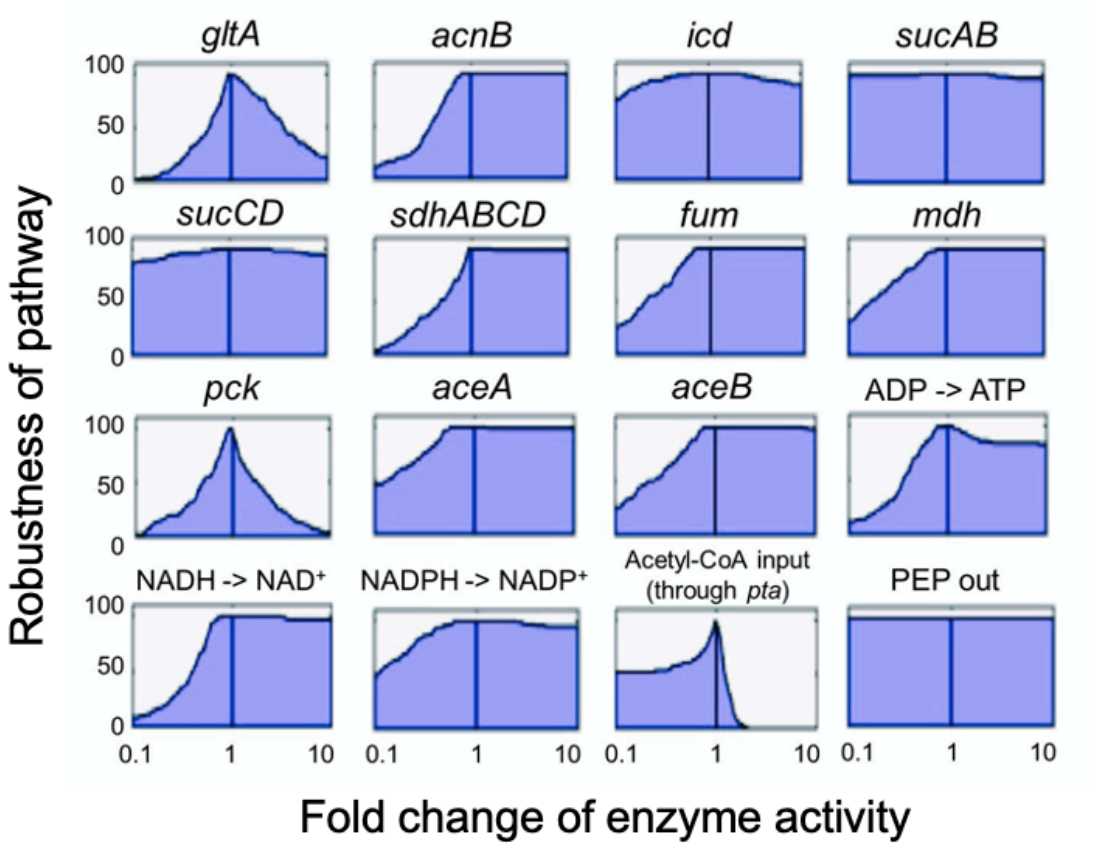

Figure S3-5: EMRA analysis of robustness in TCA cycle, glyoxylate shunt, and Pck. The y-axis represents the fraction of models that achieve stability. The x-axis represents the levels of enzyme perturbation (>1 represents upregulation). The EMRA suggests instability occurs when Pck or GltA are too high or too low, indicating the need for balance in these pathways. The results also suggest if the acetyl-CoA supply through Pta is too high that also has a deleterious effect on stability. *pck*, phosphoenolpyruvate carboxykinase; *gltA*, citrate synthase; *acnB*, aconitate hydratase; *icd*, isocitrate dehydrogenase; *sucA*, 2-oxoglutarate decarboxylase; *sucB*, dihydrolipoyltranssuccinylase; *sucCD*, succinyl-CoA synthetase; *sdh*, succinate:quinone oxidoreductase; *fum*, fumarase; *mdh*, malate dehydrogenase; *aceA*, isocitrate lyase; *aceB*, malate synthase; *pck*, phosphoenolpyruvate carboxykinase.

3.6 References

1. Fothergill-Gilmore, L. A., & Michels, P. A. (1993). Evolution of glycolysis. *Progress in biophysics and molecular biology*, *59*(2), 105-235.

2. Flamholz, A., Noor, E., Bar-Even, A., Liebermeister, W., & Milo, R. (2013). Glycolytic strategy as a tradeoff between energy yield and protein cost. *Proceedings of the National Academy of Sciences*, *110*(24), 10039-10044.

3. Zhou, Y. J., Buijs, N. A., Zhu, Z., Qin, J., Siewers, V., & Nielsen, J. (2016). Production of fatty acid-derived oleochemicals and biofuels by synthetic yeast cell factories. *Nature communications*, *7*(1), 1-9.

4. Ingram, L. O., Conway, T., Clark, D. P., Sewell, G. W., & Preston, J. F. (1987). Genetic engineering of ethanol production in Escherichia coli. *Applied and Environmental Microbiology*, *53*(10), 2420-2425.

5. Atsumi, S., Cann, A. F., Connor, M. R., Shen, C. R., Smith, K. M., Brynildsen, M. P., ... & Liao, J. C. (2008). Metabolic engineering of Escherichia coli for 1-butanol production. *Metabolic engineering*, *10*(6), 305-311.

6. Clomburg, J. M., & Gonzalez, R. (2010). Biofuel production in Escherichia coli: the role of metabolic engineering and synthetic biology. *Applied microbiology and biotechnology*, *86*(2), 419-434.

7. Felnagle, E. A., Chaubey, A., Noey, E. L., Houk, K. N., & Liao, J. C. (2012). Engineering synthetic recursive pathways to generate non-natural small molecules. *Nature chemical biology*, *8*(6), 518-526.

8. Martin, V. J., Pitera, D. J., Withers, S. T., Newman, J. D., & Keasling, J. D. (2003). Engineering a mevalonate pathway in Escherichia coli for production of terpenoids. *Nature biotechnology*, *21*(7), 796-802.

9. Ajikumar, P. K., Xiao, W. H., Tyo, K. E., Wang, Y., Simeon, F., Leonard, E., ... & Stephanopoulos, G. (2010). Isoprenoid pathway optimization for Taxol precursor overproduction in Escherichia coli. *Science*, *330*(6000), 70-74.

10. Rodriguez, G. M., & Atsumi, S. (2014). Toward aldehyde and alkane production by removing aldehyde reductase activity in Escherichia coli. *Metabolic engineering*, *25*, 227-237.

11. Schirmer, A., Rude, M. A., Li, X., Popova, E., & Del Cardayre, S. B. (2010). Microbial biosynthesis of alkanes. *Science*, *329*(5991), 559-562.

12. Buijs, N. A., Zhou, Y. J., Siewers, V., & Nielsen, J. (2015). Long-chain alkane production by the yeast Saccharomyces cerevisiae. *Biotechnology and bioengineering*, *112*(6), 1275-1279.

13. Hamelinck, C. N., & Faaij, A. P. (2006). Outlook for advanced biofuels. *Energy policy*, *34*(17), 3268-3283.

14. Bogorad, I. W., Lin, T. S., & Liao, J. C. (2013). Synthetic non-oxidative glycolysis enables complete carbon conservation. *Nature*, *502*(7473), 693-697.

15. Roseman, S., & Meadow, N. D. (1990). Signal transduction by the bacterial phosphotransferase system. *J. Biol. Chem*, *265*(6), 2993-2996.

16. Grill, J. P., Crociani, J., & Ballongue, J. (1995). Characterization of fructose 6 phosphate phosphoketolases purified from Bifidobacterium species. *Current microbiology*, *31*(1), 49-54.

17. Sgorbati, B., Biavati, B., & Palenzona, D. (1995). The genus Bifidobacterium. *The genera of lactic acid bacteria* (pp. 279-306). Springer, Boston, MA.

18. Kocharin, K., Siewers, V., & Nielsen, J. (2013). Improved polyhydroxybutyrate production by Saccharomyces cerevisiae through the use of the phosphoketolase pathway. *Biotechnology and bioengineering*, *110*(8), 2216-2224.

19. de Jong, B. W., Shi, S., Siewers, V., & Nielsen, J. (2014). Improved production of fatty acid ethyl esters in Saccharomyces cerevisiae through up-regulation of the ethanol degradation pathway and expression of the heterologous phosphoketolase pathway. *Microbial cell factories*, *13*(1), 39.

20. Chinen, A., Kozlov, Y. I., Hara, Y., Izui, H., & Yasueda, H. (2007). Innovative metabolic pathway design for efficient l-glutamate production by suppressing CO2 emission. *Journal of bioscience and bioengineering*, *103*(3), 262-269.

21. Datsenko, K. A., & Wanner, B. L. (2000). One-step inactivation of chromosomal genes in Escherichia coli K-12 using PCR products. *Proceedings of the National Academy of Sciences*, *97*(12), 6640-6645.

22. Jiang, Y., Chen, B., Duan, C., Sun, B., Yang, J., & Yang, S. (2015). Multigene editing in the Escherichia coli genome via the CRISPR-Cas9 system. *Applied and environmental microbiology*, *81*(7), 2506-2514.

23. Enyeart, P. J., Chirieleison, S. M., Dao, M. N., Perutka, J., Quandt, E. M., Yao, J., ... & Ellington, A. D. (2013). Generalized bacterial genome editing using mobile group II introns and Cre-lox. *Molecular systems biology*, *9*(1), 685.

24. Bogorad, I. W., Chen, C. T., Theisen, M. K., Wu, T. Y., Schlenz, A. R., Lam, A. T., & Liao, J. C. (2014). Building carbon–carbon bonds using a biocatalytic methanol condensation cycle. *Proceedings of the National Academy of Sciences*, *111*(45), 15928-15933.

25. Tan, Y., & Liao, J. C. (2012). Metabolic ensemble modeling for strain engineers. *Biotechnology journal*, *7*(3), 343-353.

26. Lee, Y., Rivera, J. G. L., & Liao, J. C. (2014). Ensemble modeling for robustness Analysis in engineering non-native metabolic pathways. *Metabolic engineering*, *25*, 63-71.

27. Wright, J. A., & Sanwal, B. D. (1969). Regulatory mechanisms involving nicotinamide adenine nucleotides as allosteric effectors II. Control of phosphoenelpyruvate carboxykinase. *Journal of Biological Chemistry*, *244*(7), 1838-1845.

28. Schaaper, R. M. (1988). Mechanisms of mutagenesis in the Escherichia coli mutator mutD5: role of DNA mismatch repair. *Proceedings of the National Academy of Sciences*, *85*(21), 8126-8130.

29. Seta, F. D., Boschi-Muller, S., Vignais, M. L., & Branlant, G. (1997). Characterization of Escherichia coli strains with gapA and gapB genes deleted. *Journal of bacteriology*, *179*(16), 5218-5221.

30. Nakahigashi, K., Toya, Y., Ishii, N., Soga, T., Hasegawa, M., Watanabe, H., ... & Tomita, M. (2009). Systematic phenome analysis of Escherichia coli multiple-knockout mutants reveals hidden reactions in central carbon metabolism. *Molecular systems biology*, *5*(1), 306.

31. Grabar, T. B., Zhou, S., Shanmugam, K. T., Yomano, L. P., & Ingram, L. O. (2006). Methylglyoxal bypass identified as source of chiral contamination in L (+) and D (–)-lactate fermentations by recombinant Escherichia coli. *Biotechnology letters*, *28*(19), 1527-1535.

32. Boschi-Muller, S., Azza, S., Pollastro, D., Corbier, C., & Branlant, G. (1997). Comparative enzymatic properties of gapB-encoded erythrose-4-phosphate dehydrogenase of Escherichia coli and phosphorylating glyceraldehyde-3-phosphate dehydrogenase. *Journal of Biological Chemistry*, *272*(24), 15106-15112.

33. Chen, X., Schreiber, K., Appel, J., Makowka, A., Fähnrich, B., Roettger, M., ... & Gutekunst, K. (2016). The Entner–Doudoroff pathway is an overlooked glycolytic route in cyanobacteria and plants. *Proceedings of the National Academy of Sciences*, *113*(19), 5441-5446.

34. Görke, B., & Stülke, J. (2008). Carbon catabolite repression in bacteria: many ways to make the most out of nutrients. *Nature Reviews Microbiology*, *6*(8), 613-624.

35. Maloy, S. R., & Nunn, W. D. (1982). Genetic regulation of the glyoxylate shunt in Escherichia coli K-12. *Journal of Bacteriology*, *149*(1), 173-180.

36. Shimada, T., Fujita, N., Yamamoto, K., & Ishihama, A. (2011). Novel roles of cAMP receptor protein (CRP) in regulation of transport and metabolism of carbon sources. *PloS one*, *6*(6), e20081.

37. Nakano, M., Ogasawara, H., Shimada, T., Yamamoto, K., & Ishihama, A. (2014). Involvement of cAMP-CRP in transcription activation and repression of the pck gene encoding PEP carboxykinase, the key enzyme of gluconeogenesis. *FEMS microbiology letters*, *355*(2), 93-99.

38. Kotlarz, D., Garreau, H., & Buc, H. (1975). Regulation of the amount and of the activity of phosphofructokinases and pyruvate kinases in Escherichia coli. *Biochimica et Biophysica Acta (BBA)-General Subjects*, *381*(2), 257-268.

39. Weisser, P., Krämer, Reinhard., Sahm, H., & Sprenger, G. A. (1995). Functional expression of the glucose transporter of Zymomonas mobilis leads to restoration of glucose and fructose uptake in Escherichia coli mutants and provides evidence for its facilitator action. *Journal of Bacteriology*, *177*(11), 3351-3354.

40. Meyer, D., Schneider-Fresenius, C., Horlacher, R., Peist, R., & Boos, W. (1997). Molecular characterization of glucokinase from Escherichia coli K-12. *Journal of bacteriology*, *179*(4), 1298-1306.

41. Babul, J., & Guixé, V. (1983). Fructose bisphosphatase from Escherichia coli. Purification and characterization. *Archives of biochemistry and biophysics*, *225*(2), 944-949.

42. Hines, J. K., Fromm, H. J., & Honzatko, R. B. (2006). Novel allosteric activation site in Escherichia coli fructose-1, 6-bisphosphatase. *Journal of Biological Chemistry*, *281*(27), 18386-18393.

43. Steinsiek, S., & Bettenbrock, K. (2012). Glucose transport in Escherichia coli mutant strains with defects in sugar transport systems. *Journal of bacteriology*, *194*(21), 5897-5908.

44. Valentin-Hansen, P., Søgaard-Andersen, L., & Pedersen, H. (1996). A flexible partnership: the CytR anti-activator and the cAMP–CRP activator protein, comrades in transcription control. *Molecular microbiology*, *20*(3), 461-466.

45. Quail, M. A., & Guest, J. R. (1995). Purification, characterization and mode of action of PdhR, the transcriptional repressor of the pdhR–aceEF–lpd operon of Escherichia coli. *Molecular microbiology*, *15*(3), 519-529.

46. Hengge-Aronis, R. (1996). Back to log phase: σS as a global regulator in the osmotic control of gene expression in Escherichia coli. *Molecular microbiology*, *21*(5), 887-893.

47. Dong, T., & Schellhorn, H. E. (2009). Control of RpoS in global gene expression of Escherichia coli in minimal media. *Molecular Genetics and Genomics*, *281*(1), 19-33.

48. Avison, M. B., Horton, R. E., Walsh, T. R., & Bennett, P. M. (2001). Escherichia coli CreBC is a global regulator of gene expression that responds to growth in minimal media. *Journal of Biological Chemistry*, *276*(29), 26955-26961.

49. Oberto, J. (2010). FITBAR: a web tool for the robust prediction of prokaryotic regulons. *BMC bioinformatics*, *11*(1), 554.

50. Plumbridge, J., & Kolb, A. (1995). Nag repressor–operator interactions: protein–DNA contacts cover more than two turns of the DNA helix. *Journal of molecular biology*, *249*(5), 890-902.

51. Fandi, K. G., Ghazali, H. M., Yazid, A. M., & Raha, A. R. (2001). Purification and N-terminal amino acid sequence of fructose-6-phosphate phosphoketolase from Bifidobacterium longum BB536. *Letters in applied microbiology*, *32*(4), 235-239.

52. Meile, L., Rohr, L. M., Geissmann, T. A., Herensperger, M., & Teuber, M. (2001). Characterization of the D-xylulose 5-phosphate/D-fructose 6-phosphate phosphoketolase gene (xfp) from Bifidobacterium lactis. *Journal of bacteriology*, *183*(9), 2929-2936.

53. Liu, L., Zhang, L., Tang, W., Gu, Y., Hua, Q., Yang, S., ... & Yang, C. (2012). Phosphoketolase pathway for xylose catabolism in Clostridium acetobutylicum revealed by 13C metabolic flux analysis. *Journal of bacteriology*, *194*(19), 5413-5422.

54. Schramm, M., Klybas, V., & Racker, E. (1958). Phosphorolytic cleavage of fructose-6-phosphate by fructose-6-phosphate phosphoketolase from Acetobacter xylinum. *Journal of Biological Chemistry*, *233*(6), 1283-1288.

55. Tracy, B. P., Jones, S. W., Fast, A. G., Indurthi, D. C., & Papoutsakis, E. T. (2012). Clostridia: the importance of their exceptional substrate and metabolite diversity for biofuel and biorefinery applications. *Current opinion in biotechnology*, *23*(3), 364-381.

56. Fast, A. G., & Papoutsakis, E. T. (2012). Stoichiometric and energetic analyses of non-photosynthetic CO2-fixation pathways to support synthetic biology strategies for production of fuels and chemicals. *Current Opinion in Chemical Engineering*, *1*(4), 380-395.

4 Characterization of growth in an evolved *E. coli* strain adapted to non-oxidative glycolysis and evaluation of mutations using CRISPR-Cas9

Synthetic non-oxidative glycolysis (NOG) bypasses pyruvate formation to directly generate stoichiometric amounts of two-carbon (C2) metabolites, offering the potential to produce various C2-derived products at unprecedented yields. An *E. coli* strain with its native glycolytic pathways removed was constructed for non-oxidative glycolysis-dependent growth by a combination of rational design and evolution, and this strain may represent attractive host for biotechnological purposes. Sequencing of the evolved NOG strain revealed ~50 mutations. To evaluate the effect of several mutations in this strain, a previously reported protocol for genome editing in *E. coli* using CRISPR-Cas9 was adapted to fix these mutations. A transposon insertion in *ptsG*, was found to be essential for growth in both glucose and glucose plus acetate media, and another transposon insertion in *rpoS* also contributed to growth in the strain. Interestingly, fixing a deleterious promotor truncation for *pck* was found to increase the growth rate of the NOG strain. After the evolution of a robust NOG pathway, the upregulation of Pck may have helped the cell better balance gluconeogenic and TCA cycle fluxes, underscoring how this junction appears to be very important for NOG growth. Additionally, the effect of the plasmids in the NOG strain for growth was also evaluated. In particular, the overexpression of Tkt was determined to be extremely important for NOG-based growth.

4.1 Introduction

CRISPR-Cas9 has emerged as one of the most powerful tools available for genome editing.[1] A group of DNA sequences defined as CRISPRs (clustered regularly interspaced palindromic repeats) have been discovered in *E. coli* and many other prokaryotic organisms in

both Bacteria and Archaea domains.[2,3,4] Although their function was initially uncertain, they were later hypothesized to comprise a defensive mechanism against foreign replicons such as bacteriophage and plasmid genes.[5] Evidence for a defensive mechanism was uncovered when the unique spacer sequences contained within CRISPRs were discovered to have homology with bacteriophage or conjugative plasmid sequences.[6] Moreover, it was reported that CRISPR sequences were often located adjacent to CRISPR-associated (*cas*) genes whose products contained endonuclease and helicase activity.[7] Experimental evidence was later shown directly linking CRISPR sequences to acquired phage resistance in bacteria.[8]

Though multiple CRISPR/Cas mechanisms exist, one of the best described CRISPR/Cas systems is from the bacterium *Streptococcus pyrogenes*. This system relies on the co-transcription of a crRNA and a *trans*-activating crRNA (tracrRNA), as well as the Cas9 endonuclease.[9] The crRNA and tracrRNA form a complex to direct Cas9 to the appropriate cut site. Once directed to a particular target, Cas9 will cut any sequence immediately 5' to a short protospacer adjacent motif (PAM), which would be part of an invading genome but not the CRISPR loci.[10] This system was simplified by fusing the crRNA and tracrRNA into a single guide RNA (sgRNA) molecule consisting of a 20 nucleotide sequence with homology to the target site at the 5' end and the Cas9 recognition sequence at the 3' end.[10] This hybrid system has become a robust system for genome engineering. To maintain cell viability double-stranded breaks introduced by Cas9 must be fixed by nonhomologous end joining or homology-directed repair, allowing sequences to be added, removed or mutated as desired.[11]

In recent years, this modified CRISPR/Cas9 system has been widely applied for the manipulation of many organisms, including humans,[12,13] yeast,[14] and plants.[15]

CRISPR-Cas9 has also greatly facilitated genome engineering in bacteria by removing the need for selectable markers. A fast and efficient two-component system for genome engineering in *E. coli* was developed that uses CRISPR-Cas9 to induce double-stranded breaks in the chromosome and λ Red recombinase for genome repair using homologous recombination.[16]

Recently, an evolved *E. coli* strain was developed has been adapted to grow on non-oxidative glycolysis (NOG), potentially allowing it to produce acetyl-CoA and other two-carbon (C2) derived products at 100% yield.[17,18] NOG growth was implemented through a combination of evolution and rational design through gene knockout and gene overexpression on two plasmids, pPL274* and pTW371. The resulting strain's metabolism was fundamentally rewired as it synthesizes C2 metabolites from sugar before three-carbon (C3) metabolites. C3 metabolites are produced from C2 metabolites using native carbon scavenging pathways. The evolution of the NOG strain was divided into two phases. The first phase improved growth in glucose plus acetate media by upregulating carbon scavenging pathways, which are normally subject to catabolite repression. The second phase established NOG dependent growth on glucose. Since this strain was adapted to grow on synthetic metabolism, it was of great interest to characterize how the evolved strain adapted to its new growth schematic.

Next-generation sequencing was used to identify chromosomal mutations that may have aided the development of NOG growth, and more than 50 mutations were elucidated, with the majority being gene knockouts due to transposon insertion (TI).[18] While a discussion of these mutations' potential effect on NOG-based growth was previously reported in the study,[18] their effect on growth was not directly evaluated. Here, the previously described CRISPR-Cas9 system[16] was applied to characterize several mutations in the NOG strain by reverting the mutations back to their original sequence. We also tested the contribution of the two plasmids in the evolved NOG

strain for growth and characterized the effect of a mutation that occurred during evolution on one of the growth plasmids.

4.2 Materials and Methods

4.2.1 Medium and cultivation

All *E. coli* strains were cultured by rotary shaking (250 rpm, New Brunswick Scientific) at 30 or 37 degrees. Culture at 30 degrees was necessary when maintaining pCas9 due to temperature sensitive replication. All media ingredients were purchased through Fisher Scientific unless otherwise noted. Growth media contained 10 g/L glucose, 1x m9 salts, 0.2 mM $CaCl_2$, 2 mM $MgSO_4$, (Sigma Aldrich) and vitamin mix (0.02 g/L pyridoxamine dihydrochloride (Sigma Aldrich), 4-aminobenzoic acid (Sigma Aldrich), 0.002 g/L biotin, 0.002 g/L B12 and 0.01 g/L thiamin). Strains were induced with 10 mM arabinose (Sigma Aldrich) for 2 to 3 hours prior to harvesting for electrocompetent transformation to induce the expression of lamda red recombinase.

4.2.2 Strains and plasmids

The evolved NOG strain was obtained from Lin, *et. al*[18]. The previously reported pTarget and pCas9 series[16] were obtained through addgene. All primers for the construction of sgRNA plasmids or donor DNA sequences were purchased through Integrated DNA Technologies (idtdna.com). PCR fragments were amplified using KOD Xtreme Hot-Start DNA polymerase (EMD Milipore). *E. coli* DH10B (NEB) electrocompetent cells were used for cloning. For plasmid construction, each fragment contained 20-30 bp overlapping sequences and were mixed at equimolar amounts. Plasmids were assembled using HIFI Assembly Master (NEB). Fragments

contained 20-30 bp overlaps and were mixed at equimolar amounts. Plasmids were verified by sequencing (Laragen, Culver City, CA). Genome edits were verified by colony PCR and sequencing (Laragen, Culver City, CA). Strain and plasmid lists can be found in Appendix I and Appendix II respectively.

4.2.3 CRISPR-Cas9 transformations

Linear donor DNA was constructed using SOE with 20 bp overlapping sequences. *cas9* was expressed on pCas9 and targeted to cut site by sgRNA containing 20 bp homology region and expressed on the pTarget plasmids. The removal of PAM sites was achieved by introducing a synonymous mutation to prevent further cutting. Recombination of the donor DNA was facilitated by expressing the lambda red recombinase on pCas9 under the arabinose promotor. Cultures were induced with 10 mM arabinose for ~3 hours prior to transformation. *E. coli* was made electrocompetent by washing twice with ice cold MQ water and twice with 10% glycerol. At least 100 ng pTarget and 500 ng donor DNA was transformed.

4.2.4 Growth curves and growth rate

Cultures were grown overnight in LB media and inoculated (1%) into preculture media (growth media supplemented with 0.05% cas amino acids). Precultures were harvested at OD_{600} ~0.8-1.0, centrifuged at 6000 rpm for 5 min to remove supernatant, and resuspended into growth media at a starting OD_{600} of 0.1. Specific growth rate was calculated by fitting logarithmic growth to exponential regression and obtaining the exponential growth constant, B.

4.2.5 Pck enzyme assay

Strains for the Pck assay were grown overnight in minimal glucose media plus 1% cas amino acids. Cells were lysed by Bugbuster (EMD Milipore) and concentrations were determined by Bradford assay. The Pck assay conditions were modified from a previously described coupled assay that measures NADH consumption at OD_{340}.[18] The assay conditions contained 100 mM Tris-HCl (pH 7.5), 5 mM $MgCl_2$, 0.4 mM NADH, 1 mM ADP, 50 mM $NaHCO_3$, 5 mM phosphoenolpyruvate, 1U malate dehydrogenase.

4.3 Results

4.3.1 ptsG transposon insertion was essential for NOG based growth

One of the most notable mutations in the evolved NOG strain was a transposon insertion in *ptsG*.[18] This mutation was first detected in the strain NOG6, which was isolated after the initial evolution on glucose plus acetate.[18] The *ptsG* enzyme was inserted with a ~1.4 kb sequence, effectively knocking out this enzyme. PtsG is a component of the glucose-specific phosphotransferase (PTS) system, a well described system for the uptake of various sugars in *E. coli*.[19] An overview of the phosphotransferase system is described in Figure 4-1.

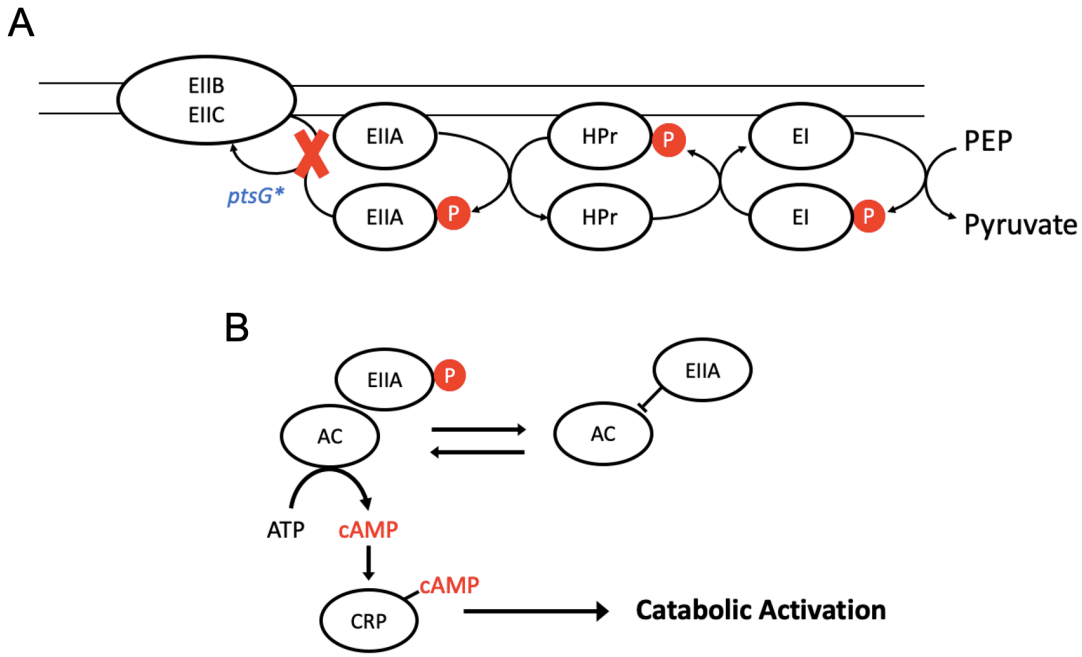

Figure 4-1: Overview of phosphotransferase (PTS) system in *E. coli*. The *ptsG* mutation likely disrupted the phosphate transfer from EIIA to PtsG domains EIIB and EIIC. When EIIA remains in the phosphorylated state, adenylate cyclase (AC) is activated to carry out the biosynthesis of cyclic-AMP (cAMP). cAMP forms a complex with the cAMP receptor protein (CRP) to activate many catabolic genes.

PtsG is the last enzyme in the chain, it receives a phosphate from EIIA (Crr) which it then uses it to phosphorylate glucose.[18] The phosphorylation state of EIIA is important for global regulation in *E. coli*. When EIIA is phosphorylated the biosynthesis of cyclic-AMP (cAMP) by adenylate cyclase is induced.[20] cyclic-AMP forms a complex with the cyclic-AMP receptor protein (CRP) to activate many catabolic genes.[21] Therefore, this mutation was predicted to be beneficial to the NOG growth schematic by increasing intracellular cAMP levels. Relative to the precursor strain, it was determined that the evolved NOG strain had higher cAMP levels and upregulated the transcription of catabolic genes such as *pdhR*, *fumA*, and *sdhA*.[18] However, the effect of this mutation on growth was not directly analyzed.

Thus, we evaluated the effect of fixing this mutation in NOG21. This was achieved in an NOG21 derivative containing plasmids removed, NOG22. While NOG26 had a faster growth rate than NOG21, occasional loss of phenotype was observed in this strain. Please see Appendix I and II for strain and plasmid lists.

In order to fix the *ptsG* mutation previously described pCas9/pTarget CRISPR-Cas9[16] was used to reconstruct the wild-type PtsG sequence in NOG22, by effectively knocking out the transposon insertion. To remove the protospacer, a synonymous mutation needed to be implemented in the *ptsG* sequence, but the amino acid sequence was unaffected. Following, the reconstitution of PtsG, the resulting strain was designated NOG32 and was transformed with pPL274* and pTW371 to test growth. Interesting, we found that NOG32/pPL274*/pTW371 had no growth phenotype at all in both glucose and glucose plus acetate media. To ensure that the observed loss of phenotype was due to the designed edit and not off-target effects, we knocked out the intact *ptsG* in NOG32. We observed that the growth phenotype in glucose media in NOG32Δ*ptsG*/pPL274*/pTW371 was restored to the original growth phenotype of NOG22/pPL274*/pTW371, verifying that the loss of phenotype was due to an intact PtsG and that this mutation was essential for NOG-based growth (Figure 4-2). Since the *ptsG* mutation was linked to an increased in intracellular cAMP in the evolved NOG strain, these results suggested the reorganization of global regulation was a significant factor for NOG-based growth.

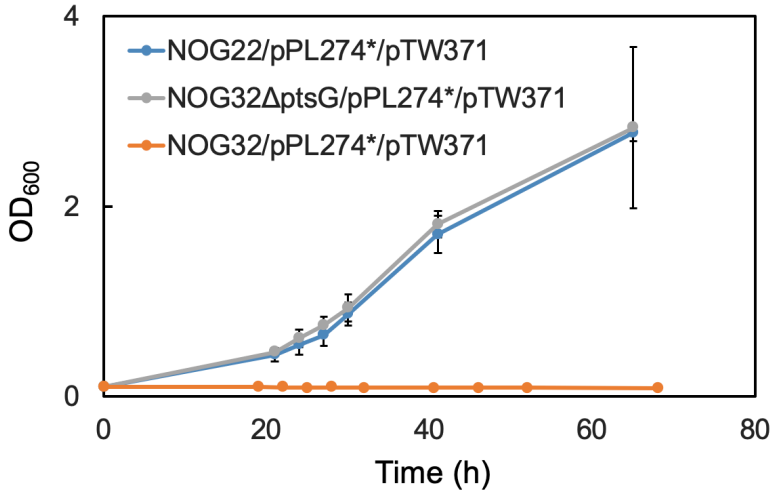

Figure 4-2: Growth curve in glucose minimal media of strains with *ptsG* transposon insertion fixed. The *ptsG* mutation was fixed in NOG22 to create NOG32. The growth phenotype of NOG32 on glucose media was completely abolished. Knocking out *ptsG* in NOG32 restored the growth on glucose, demonstrating loss of phenotype was due to the designed edit and not off target effects. All strains contained growth plasmids pPL274* and pTW371

4.3.2 rpoS transposon insertion contributes to NOG based growth

The next mutation evaluated in the evolved NOG strain was a transposon insertion in another gene, *rpoS*, which encodes the alternative sigma factor σ^S.[18] This mutation was observed following the development of growth on glucose media (i.e. in NOG21).[18] The mutation was not observed in some intermediate strains isolated during the evolution on glucose, indicating the mutation was expected to be beneficial but not essential. RpoS is involved in the control of the general stress response in E. coli.[22] Since *rpoS* was found to downregulate genes important for NOG growth, such as the components of the TCA cycle, it was expected the *rpoS* mutation should benefit NOG growth.[18,23,24] We restored RpoS in NOG22 again using the previously described pCas9/pTarget CRISPR-Cas9 system.[16] The resulting strain was termed NOG33. We tested growth of NOG33/pPL274*/pTW371 in glucose minimal media and found its growth rate was reduced to 82% of NOG22/pPL274*/pTW371 (Figure 4-3). This result suggested the *rpoS*

mutation contributes to the growth phenotype on glucose but was not indispensable for it, which was consistent with our initial expectations.

4.3.3 Fixing promotor truncation in edited pck construct increases growth rate

Pck is a key enzyme for NOG-based growth since it is used by to convert TCA cycle intermediates into essential precursors in lower glycolysis. Part of the rational design in constructing the initial evolution strain PHL13 was to upregulate Pck.[18] To this end, the endogenous *pck* promotor was replaced with P_L*lac*O_1 to avoid endogenous transcriptional repression by cAMP-CRP.[25] However, following evolution to establish robust growth on glucose plus acetate media, the designed promotor was found to have been truncated following evolution in glucose plus acetate media, reducing Pck activity in strain lysates.[18] It was predicted the this mutation occurred to balance gluconeogenic and TCA flux, since high Pck activity could drain TCA cycle intermediates and preclude acetyl-CoA condensation into the TCA cycle. The deleterious effect of strong Pck activity was predicted using Ensemble Modeling Robustness Analysis (EMRA), and it was assumed that the *pck* promotor truncation in the NOG strain helped to balance the relative activities *in vivo*.[18,26] However, the EMRA analysis also predicted that if GltA activity or rate of acetyl-CoA supply is too high, the robustness also decreases. A mutation was also observed that knocked down activity of Pta, which is responsible for the supply of acetyl-CoA, further demonstrating how the cell sought to adjust the relative activities of these pathways. These results suggested the interface of the TCA cycle and gluconeogenesis represents a key junction for NOG-based growth.

To evaluate how the *pck* mutation affects growth, we restored the *pck* promotor sequence in the evolved NOG21 strain using CRISPR-Cas9 to the original designed P_L*lac*O_1 sequence. Pck

activity in the resulting strain was increased about fivefold (Figure 4-3), indicating successful restoration of the Pck promotor. The resulting strain was designated NOG34. Interestingly, following plasmid retransformation, NOG34/pL274*/pTW371 had a growth rate about 15% faster than NOG22/pPL274*/pTW371 in glucose minimal media (Figure 4-3).

Though this was contrary to our prediction that increased Pck activity would be deleterious, we reasoned that a change in intracellular conditions following the development of robust NOG growth could make increased Pck beneficial. When the mutation occurred, the strain was adapting to grow on glucose plus acetate in conditions where acetate supply was intentionally limited.[18] It is plausible that acetate consumption was slow in this condition, resulting in a weak rate of acetyl-CoA supply. Thus, the strong Pck construct may have been deleterious initially since its competing pathway was slow. However, following the establishment of a robust NOG pathway in NOG21, it is likely the rate of acetyl-CoA supply increased since the cell was now degrading sugar to C2. Therefore, the strong Pck construct may be beneficial in NOG21 since its competing pathway was upregulated.

4.3.4 Test of pta overexpression in NOG22 and NOG34

The EMRA analysis of the TCA/GS for NOG-based growth reported balancing acetyl-CoA supply through Pta, and carbon flux out of the TCA cycle through Pck was necessary for robustness.[17] Mutations knocking down activity were detected in *pta* and the *pck* promotor during the initial evolution on glucose plus acetate media, suggested the strain sought to balance the activities of these enzymes. To evaluate how increased *pta* expression might affect growth in both NOG22 and NOG34, we cloned *pta* onto pTW371, creating pJD581. pJD581 was transformed into NO22/pPL274* and NOG34/pPL274*. We found that while growth rate in both

strains dropped relative to controls not overexpressing *pta* (i.e. strains containing pPL274* and pTW371), NOG22 had a more significantly reduced growth rate than NOG34. Specifically, the growth rate in NOG22/pPL274*/pJD581 dropped by 54% relative to NOG22/pPL274*/pTW371, while the growth rate in NOG34/pPL274*/pJD581 dropped only 27% relative to NOG34/ pPL274*/pTW371 (Figure 4-3). Moreover, the specific growth rate in NOG34/pPL274*/pJD581 was 50% higher than NOG22/pPL274*/pJD581, suggesting the increased Pck activity in this strain was better able to balance the Pta overexpression.

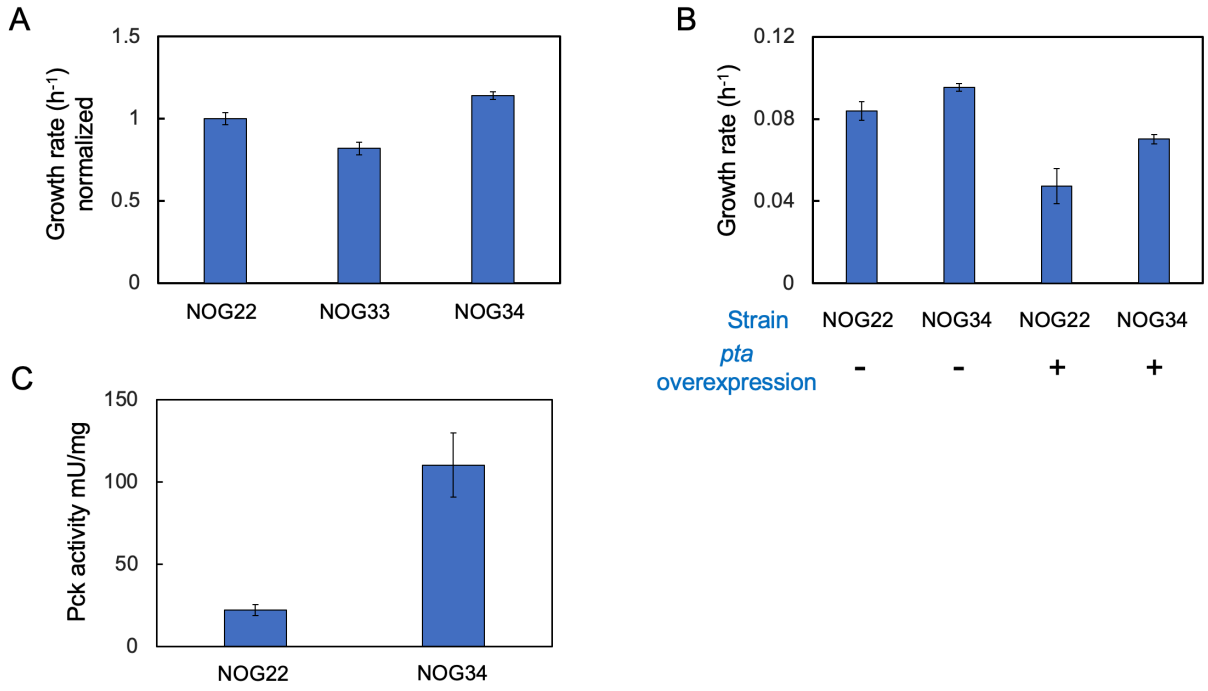

Figure 4-3: Growth characterization of mutations in NOG21 in glucose minimal media. (A) Growth rate of NOG33 (*rpoS* transposon insertion fixed) and NOG34 (*pck* promotor truncation fixed) normalized to NOG22 in glucose minimal media. All strains contained pPL274* and pTW371. (B) Growth rate of NOG22 vs. NOG34 with pPL274* and pTW371 or pPL274* and pJD581(pTW371 plus additional overexpression of *pta*) (C) Fixing promotor truncation of *pck* in NOG22 increased Pck activity in the lysate. NOG34 contained *pck* promotor truncation in NOG22 fixed.

4.3.5 Essentiality of plasmids for growth phenotype in NOG strain

NOG growth was developed by a combination of rational design and evolution.[18] While evolution was used to overcome global regulation, genes encoding for limiting enzymes in the core NOG cycle or other enzymes predicted to benefit NOG-based growth were expressed from plasmids. The isolated evolved NOG strains NOG21 and NOG26 contained two plasmids. The first, pPL274* contained an additional copy of phosphoketolase (*f/xpk)* from *Bifidobacterium adolescentis* to supplement the copy on the chromosome. However, this gene was found to be mutated and effectively knocked out by transposon insertion following evolution.[18] The plasmid pPL274* also contained highly active heterologous versions of NOG genes transaldolase (*tal*) and transketolase (*tkt2)* from *Klebsiella pneumonia* and *Methylomicrobium buryatense* respectfully; a phosphotransferase system (PTS) independent glucose uptake system consisting of the glucose facilitator gene from *Zymomonas mobilis* (*glf*) and the cytosolic glucokinase *(glk*) from *E. coli*; and finally a gene encoding an isozyme of NOG enzyme fructose-bisphosphotase that was not post-translationally inhibited by *(glpX*). The second plasmid, pTW371, contained additional copies of transketolase (*tkt1* and *tkt2*) from *M. buryatense*.

Here, we tested the essentiality of these plasmids for growth in NOG22. We compared growth in NOG22/pPL274*, NOG22/pTW371, and NOG22 to the positive control NOG22/pPL274*/pTW371 (Figure 4-4). NOG22/pPL274* initially grew at a similar rate to NOG22/pPL274*/pTW371, but its maximum OD_{600} was significantly less, only reaching about 1.8 relative to 2.5. This suggests the extra transketolases on pTW371 allow the strain to make better use of glucose by using it more efficiently, but there may be other limiting factors for growth rate besides efficient C2 formation. NOG22/pTW371 grew slightly slower than NOG22/pPL274*/pTW371, but was able to reach a similar optical density. These results

suggested there were genes on pPL274* that slightly benefit growth. NOG22 with no plasmids, however, grew much more slowly than all the other strains. Since NOG22/pTW371 grew much faster than NOG22, this suggested that overexpression of heterologous Tkt is extremely important for growth, since pTW371 contained no other genes and *tkt1* from *M. buryatense* was present on both plasmids. Thus, the strain with no plasmids was the only one with no heterologous *tkt* overexpression. This result is consistent with the prediction of the benefit to overexpressing Tkt in the pathway assay.[18]

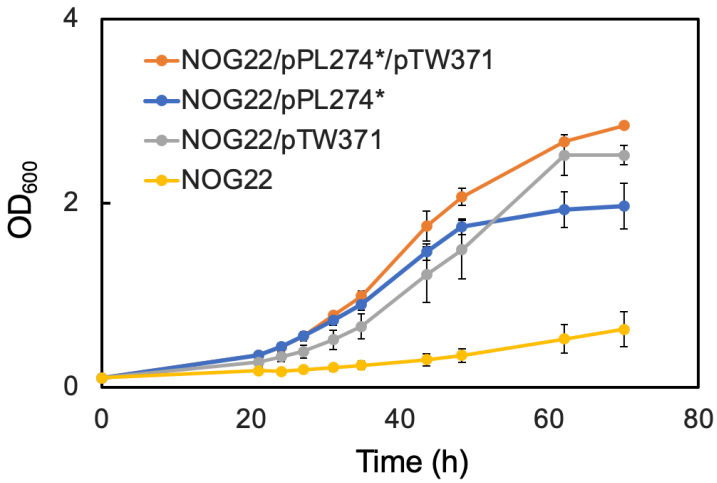

Figure 4-4: Growth curves of evolved NOG strain with growth plasmids removed in glucose minimal media. Removing pTW371 did not significantly affect growth rate initially but reduced the maximum OD_{600} that the strain could achieve. Removing pPL274* slightly reduced growth rate, but the strain ultimately reached a similar OD_{600} as the strain with both plasmids. Removing both plasmids significantly impaired the growth of NOG22. Since pTW371 only contains copies of *tkt*, this suggests Tkt overexpression gives the biggest contribution to the growth phenotype.

4.3.6 Mutation in pPL274 f/xpk during evolution was beneficial to growth

During the development of NOG based growth, a whole-pathway assay on the lysate of precursor strain NOG6 to identify potential enzymes in the NOG pathway whose activity was limiting for acetyl-phosphate (AcP) production *in vitro*. The assay determined that the activity of F/Xpk, which was originally expressed from an integrated copy on the chromosome, was limiting for AcP production.[18] To overcome this, a second copy of *f/xpk* from *Bifidobacterium adolescentis* was overexpressed on the plasmid pPL274. Following the transformation of pTW371, NOG-based growth on glucose was established. However, the evolution to improve growth on glucose, it was determined that the *f/xpk* on pPL274* had been mutated by transposon insertion.[18] Since Fpk activity is known to form a potential kinetic trap in NOG and other Fpk dependent pathways,[26,27] it was reasoned that strong Fpk could be deleterious for growth by causing decreased pathway robustness and the possible accumulation of NOG intermediates such as erythrose 4-phosphate.

To evaluate how the *f/pk* mutation on pPL274* affected grow, we transformed the original pPL274 and pTW371 into NOG22 and compared growth to NOG22/pPL274*/pTW371. NOG22/pPL274/pTW371 grew more slowly than NOG22/pPL274*/pTW371, confirming that the stronger F/Xpk construct was deleterious for growth (Figure 4-5). Previous EMRA predictions also suggested downregulating Tkt activity decreases robustness for NOG.[26] The combination of Tal and Tkt also directly competes with Fpk for F6P in NOG. Following the overexpression of *f/xpk* on pPL274, Tkt was found to be the most limiting NOG enzyme for *in vitro* AcP production in the pathway assay, possibly by balancing the stronger Fpk.[18] Therefore, to evaluate how Tkt could balance Fpk *in vivo*, we compared the relative effect of pTW371 for growth in NOG22/pPL274 and NOG22/pPL274* (Figure 4-6). pTW371 was found to have a

much stronger contribution to growth in NOG22/pPL274. Relative to NOG22/pPL274*/pTW371, NOG22/274* grew at a similar rate but did not reach the same maximum OD_{600}. On the other hand, NOG22/pPL274 barely grew at all relative to NOG22/pPL274/pTW371. This suggests the Fpk kinetic trap may have been much stronger using pPL274 relative to pPL274*, and the extra copies of *tkt* on pTW371 could help balance the intact *f/xpk* construct on pPL274. The need to balance this kinetic trap may explain why pTW371 was need for the initial establishment of growth.

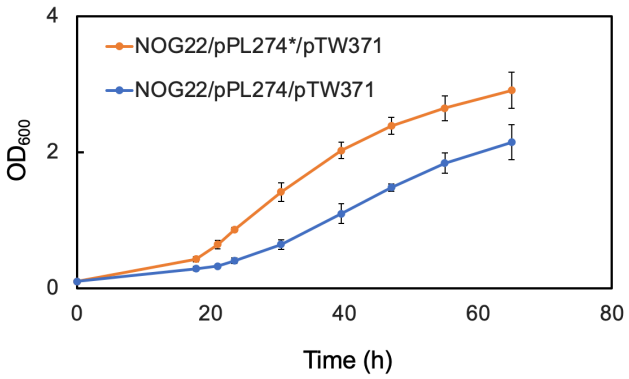

Figure 4-5: Growth curves of NOG22/pPL274*/pTW371 and NOG22/pPL274/pTW371 in minimal glucose media. The strain with the originally designed pPL274 containing intact *f/xpk* grew slower than the strain with the evolved pPL274*. This suggested a kinetic trap caused by strong Fpk was deleterious for growth.

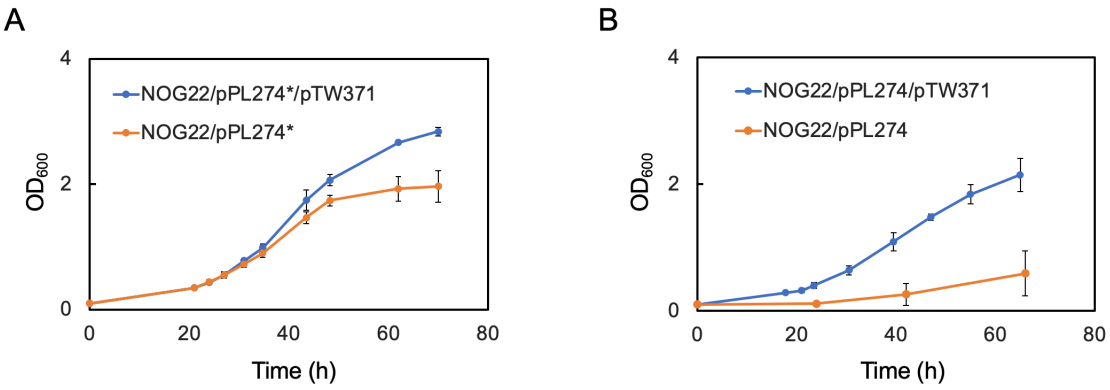

Figure 4-6: Growth curves of NOG22/pPL274* and NOG22/pPL274* with and without pTW371 in glucose minimal media. (A) Removing pTW371 from NOG22/pPL274*/pTW371 reduced maximum OD_{600} but did not significantly reduce the rate of growth. (B) Removing pTW371 from NOG22/PL274/pTW371 had a much more significant deleterious effect on growth, as NOG22/pPL274 barely grew. Since pPL274 has an intact *f/xpk*, these results suggest the extra copies of transketolase on pTW371 balance the extra Fpk activity, providing further evidence of the Fpk kinetic trap in NOG.

4.4 Discussion and conclusions

The effect of several mutations and plasmids for growth in the evolved NOG strain was determined using CRISPR-Cas9 for genome editing in the evolved NOG strain. Overall, the results are consistent with previous predictions.[18] The transposon insertion in *ptsG,* which likely inactivated the gene, was found to be essential for NOG-based growth, presumably due to the upregulation of cAMP biosynthesis that affected global regulation in the strain. Likewise, the mutation inactivating alternative sigma factor *rpoS,* also contributed to NOG based growth but was not essential. This was expected since RpoS downregulates components of the TCA cycle and glyoxylate shunt.[18] Other mutations involved in kinetic traps in NOG were evaluated. The balance between gluconeogenic flux (controlled by Pck) and TCA cycle flux (controlled by GltA and acetyl-CoA supply through Pta) was predicted to be important for robust NOG growth.[18] Following glucose plus acetate evolution, mutations were observed in both *pck* (promotor

truncation) and *pta* (point mutation) that knocked down activities of their respective proteins, demonstrating the cell trying to balance these pathways.[18] While restoring the *pck* promotor to the original designed sequence actually improved growth in the evolved NOG strain, changing intracellular conditions caused by the adaptation to NOG likely increased flux to acetyl-CoA, causing increased Pck activity to become advantageous for growth.

Likewise, the original pPL274 plasmid containing an intact second copy of *f/xpk*, was also deleterious for growth, suggesting an Fpk kinetic trap in NOG. Since pTW371 had a much stronger contribution to growth when pPL274 was used, it appeared that Tkt activity was important in balancing Fpk. Although evolution tuned the relative expression of these enzymes to the working range, it is unlikely they are fully optimized. Therefore, to improve the growth rate on NOG, high throughput genome editing tools can be applied to affect the relative expression of genes involved in these kinetic traps. Libraries of diverse mutants could be screened for improved growth on glucose media by picking fast growing colonies. Since restoring the *pck* promotor increased the growth rate of the resulting strain, there appears to be potential that further improvement of growth can be achieved by the large-scale manipulation of these constructs. Genetic techniques such as Multiplex Automated Genome Engineering (MAGE)[28] and CRISPR-Cas9 have previously been used to create large strain libraries for the improvement of phenotypes in *E. coli*.[29-31] Such strategies could be used to target the ribosome binding site (RBS) and coding region of *pck, gltA,* and *pta* to vary relative expression strength of these genes.

Additionally, to better allow the evolved NOG strain to become a host for chemical production, it would be advantageous to eliminate the need for plasmids for growth. Therefore, the genes on pPL274* (besides *tkt*) that contribute to growth should be determined. These genes could then be

integrated, and the resulting strain could be evolved to establish robust growth without plasmids. Although NOG22 has a weak growth phenotype and may be evolvable without integration, it may be difficult to sufficiently upregulate *tkt* expression from the chromosome. Also, since Tkt1 and Tkt2 were selected for improved substrate affinity[18] it is possible these versions are superior to *E. coli* transketolase for NOG dependent growth.

4.5 Appendices

4.5.1 Strain list

Strain	Genotype	Comments	Reference
BW25113	*rrnB*$_{T14}$ Δ*lacZ*$_{w116}$*hsdR514* Δ*araBAD*$_{AH33}$ Δ*rhaBAD*$_{LD78}$	Wild Type	
JCL16	BW25113/F'[*tra*D36 *proAB*$^{+}$ lacI^{q}ZΔM15(Tet^{r})]	Wild Type	
PHL13	JCL16 Δ*gapA::FRT* Δ*mgsA::FRT* Δ(*pgk gapB*)*::FRT* Δ*pfkA::FRT* Δ*iclR::FRT* Δ*poxB::cat* Δ*zwf::FRT* Δ(*edd eda*)*::(*P$_{L}$*lacO*$_{1}$*::f/xpk*$_{BA}$) ΔP$_{pck}$::P$_{L}$*lacO*$_{1}$	Precursor to NOG strain that cannot grow on glucose	Lin, P.P. *et. al*[18]
NOG21	Evolved from PHL13	PHL13 following evolution for glucose growth using NOG	Lin, P.P. *et. al*[18]
NOG22	NOG21 with growth plasmids removed	Retains NOG21 phenotype	This Study
NOG32	NOG22 with fixed *ptsG* mutation	No growth on glucose media	This Study
NOG33	NOG22 with fixed *rpoS* mutation	Weaker growth on glucose media relative to NOG22	This Study
NOG34	NOG22 with *pck* promotor truncation fixed	Stronger growth on glucose media relative to NOG22	This Study

4.5.2 Plasmid list

Plasmid	Description	Reference
pPL274	P$_{L}$*lacO*$_{1}$*::f/xpk*$_{BA}$ *glf*$_{ZM}$ *glk*$_{EC}$ tkt2$_{MB}$ *tal*$_{KP}$ *glpX*$_{EC}$ ColE *ori* Carb^{r}	Lin, PP et. al
pPL274*	P$_{L}$*lacO*$_{1}$*::f/xpk*$_{BA}$ (mutated by transposon insertion) *glf*$_{ZM}$ *glk*$_{EC}$ tkt2$_{MB}$ *tal*$_{KP}$ *glpX*$_{EC}$ ColE *ori* Carb^{r}	Lin, PP et. al
pTW371	P$_{L}$*lacO*$_{1}$*:: tkt2*$_{MB}$ *tkt1*$_{MB}$ CloDF13 *ori* Spec^{r}	Lin, PP et. al
pJD581	P$_{L}$*lacO*$_{1}$*:: tkt2*$_{MB}$ *tkt1*$_{MB}$ *pta*$_{EC}$ CloDF13 *ori* Spec^{r}	This Study

4.6 References

1. Doudna, J. A., & Charpentier, E. (2014). The new frontier of genome engineering with CRISPR-Cas9. *Science*, *346*(6213).

2. Ishino, Y., Shinagawa, H., Makino, K., Amemura, M., & Nakata, A. (1987). Nucleotide sequence of the iap gene, responsible for alkaline phosphatase isozyme conversion in Escherichia coli, and identification of the gene product. *Journal of bacteriology*, *169*(12), 5429-5433.

3. Mojica, F. J., Díez-Villaseñor, C., Soria, E., & Juez, G. (2000). Biological significance of a family of regularly spaced repeats in the genomes of Archaea, Bacteria and mitochondria. *Molecular microbiology*, *36*(1), 244-246.

4. Nelson, K. E., Clayton, R. A., Gill, S. R., Gwinn, M. L., Dodson, R. J., Haft, D. H., ... & Fraser, C. M. (1999). Evidence for lateral gene transfer between Archaea and bacteria from genome sequence of Thermotoga maritima. *Nature*, *399*(6734), 323-329.

5. Makarova, K. S., Grishin, N. V., Shabalina, S. A., Wolf, Y. I., & Koonin, E. V. (2006). A putative RNA-interference-based immune system in prokaryotes: computational analysis of the predicted enzymatic machinery, functional analogies with eukaryotic RNAi, and hypothetical mechanisms of action. *Biology direct*, *1*(1), 7.

6. Mojica, F. J., García-Martínez, J., & Soria, E. (2005). Intervening sequences of regularly spaced prokaryotic repeats derive from foreign genetic elements. *Journal of molecular evolution*, *60*(2), 174-182.

7. Jansen, R., Embden, J. D. V., Gaastra, W., & Schouls, L. M. (2002). Identification of genes that are associated with DNA repeats in prokaryotes. *Molecular microbiology*, *43*(6), 1565-1575.

8. Barrangou, R., Fremaux, C., Deveau, H., Richards, M., Boyaval, P., Moineau, S., ... & Horvath, P. (2007). CRISPR provides acquired resistance against viruses in prokaryotes. *Science*, *315*(5819), 1709-1712.

9. Deltcheva, E., Chylinski, K., Sharma, C. M., Gonzales, K., Chao, Y., Pirzada, Z. A., ... & Charpentier, E. (2011). CRISPR RNA maturation by trans-encoded small RNA and host factor RNase III. *Nature*, *471*(7340), 602-607.

10. Cencic, R., Miura, H., Malina, A., Robert, F., Ethier, S., Schmeing, T. M., ... & Pelletier, J. (2014). Protospacer adjacent motif (PAM)-distal sequences engage CRISPR Cas9 DNA target cleavage. *PloS one*, *9*(10), e109213.

11. Jinek, M., Chylinski, K., Fonfara, I., Hauer, M., Doudna, J. A., & Charpentier, E. (2012). A programmable dual-RNA–guided DNA endonuclease in adaptive bacterial immunity. *Science*, *337*(6096), 816-821.

12. Cong, L., Ran, F. A., Cox, D., Lin, S., Barretto, R., Habib, N., ... & Zhang, F. (2013). Multiplex genome engineering using CRISPR/Cas systems. *Science*, *339*(6121), 819-823.

13. Mali, P., Yang, L., Esvelt, K. M., Aach, J., Guell, M., DiCarlo, J. E., ... & Church, G. M. (2013). RNA-guided human genome engineering via Cas9. *Science*, *339*(6121), 823-826.

14. DiCarlo, J. E., Norville, J. E., Mali, P., Rios, X., Aach, J., & Church, G. M. (2013). Genome engineering in Saccharomyces cerevisiae using CRISPR-Cas systems. *Nucleic acids research*, *41*(7), 4336-4343.

15. Jiang, W., Zhou, H., Bi, H., Fromm, M., Yang, B., & Weeks, D. P. (2013). Demonstration of CRISPR/Cas9/sgRNA-mediated targeted gene modification in Arabidopsis, tobacco, sorghum and rice. *Nucleic acids research*, *41*(20), e188-e188.

16. Jiang, Y., Chen, B., Duan, C., Sun, B., Yang, J., & Yang, S. (2015). Multigene editing in the Escherichia coli genome via the CRISPR-Cas9 system. *Applied and environmental microbiology*, *81*(7), 2506-2514.

17. Bogorad, I. W., Lin, T. S., & Liao, J. C. (2013). Synthetic non-oxidative glycolysis enables complete carbon conservation. *Nature*, *502*(7473), 693-697.

18. Lin, P. P., Jaeger, A. J., Wu, T. Y., Xu, S. C., Lee, A. S., Gao, F., ... & Liao, J. C. (2018). Construction and evolution of an Escherichia coli strain relying on nonoxidative glycolysis for sugar catabolism. *Proceedings of the National Academy of Sciences*, *115*(14), 3538-3546.

19. Deutscher, J., Francke, C., & Postma, P. W. (2006). How phosphotransferase system-related protein phosphorylation regulates carbohydrate metabolism in bacteria. *Microbiology and molecular biology reviews*, *70*(4), 939-1031.

20. Steinsiek, S., & Bettenbrock, K. (2012). Glucose transport in Escherichia coli mutant strains with defects in sugar transport systems. *Journal of bacteriology*, *194*(21), 5897-5908.

21. De Crombrugghe, B., Busby, S., & Buc, H. (1984). Cyclic AMP receptor protein: role in transcription activation. *Science*, *224*(4651), 831-838.

22. Hengge-Aronis, R. (1996). Back to log phase: σS as a global regulator in the osmotic control of gene expression in Escherichia coli. *Molecular microbiology*, *21*(5), 887-893.

23. Dong, T., & Schellhorn, H. E. (2009). Control of RpoS in global gene expression of Escherichia coli in minimal media. *Molecular Genetics and Genomics*, *281*(1), 19-33.

24. Battesti, A., Majdalani, N., & Gottesman, S. (2011). The RpoS-mediated general stress response in Escherichia coli. *Annual review of microbiology*, *65*, 189-213.

25. Nakano, M., Ogasawara, H., Shimada, T., Yamamoto, K., & Ishihama, A. (2014). Involvement of cAMP-CRP in transcription activation and repression of the pck gene encoding PEP carboxykinase, the key enzyme of gluconeogenesis. *FEMS microbiology letters*, *355*(2), 93-99.

26. Lee, Y., Rivera, J. G. L., & Liao, J. C. (2014). Ensemble Modeling for Robustness Analysis in engineering non-native metabolic pathways. *Metabolic engineering*, *25*, 63-71.

27. Bogorad, I. W., Chen, C. T., Theisen, M. K., Wu, T. Y., Schlenz, A. R., Lam, A. T., & Liao, J. C. (2014). Building carbon–carbon bonds using a biocatalytic methanol condensation cycle. *Proceedings of the National Academy of Sciences*, *111*(45), 15928-15933.

28. Wang, H. H., Isaacs, F. J., Carr, P. A., Sun, Z. Z., Xu, G., Forest, C. R., & Church, G. M. (2009). Programming cells by multiplex genome engineering and accelerated evolution. *Nature*, *460*(7257), 894-898.

29. Wang, H. H., Kim, H., Cong, L., Jeong, J., Bang, D., & Church, G. M. (2012). Genome-scale promoter engineering by coselection MAGE. *Nature methods*, *9*(6), 591-593.

30. Zhu, X., Zhao, D., Qiu, H., Fan, F., Man, S., Bi, C., & Zhang, X. (2017). The CRISPR/Cas9-facilitated multiplex pathway optimization (CFPO) technique and its application to improve the Escherichia coli xylose utilization pathway. *Metabolic engineering*, *43*, 37-45.

31. Liang, L., Liu, R., Garst, A. D., Lee, T., Beckham, G. T., & Gill, R. T. (2017). CRISPR EnAbled Trackable genome Engineering for isopropanol production in Escherichia coli. *Metabolic engineering*, *41*, 1-10.

5 Production of ethanol, a reduced liquid fuel in an NOG-dependent strain using external electron supply

The use of petroleum as transportation fuel is a leading contributor to atmospheric CO_2 levels and climate change. Microbially-produced liquid fuels (i.e. biofuels) are promising alternatives to petroleum but their economic competitiveness is often limited by high feedstock costs. This problem is exacerbated by the inherent carbon loss in endogenous metabolic pathways that microbes use to produce two-carbon (C2) metabolites, which are precursors to important biofuels such as ethanol and butanol. To generate C2, the three-carbon (C3) metabolite pyruvate is decarboxylated, releasing one third of input carbon as CO_2, effectively capping the maximum carbon yield of C2-derived biofuels to 67%. The recent design of a synthetic non-oxidative glycolysis (NOG), which bypasses C3 production to directly generate C2 equivalents at stoichiometric yields, could improve the theoretical yield of C2-derived biofuel to 100%. Here, we sought to engineer a previously constructed NOG-dependent strain for ethanol production using the NOG pathway. By supplying external reducing power in the form of formate, we were able improve molar ethanol yields on glucose in anaerobic conditions from 0.26 to 0.82, validating reductive fermentation can be used for ethanol production in NOG. Further improvement of ethanol yields appears to limited by the supply of ATP, which could be overcome by incorporating respiration under microaerobic conditions.

5.1 Introduction

Climate change represents a major threat to society and is caused in large part due to carbon emissions from the burning of fossil fuels.[1,2] Recently, atmospheric concentrations of greenhouse gas CO_2 have risen beyond 400 ppm for the first time in humanity's existence, and

continues to rise drastically.[3] In addition, the extraction of fossil fuels can also be damaging to the environment through processes such as hydraulic fracking.[4] Therefore, it is of great importance to develop sustainable alternative technologies to fossil fuels. Liquid fuels obtained from renewable feedstocks, commonly known as biofuels, are promising alternatives since they reduce dependence on petroleum and reduce harmful carbon emissions.[5,6] Microbial hosts such as *E. coli* and yeast have applied for the production of a wide range of biofuels, including ethanol,[7] butanol[8-10] and isobutanol.[11-12] Ethanol is the most widely produced biofuel worldwide, but advanced biofuels like isobutanol and butanol have higher energy density and are compatible current infrastructure that is designed for petroleum-based fuels.[13,14]

However, despite incentives designed to enhance their usage as transportation fuel, biofuels still struggle to compete economically with petroleum. For most biofuel processes, high feedstock costs represent one of the most significant economic constraints on process profitability.[15,16] A major contributing factor to this problem is the inherent carbon-inefficiency with which endogenous microbial metabolism produces biofuels derived from two-carbon (C2) metabolites, including ethanol and butanol. Essentially all organisms initially degrade carbohydrates into pyruvate, a three-carbon (C3) metabolite using a variation of the conserved glycolytic pathways, such as the Embden-Meyerhof-Parnas (EMP) or Entner-Doudoroff (ED) pathway.[17] Pyruvate is then decarboxylated to generate one mol of CO_2 and one mol of C2 precursor. This loss of carbon effectively turns one-third of the feedstock into wasted material, not only imposing a significant economic constraint but also increasing the emissions of harmful CO_2. While no native pathway exists that bypasses C3 formation to generate C2, a synthetic non-oxidative glycolysis (NOG) pathway was devised and shown to directly degrade sugar into C2 equivalents at 100% yield *in vivo* and *in vitro* without the generation or consumption of reducing

equivalents.[18] The development of NOG generated considerable excitement, as it opened the door for C2-derived products to be produced at 100% yield while eliminating CO_2 emission. Recently, an *E. coli* strain with its native glycolytic pathways deleted was adapted to grow on NOG using a combination of evolution and rational design.[19] The resulting NOG strain has a distinct metabolic profile, as it generates C2 metabolites before generating C3 metabolites, and is a promising host for the production of ethanol and butanol using NOG. Here, we sought to engineer this previously developed NOG strain for ethanol production using the NOG pathway. Although NOG can potentially allow the production of C2-derived biofuel at 100% yield, there are also NOG-specific challenges that need to be addressed. Firstly, NOG does not generate the necessary reducing equivalents to reduce C2 precursors to alcohol. Therefore, electrons must be supplied externally to obtain the necessary reducing equivalents to produce ethanol. NOG-based ethanol production is shown in Figure 5-1.

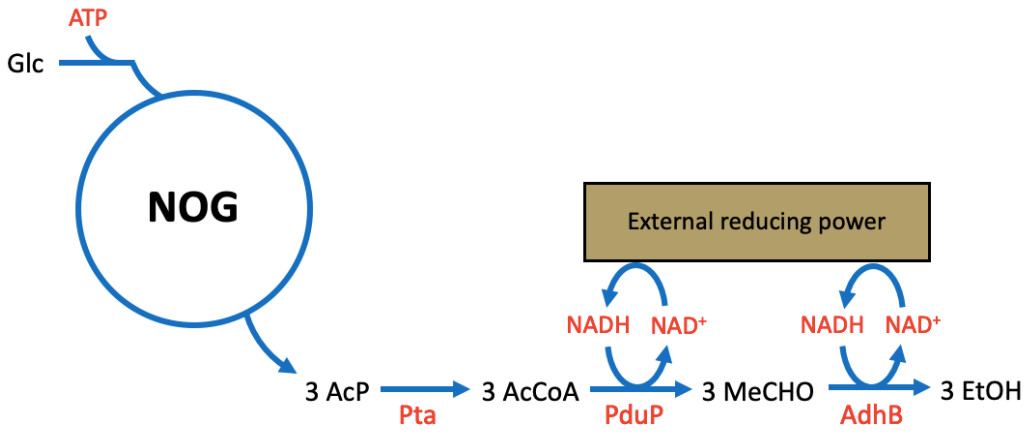

Figure 5-1: Overview of NOG-based ethanol production using reductive fermentation. External reducing power can be obtained from hydrogen or formate, both of which can be generated from renewable resources.

An external supply of reducing power can be achieved by feeding formate or hydrogen to cells expressing formate dehydrogenase (Fdh) or hydrogenase. Versions of these enzymes that are soluble, oxygen-tolerant, and NADH-dependent have already been successfully expressed in *E. coli*.[20-21] Both formate and hydrogen can be generated renewably using electricity from the reduction of CO_2 and electrolysis of water respectively.[22-24]

In addition to the external supply of reducing power, another challenge in NOG-based alcohol production is the inherent ATP deficit. The net reaction for the production of 100% ethanol using NOG is shown in Equation 5.1:

$$\text{Glucose} + 1\ \text{ATP} + 6\ \text{NADH} \rightarrow 3\ \text{Ethanol} + 1\ \text{ADP} + 6\ \text{NAD}^+ \qquad \textbf{5.1}$$

In addition to the 6 mol of NADH required to reduce glucose Equation 5.1 shows one mol of ATP is required for each mol of glucose consumed for 100% ethanol yield. In NOG, acetate production from AcP can supply ATP under anaerobic conditions, but since this comes at the expense of ethanol production, theoretical yields of ethanol would ultimately require another ATP source. This can be achieved supplying excess reducing power, which can be converted to ATP using endogenous respiratory pathways in the presence of electron acceptors such as oxygen.[25]

In the following, we sought to apply the previously developed NOG strain[19] for ethanol production under reductive conditions, using formate as the electron donor. Initially, we sought to carry out production anaerobically while relying on acetate production for ATP, to establish ethanol production without competing with respiration. Characterization of the production in NOG strains expressing Fdh found a positive correlation between formate consumption and

ethanol yields, verifying that reductive fermentation can be applied for ethanol production in the NOG strain. Increasing formate consumption was also linked to reduced acetate yields. Eventually, when formate consumption became too high, cells were no longer able to uptake sugar, suggesting an ATP limitation precluded further improve ethanol production. We attempted to overcome ATP limitation by feeding G6P, bypassing the ATP requirement for sugar phosphorylation. However, ethanol yields dropped significantly on G6P media due to apparent limited flux through the ethanol pathway and/or presence of alternative electron sinks. Additionally, we observed increasing formate consumption may also lead to a loss of robustness in the NOG pathway due to an observed drop in overall C2 yields when formate consumption was highest, possibly due to reductive stress. To further increase ethanol yields in glucose media, the production must be integrated with respiration, which can supply ATP through the additional input of reducing equivalents. Respiration could also act as a potential purge for NAD(P)H if conditions within the cell become too reductive.

5.2 Materials and Methods

5.2.1 Medium and cultivation

All *E. coli* strains were cultured by rotary shaking (250 rpm, New Brunswick Scientific) at 37 degrees. All media ingredients were purchased through Fisher Scientific unless otherwise noted. Production media contained 50 mM glucose or Glucose 6-Phospahte (Sigma Aldrich), 1x m9 salts, 0.2 mM $CaCl_2$, 2 mM $MgSO_4$, (Sigma Aldrich), 100 mM MOPS buffer, and vitamin mix (0.02 g/L pyridoxamine dihydrochloride (Sigma Aldrich), 4-aminobenzoic acid (Sigma Aldrich), 0.002 g/L biotin, 0.002 g/L B12 and 0.01 g/L thiamin). Production media was titrated to ~pH 7 using NaOH. Sodium formate or sodium nitrate was added as required to the production media.

5.2.2 Strains and plasmids

The evolved NOG strain, pPL274* and pTW371 were obtained from Lin, P.P. *et. al*[19]. All primers for the construction of ethanol production plasmids were purchased through Integrated DNA Technologies (idtdna.com). PCR fragments were amplified using KOD Xtreme Hot-Start DNA polymerase (EMD Milipore). *E. coli* DH10B (NEB) electrocompetent cells were used for cloning. For plasmid construction, each fragment contained 20-30 bp overlapping sequences and were mixed at equimolar amounts. Plasmids were assembled using HIFI Assembly Master (NEB). Fragments contained 20-30 bp overlaps and were mixed at equimolar amounts. Plasmids were verified by sequencing (Laragen, Culver City, CA). See Appendix II for plasmid list.

5.2.3 Anaerobic ethanol production

Strains were prepared for fermentation by cultivation in LB plus glucose media as previously described.[19] Cell culture was induced with 1 mM IPTG (Zymo scientific) at OD_{600} 0.7-1.0 for 14-17 hr. Induced cultures were centrifuged and washed once with production media containing no carbon source before resuspension in production media anaerobically to $OD_{600} \sim 20$. Intermediate time points were taken anaerobically, and final time points were taken between 20-24 hr.

5.2.4 Quantification of samples from ethanol production

Samples were analyzed using gas chromatography with flame ionization detection (Agilent) or HPLC (Thermo Scientific VWD and Refractomax detectors). The HPX-87H column (BioRad) was used for HPLC analysis.

5.2.5 Whole pathway assay

To identify limiting enzymes for ethanol production a similar whole-pathway was used as was described previously.[19] Cells for the assay were obtained by recovering cell pellet from production time point 4 hr into packed cell production. Cell lysates were obtained by Bugbuster and protein concentrations were measured by Bradford assay. The assay mixture contained 50 mM phosphate buffer (pH7.5), 5 mM $MgCl_2$, 0.2 mM NAD^+, 0.2 mM CoA, 25 mM AcP, and 50 mM formate. 40 ug strain lysate was used, which was supplemented with 10 ug of purified enzymes to establish a positive control. In this assay, formate was oxidized by Fdh, generating the NADH necessary to reduce AcP to ethanol, and the effect of removing individual purified enzymes on ethanol production was evaluated. The reaction was incubated at 37 degrees. Ethanol was detected on GC-FID (Agilent).

5.2.6 PduP assay

PduP activity was calculated by coupled assay measuring *in vitro* NADH consumption at OD_{340}.[26] The extinction coefficient for NADH was (6220 M^{-1} cm^{-1}). Cells for the assay were obtained by recovering cell pellet from production time point 4 hr into packed cell production. Cell lysates were obtained by Bugbuster and protein concentrations were measured by Bradford assay. The reaction mixture contained 20 mM ACP, 0.5 mM NADH, 0.5 mM CoA, 5 mM $MgCl_2$, >1U Pta, >1U Adh, and 40 μg strain lysate.

5.2.7 Fdh assay

Fdh activity was calculated by coupled assay measuring *in vitro* NADH production at OD_{340}.[27] The extinction coefficient for NADH was (6220 M^{-1} cm^{-1}). Cells for the assay were obtained by

recovering cell pellet from production time point 4 hr into packed cell production. Cell lysates were obtained by Bugbuster and protein concentrations were measured by Bradford assay. The reaction mixture contained 0.5 mM NAD^+, 50 mM formate and 40 μg strain lysate.

5.2.8 Glucose 6-phosphate quantification

Concentrations of glucose 6-phosphate (G6P) were determined using the Glucose 6-Phosphate Assay Kit (Abcam). G6P was quantified according to the manufacturers' instructions.

5.2.9 Metabolite extraction and analysis

Metabolites were extracted similar to as previously.[28] Metabolites were extracted from approximately 10^9 cells. Samples were run on LC-MS and analyzed with Tracefinder. LC-MS operation and sample analysis was performed by the UCLA Metabolomics center at (Los Angeles, CA)

5.2.10 CRISPR Cas9 for gene knockout

CRISPR-Cas9 knockout of SrlD was carried out using an adapted protocol for CRISPR-Cas9 in *E. coli*.[29] Linear donor DNA was constructed using SOE with 20 bp overlapping sequences. Cas9 was expressed on pCas9 and targeted to cut site by sgRNA containing 20 bp homology region and expressed on the pTarget plasmids. The removal of PAM by placing the PAM inside the deleted *srlD* gene. Recombination of the donor DNA was facilitated by expressing the lambda red recombinase on pCas9 under the arabinose promotor. Cultures were induced with 10 mM arabinose for ~3 hours prior to transformation. *E. coli* was made electrocompetent by washing

twice with ice cold MQ water and twice with 10% glycerol. At least 100 ng pTarget and 500 ng donor DNA was transformed. Positive clone was verified by colony PCR and sequencing

5.3 Results

5.3.1 Overexpression of ethanol pathway

To demonstrate ethanol production in the NOG strain using reductive fermentation, formate was chosen over hydrogen as the electron donor due to its high solubility. The production of ethanol from the output of NOG, acetyl-phosphate (AcP), using formate as the electron donor can be achieved using a three-enzyme pathway. Phosphotransacetylase (Pta), which is a component of NOG-based growth, converts AcP to acetyl-CoA; propionyl-CoA dehydrogenase (PduP), reduces acetyl-CoA to acetaldehyde using NADH as the electron donor; and alcohol dehydrogenase (Adh), which reduces acetaldehyde into ethanol. A fourth enzyme, formate dehydrogenase (Fdh) is used to supply the NADH from formate oxidation. While *E. coli* already contains versions of all the enzymes, its Fdh isozymes do not use NADH as a cofactor, and its primary acetyl-CoA reducing enzyme, AdhE, is transcriptionally repressed and allosterically inhibited in aerobic conditions,[30] under which NOG-based ethanol production may potentially need to be carried out due to the requirement of respiration. Therefore, heterologous versions of *fdh*, *pduP*, and *adh* were all further expressed in the NOG strain to support ethanol production. Since *pta* overexpression is predicted to form a kinetic trap that is detrimental to NOG-growth,[19] we did not initially plan to alter the expression of this gene in the NOG strain.

An NADH dependent Fdh from Candida boidnii is well characterized and previously expressed in *E. coli*, so this gene was chosen to supply the Fdh enzyme.[21] While ethanol is generally produced via pyruvate decarboxylation rather than direct reduction of acetyl-CoA reduction, a study prospected oxygen-tolerant CoA reducing enzymes (PduP) for their activity on acetyl-CoA

and other CoA molecules.[31] PduP from *Salmonella enterica* was found to be among the best to reduce acetyl-CoA, and support high ethanol titers *in vivo* using cyanobacteria.[31] Finally, AdhB from *Zymomonas mobilis,* which is typically used to reduce acetaldehyde in ethanol production.[7] The genes *fdh, pduP*, & *adhB* were cloned onto a separate plasmid backbone from pPL274* & pTW371 containing a p15A origin, creating plasmid pJD403. This origin was reported to be compatible with pPL274* (ColE) and pTW371 (CloDF13), theoretically making it to use in a three-plasmid system with the growth plasmids.[32] This plasmid was then transformed directly into NOG21, the previously reported evolved NOG strain,[19] yielding NOG21/pPL274*/pTW371/pJD403. The NOG strain used plasmids pPL274* and pTW371 for growth. See Appendix I and Appendix II for complete strain and plasmid lists.

We tested the capability of NOG21/pPL274*/pTW371/pJD403 to produce ethanol in anaerobic conditions. While ethanol production will ultimately require microaerobic conditions to achieve theoretical yields, oxygen competes with the ethanol pathway for NADH and could lead to excess carbon oxidation in the TCA cycle. Therefore, we planned to initially establish ethanol production in anaerobic conditions to validate reductive fermentation can be used to produce ethanol, relying on acetate production for ATP, before incorporating respiration. We tested production in media containing with 50 mM formate and 50 mM glucose. We found that the resulting strain did not consume formate during anaerobic production. Following the failure to observe significant formate consumption in this strain, we considered that poor expression of some or all ethanol pathway enzymes may be the cause. In order to evaluate potentially limiting enzymes in the ethanol pathway, a pathway assay similar to as previously described was used.[19]

An overview of the pathway assay for ethanol production is shown in Figure 5-2. AcP, the output of NOG, was the input, and formate was supplied as the source reducing power. Ethanol was quantified on GC.

NOG21/pPL274*/pTW371/pJD403 lysates were supplemented with purified Pta (*E. coli*), Fdh, (*C. boidnii*), PduP (*S. enterica*), and Adh (*S. cerevisiae*), and the effect of removing individual enzymes from the protein mix was observed. The results, shown in Figure 5-2 demonstrated that measurable quantities of ethanol were dependent on the addition purified PduP, while removing purified Fdh resulting in barely quantifiable amounts of ethanol. This indicated these enzymes were not significantly present in the lysate to sustain the *in vitro* production of ethanol. Therefore, it appeared that the third plasmid backbone did not represent an effective expression construct for the ethanol production genes. While significant ethanol productivity was observed in the case where purified Adh was removed, *E. coli* already contains a significant number of endogenous alcohol dehydrogenases which potentially compensated for poor plasmid expression of *adhB*.[33]

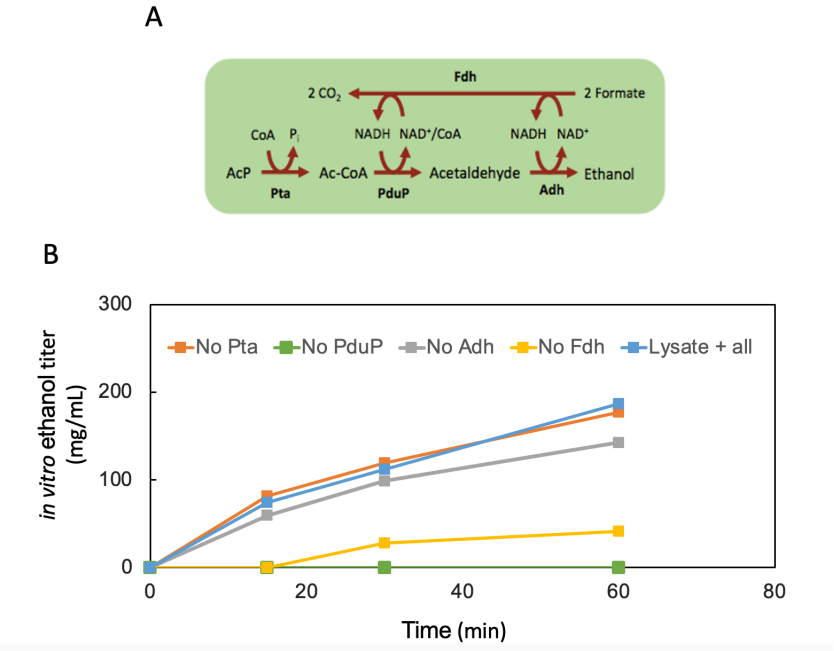

Figure 5-2: Pathway assay to detect limiting enzymes in ethanol pathway. (A) Overview of the pathway assay. Acetyl-phosphate (AcP) is the starting point of the assay and gets converted to ethanol using phosphotransacetylase (Pta), propionyl-CoA dehydrogenase (PduP) and alcohol dehydrogenase (Adh). The NADH required to drive the ethanol pathway is derived from the oxidation of formate by Fdh. Ethanol product is quantified on GC-FID. (B) Pathway assay result in NOG22/pPL274*/pTW371/pJD403 lysate. No ethanol was detected following the removal of purified PduP, and purified Fdh was found to be strongly limiting for ethanol productivity. These results suggested low activity in PduP and Fdh could be result of low expression in construct on third plasmid.

5.3.2 Combination of fdh overexpression and media formate precludes sugar consumption in NOG strain

Since the expression of multiple genes from the third backbone was insufficient, it was considered that utilizing this three-plasmid system did not represent and effective platform for expression of the ethanol pathway. Therefore, we next investigated expressing the ethanol genes on one of the two growth plasmids to allow for a simpler two plasmid system. pTW371 was chosen to harbor the ethanol pathway genes due to its smaller size relative to pPL274*. Initially, only *fdh* was cloned onto pTW371 yielding the new plasmid pJD225. *fdh* was expressed

downstream of the transketolases on the same operon. This plasmid was transformed into NOG22/pPL274*, where NOG22 was NOG21 following plasmid removal. Production was carried out in production media supplemented with 40 mM formate to test the ability of NOG22/pPL274*/pJD225 to consume formate.

Interestingly, NOG22/pPL274*/pJD225 was not able to consume glucose in formate supplemented media (Figure 5-3). The loss of sugar uptake was found to dependent on the combination of both media formate and the presence of Fdh. The control strain not expressing *fdh* consumed about the same amount of sugar over the production whether or not formate was present in the media.

A potential explanation for this phenotype is that when formate gets consumed quickly, there could be a disruption of the intracellular redox balance due to lack of available electron acceptors present to receive electrons from NADH. This could cause reductive stress, leading to an inability to consume sugar.[34] *E. coli* can't use its normal fermentative products such as lactate and succinate since generating these products does not consume NADH in NOG-based metabolism. While E. coli with fermentative pathways knocked out cannot consume sugar anaerobically, this is due to the requirement of NAD^+ for the EMP, so the reason for a lack of sugar uptake in the NOG strain is likely due to a different mechanism. Although the ethanol production represents a potential electron sink,[35-36] the ethanol pathway was not overexpressed in this strain, so it's possible the activity of these enzymes was limiting their ability to function as an effective electron sink.

5.3.3 Addition of nitrate, an anaerobic electron acceptor, allows NOG22/pPL274/pJD225 to consume glucose in formate-supplemented production media*

To evaluate whether the addition of an electron sink could rescue anaerobic sugar consumption in NOG22/pPL274*/pJD225, we repeated production with 40 mM formate along with the addition of 40 mM nitrate. Nitrate is the preferred anaerobic electron acceptor in *E. coli,* so supplying nitrate should provide the cell with a robust electron sink.[25] We observed that the addition of nitrate was able to rescue sugar consumption in NOG22/pPL274*/pJD225 in formate media (Figure 5-3). Additionally, we observed NOG22/pPL274*/pJD225 consumed all media formate in glucose/formate/nitrate media, demonstrating the ability to consume formate *in vivo* (data not shown). This result supported the hypothesis that a lack of a robust electron sink was the reason why NOOG22/pPL274*/pJD225 could not consume sugar in glucose plus formate media.

5.3.4 Replacement of nitrate with the ethanol pathway for the electron sink

Since the addition an electron sink allowed NOG22/pPL274*/pJD225 to uptake sugar in glucose plus formate media we planned to replace nitrate with ethanol production by overexpressing the ethanol pathway on top of *fdh*. Ethanol pathway genes *pduP* (*S. enterica)* and *adhB (Z. mobilis)* were cloned onto pJD225 to construct pJD428, and this plasmid was transformed into the NOG strain to give NOG22/PL274*/pJD428. To verify successful overexpression of the ethanol pathway, the same whole-pathway assay as was carried out in Fig. 5-2 was carried out with lysate from NOG22/pPL274*/pJD428. Functional expression of all enzymes was verified as *in vitro* ethanol production occurred when any of the purified pathway enzymes was removed from the positive control mix. Compared to the positive control, PduP was the most limiting enzyme

in lysate for ethanol production, as ethanol productivity dropped 40% following the removal of PduP (Figure 5-3).

To test whether the overexpression of the ethanol pathway improved the strain's capability to consume sugar in formate-supplemented media, production in NOG22/pPL274*/pJD225 and NOG22/pPL274*/pJD428 at different concentrations of formate was compared. Media formate concentrations of 10, 20 and 30 mM formate.

However, overexpression of the ethanol pathway did not significantly improve the strain's ability to consume sugar in formate-supplemented production media. Total sugar consumption vs. media formate for NOG22/pPL274*/pJD225 & NOG22/pPL274*/pJD428 is shown in Figure 5-3. The data show that both strains failed to consume sugar when concentrations of media formate was 20 mM and above. Potential reasons for the failure to improve the formate threshold for sugar uptake could be that limitations in carbon flux to acetyl-CoA were more limiting than ethanol pathway activity, or that other mechanisms were causing the impairment of sugar uptake.

Pta limitation was also evaluated using a similar *in vitro* assay to the pathway assay (Figure S5-1), although NADH was added as the electron donor rather than formate. AcP was supplied as the starting point and NADH consumption was detected at OD_{340}. It was found that removing Pta from the reaction mix did not significantly reduce overall activity of the pathway (Fig 5S-2). However, the K_m of Pta is relatively high in the acetyl-CoA forming direction. Thus there may be a greater kinetic limitation in this enzyme if *in vivo* concentrations of AcP are too low.[37]

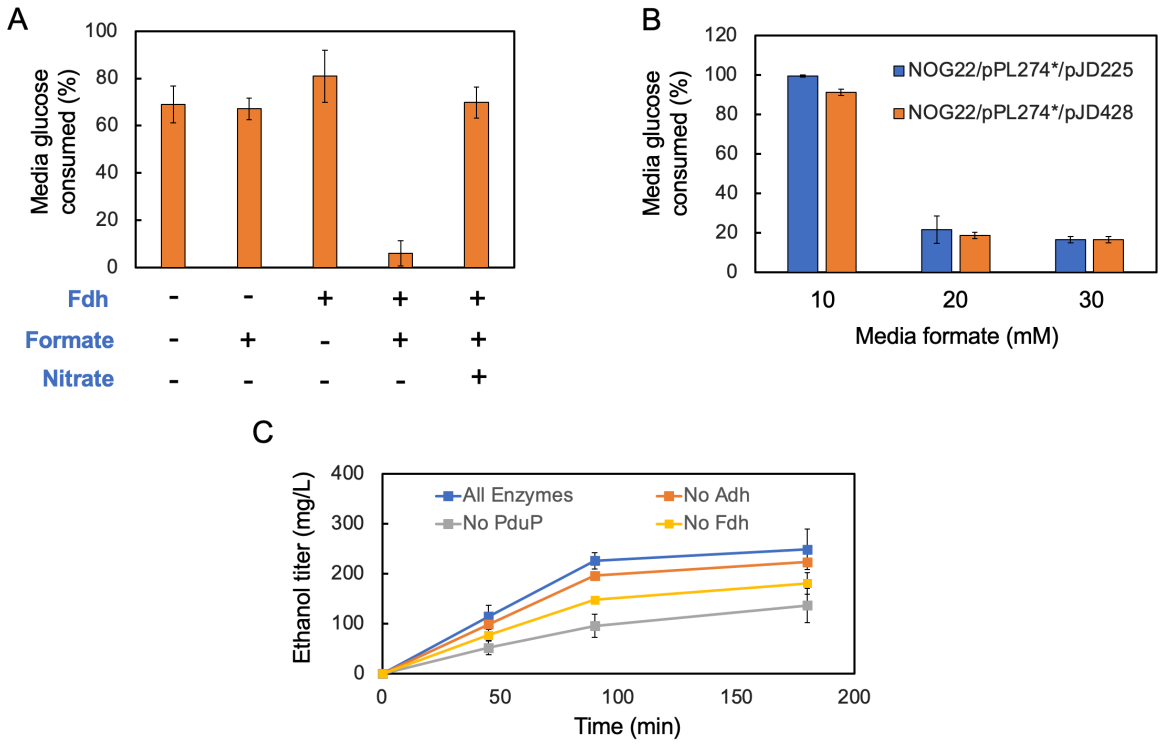

Figure 5-3: Production results in NOG22/pPL274*/pJD225 and NOG22/pPL274*/pJD428 and pathway assay of NOG22/pPL274*/pJD428. (A) Total sugar consumption over 24 hr production in NOG22/pPL274*/pTW371 (-Fdh) or NOG22/pPL274*/pJD225 (+Fdh). The combination of Fdh and media formate significantly reduced total sugar consumption. Sugar consumption was restored by the addition of an electron sink (nitrate). (B) Total sugar consumption over production vs. media formate concentration in strain expressing *fdh* only (NOG22/pPL274*/pJD225) and strain expressing (*fdh* + *pduP* + *adhB*). The additional expression of the ethanol pathway enzymes did not improve the formate threshold for sugar consumption. (C) *in vitro* pathway assay in NOG22/pPL274*/pJD428 lysate. Ethanol production was observed when all purified enzymes were removed, verifying successful expression of the ethanol pathway enzymes. PduP was the most limiting enzyme for ethanol productivity.

5.3.5 Production characterization in glucose/formate/nitrate media

Since the addition of nitrate to glucose plus formate production media was able to rescue anaerobic sugar consumption in NOG22/pPL274*/pJD225, we reasoned we could use nitrate to allow for better characterization of production in NOG22/pPL274*/pJD428. Since strains expressing Fdh were unable to uptake sugar and produce products with even a minimal amount of formate in the media, it was difficult to determine how formate consumption affected the

production phenotype. Thus, we speculated that if we can improve the maximum formate threshold by small additions of nitrate, we could test production over a wider range of formate concentrations and thus better characterize production. Although we could also similarly characterize the production using oxygen instead, nitrate has several advantages under these particular circumstances, even if it is a more scalable electron acceptor. Relative to oxygen, it is more straightforward to keep nitrate levels consistent across samples since it can be directly added to the media. For oxygen, the rate of supply would be controlled by the rate of oxygen transfer from the reactor headspace, so small variations in amount of headspace (e.g. after taking samplings), reactor orientation, or shaking rate could cause differences in the rate of oxygen transfer to the liquid media. Since we wanted to change the amount of media formate while keeping all other factors constant, being able to stringently control the amount of electron acceptor was extremely important. Moreover, unlike with oxygen, the consumption of nitrate can be directly measured. We found that adding 10 mM nitrate was able to increase the media formate threshold in NOG22/pPL274*/pJD428 from between 10 to 20 mM formate to between 50-70 mM formate (Figure S5-2). Therefore, these new conditions allow us to test production across a wider range of formate concentrations and thus gather more information regarding how formate affects the production phenotype.

5.4.6 Time course characterization of NOG22/pPL274/pJD428* production in glucose/formate/nitrate media*

To evaluate how formate affect production in glucose/nitrate formate media, a time course of production was carried out at 50 mM formate, near the threshold at which NOG22/pPL274*/pTW371 could produce without significant impairment of sugar uptake

(Figure 5-4). The results clearly demonstrate that glucose consumption is inhibited when the cells are consuming formate, as glucose consumption did not occur until after media formate was exhausted, after about 12 hours into production. With 30 mM media formate, glucose consumption happened much sooner (Figure S5-3). Given how formate and glucose were consumed, we reasoned that the activity of Fdh in NOG22/pPL274*/pJD428 might be too strong, resulting in imbalanced formate uptake preventing the strain from consuming glucose and formate simultaneously. It was also difficult to further characterize the results due to large variations in sugar consumption phenotypes between biological replicates. Furthermore, since very little glucose was consumed during the period where the cell consumed formate, we couldn't reliably analyze those data points since very little glucose was consumed and very little product was produced. Therefore, we reasoned that reducing Fdh activity in the strain could lead to better interpretable results.

5.4.7 Isolation of NOG22/pJD428 mutant with reduced Fdh activity

In a previous attempt to overcome potential PduP limitation in NOG22/pPL274*/pJD428, which was elucidated as the most limiting enzyme for ethanol productivity in the pathway assay, we developed a mutant strain that had knocked down Fdh activity relative to NOG22/pPL274*/pJD428. To increase the activity of PduP, we cloned another copy of the *S. enterica pduP* onto pPL274*, replacing the mutated version of *f/xpk* on pPL274*. This new plasmid was designated pJD437. When NOG growth was established, limitation in Tkt uncovered by the pathway assay in the NOG22/pPL274 lysate was fixed by the overexpression of *tkt1* and second copy of *tkt2* from *M. buryatense* on pTW371, supplementing the *tkt2* on pPL274.[19] We attempted to pursue a similar strategy here.

After pJD437 was transformed into NOG22/pJD428, an enzyme assay was performed to evaluate whether the new copy of PduP increased PduP activity relative to NOG22/pPL274*/pJD428. Surprisingly, specific PduP activity in the lysate of NOG22/pJD437/pJD428, decreased dramatically relative to NOG22/pPL274*/pJD428, about to the level of the negative control NOG22/pPL274*/pTW371 (Figure 5-4). We also tested Fdh activity and found it was also decreased, though unlike with PduP it was still clearly overexpressed relative to the negative control (Figure 5-4).

Following this result, we speculated that mutations on plasmid pJD428 may have occurred, thus knocking down enzyme activity in NOG22/pJD437/pJD428. After sequencing, we discovered an insertion sequence on pJD428 had occurred between *fdh* and *pduP* (Figure S5-4). This mutated version of pJD428 was designated pJD428*. Although the resulting strain NOG22/pJD437/pJD428* did not have the phenotype we originally intended, we wished to evaluate how the lower activity of Fdh would affect production.

5.4.8 Production in NOG22/pJD437/pJD428 mutant with reduced Fdh activity*

To compare production in NOG22/pJD437/pJD428* to NOG22/pPL274*/pJD428, we carried out a production time course in 50 mM glucose, 50 mM formate and 10 mM nitrate. Comparing the results to NOG22/pPL274*/pJD428, which could not robustly consume glucose until formate was exhausted, we observed that NOG22/pJD437/pJD428* was able to simultaneously utilize both glucose and formate without significant impairment of glucose consumption, suggesting the reduced Fdh activity allowed the cells to better balance glucose and formate consumption. The time course of sugar/formate consumption between the two strains is listed in Figure 5-4.

Since NOG22/pJD437/pJD428* had significantly reduced PduP activity, we next tested whether this adversely affected ethanol yields in this strain (Figure 5-4). Interestingly, in conditions with 50 mM formate and 10 mM nitrate NOG22/pJD437/pJD428* had a higher final molar ethanol yield on glucose at the end of the time course (t=20 hr) than NOG22/pPL274*/pJD428, 0.82 compared to 0.49. This indicated that balanced consumption of formate glucose appeared to be more important for ethanol yield than PduP activity. Moreover, NOG22/pPL274*/pJD225, which expressed Fdh but not the ethanol pathway, had the same ethanol yield as NOG22/pPL274*/pJD428, indicating PduP overexpression did not significantly affect ethanol yields under this condition. However, NO22/pPL274*/pTW371, a control expressing neither Fdh nor PduP, produced no ethanol. This indicates Fdh was necessary for ethanol production in media containing glucose, formate and nitrate. NO22/pPL274*/pTW371 also did not consume significant amounts of formate, while strains expressing Fdh consumed >90% formate. (data not shown). This increased ethanol yield in NOG22/pJD437/pJD428* appeared to be due to the strains ability to balance formate and glucose consumption. Since NOG22/pPL274*/pJD428 did not consume much glucose until formate was exhausted, there may have been limited amounts of acetyl-CoA available to be reduced. This was further evident from the fact that NOG22/pPL274*/pJD428 consumed all media nitrate, while NOG22/pJD437/pJD428* did not (Figure S5-5). The reduced Fdh activity in NOG22/pJD437/pJD428* also had an improved the threshold for formate consumption in 10 mM nitrate media, as the strain was able to consume sugar with up to 100 mM formate.

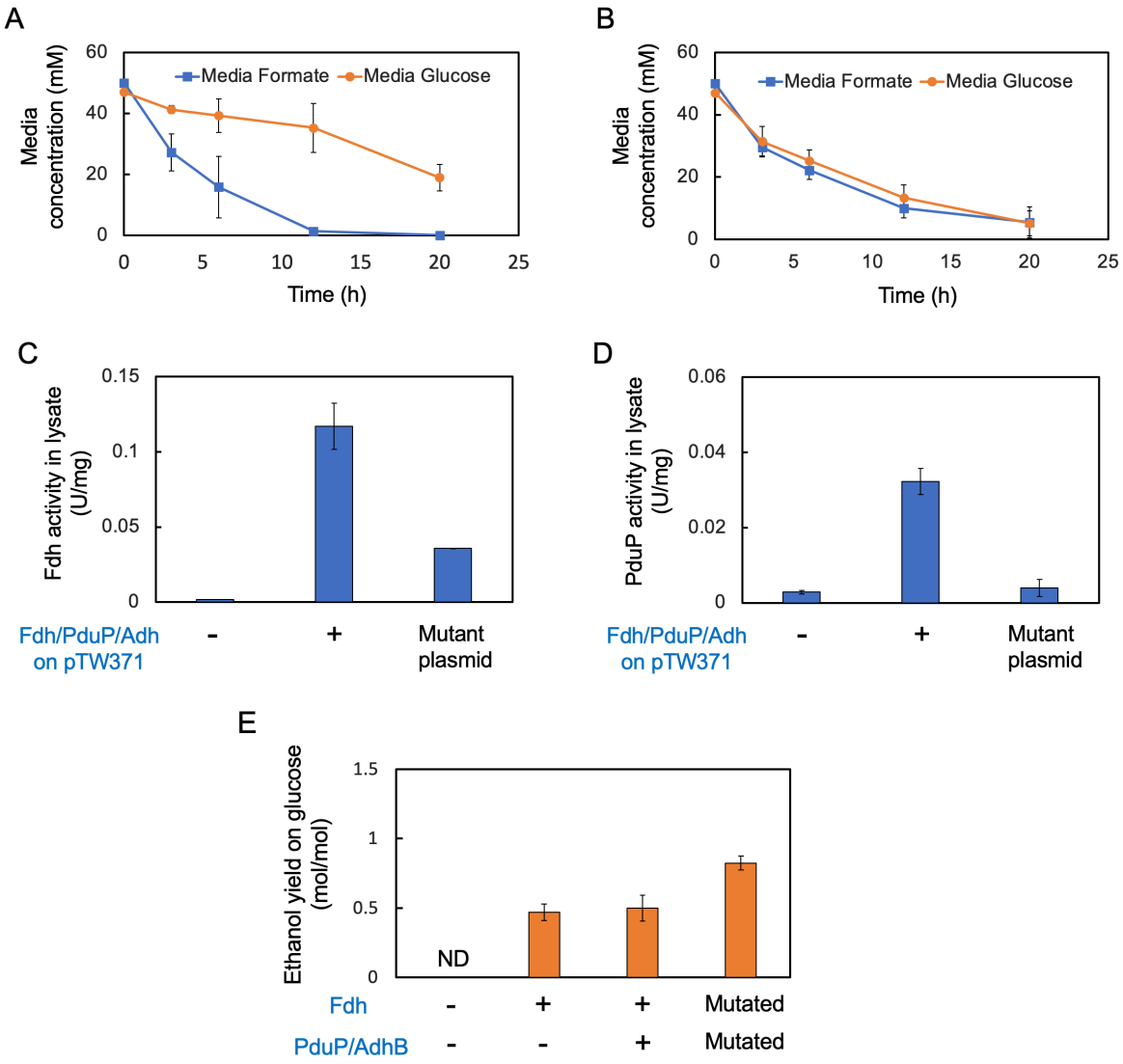

Figure 5-4: Comparison of production results in NOG22/pPL274*/pJD428 and NOG22/pJD437/pJD428*. The plasmid pJD428* contained a mutation between *fdh* and *pduP*. (A) Time course of glucose and formate consumption during production in NOG22/pPL274*/pJD428 in media containing 50 mM glucose, 50 mM formate and 10 mM nitrate. (B) Time course of glucose and formate consumption during production in NOG22/pJD437/pJD428* in media containing 50 mM glucose, 50 mM formate, and 10 mM nitrate. (C) Fdh activity in strain lysates. Negative control is NOG22/pPL274*/pTW371. The mutation on pJD428* in NOG22/pJD437/pJD428* knocked down Fdh activity relative to NOG22/pPL274*/pJD428. (D) PduP activity in strain lysates. Negative control is NOG22/pPL274*/pTW371. The mutation on pJD428* in NOG22/pJD437/pJD428* appeared to completely eradicate PduP overexpression (E) Final molar ethanol yield on glucose in 50 mM glucose, 50 mM formate and 10 mM nitrate media. NOG22/pPL274*/pTW371 did not express Fdh or PduP and produced no ethanol. NOG22/pPL274*/pJD225 overexpressed Fdh only and had an ethanol yield of 0.5. NOG22/pPL274*/pJD428 overexpressed Fdh, PduP and AdhB and had an ethanol yield of 0.5. NOG22/pJD437/pJD428* had an insertion knocking down Fdh/PduP activity an ethanol yield of 0.82.

*5.4.9 Characterization of production in NOG22/pJD437/pJD428**

Although NOG22/pJD437/pJD428* contained mutations knocking down its Fdh and PduP activity, it was a slightly better ethanol producer and was able to simultaneously utilize formate and glucose in the glucose/formate/nitrate media. Although, NOG22/pJD437/pJD428* may not be the most promising ethanol producing strain in the long run due to its low expression of pathway enzymes, we reasoned that this strain could be better used to characterize how formate affected production in anaerobic conditions relative to NOG22/pPL274*/pJD428 for a couple of reasons. Firstly, since it had an improved threshold for media formate relative to NOG22/pPL274*/pJD428. Thus, we could test production over a wider range of formate concentrations. Since NOG22/pPL274*/pJD428 had a dramatic change in phenotype over relatively small intervals, obtaining consistent, repeatable results was challenging. Secondly, since sugar and glucose could be consumed simultaneously, we could obtain data points from when the cell was consuming both formate and glucose.

To characterize the production, glucose and nitrate in the production media were held constant to 50 mM and 10 mM respectively, while the concentration of formate was varied at intervals of 0, 30, 50, 80, & 100 mM. About 100 mM formate represented the upper limit for formate at which NOG22/pJD437/pJD428* could still consume reasonable (~25-33%) amounts of sugar. Samples were obtained 12 hours into production, allowing enough glucose to be consumed to obtain reliable results but before the media formate was completely exhausted in any case that contained formate. The results of this experiment are shown in Figure 5-5. Firstly, we determined that increasing media formate increased specific formate consumption in the strain, represented by the ratio of formate to glucose consumption. Since strains with more formate consumed less glucose, we reasoned the ratio of formate and glucose consumption provided a

better representation of how the cell consumed formate that absolute formate consumption. Moreover, the ratio of formate consumption directly relates to achievable ethanol yields. To convert one glucose into three ethanol, the cell must consume at least 6 mols of formate per mols of glucose. We found that at the highest formate condition, the formate/glucose consumption ratio was 1.91, which was about three-fold lower than what is required for maximum ethanol yields.

Increased formate/glucose consumption was linked to increasing ethanol yield, demonstrating how formate can be used to drive ethanol production in reductive fermentation. Although ethanol yields did not increase over 50 mM formate, the ratio of ethanol over acetate continued to increase, demonstrating the cells still increasingly favor ethanol production at formate concentrations 80 and above. This was offset by a drop in overall C2 yields, may decrease due to the manifestation of competing pathways for NADH and/or cell stress, possibly due to heavily reductive intracellular conditions. This stress could potentially cause a loss of robustness through the NOG pathway. A baseline ethanol yield of 0.23 mol ethanol/mol glucose was observed in the 0 mM formate condition. The NADH here was likely obtained through minor pathways in the TCA cycle leading to oxidation of carbon. However, the addition of formate was able to increase molar ethanol yield about four folds to 0.8. As previously mentioned, the total glucose consumption decreased relative increased media formate, and the severity of this was most pronounced at 80 mM formate and above. A time course of glucose consumption found that at the high formate condition of 100 mM, almost no glucose was consumed after 6 hours (Figure S5-6). The failure to consume sugar in high formate conditions appeared to be linked a limitation in ATP supply shown by low acetate yields in the condition where sugar consumption becomes impaired. In general, acetate yields decreased with increasing formate consumption, as was

expected when the cell diverted more C2 towards ethanol. However, in the 80 mM or 100 mM formate condition, the molar acetate yield on glucose approached 1.0, or the minimum required to sustain sugar uptake. Since one mol of ATP is required per mol of glucose consumed, at least one acetate must be produced to regenerate that ATP if sugar uptake is to be sustained. This suggested that ATP limitation due to reduced acetate yields could be responsible for the impairment of sugar uptake in conditions with high media formate. Although nitrate consumption can supply ATP, the consumption of nitrate was likely not high enough to be fully compensate, potentially due to limitations in nitrate consumption. While these results demonstrated increasing formate consumption was linked to increasing ethanol yields, it appeared that eventually ATP limitation capped the cells ability to consume formate and thus further ethanol yields. Moreover, this effect was likely exacerbated by the reduced C2 yield in the high formate conditions, which accelerated the drop in acetate yields. To further improve ethanol production, it would be necessary to use respiration to overcome the ATP limitation. Since oxygen is a more desirable electron acceptor than nitrate due its higher proton yield, availability, and lack of toxic byproducts, we believe transitioning the production to microaerobic conditions represents a better strategy than attempting to engineer nitrate consumption. However, the issue regarding the drop in C2 yields under conditions of high formate consumption may need further understanding to ensure it doesn't become problematic under microaerobic conditions.

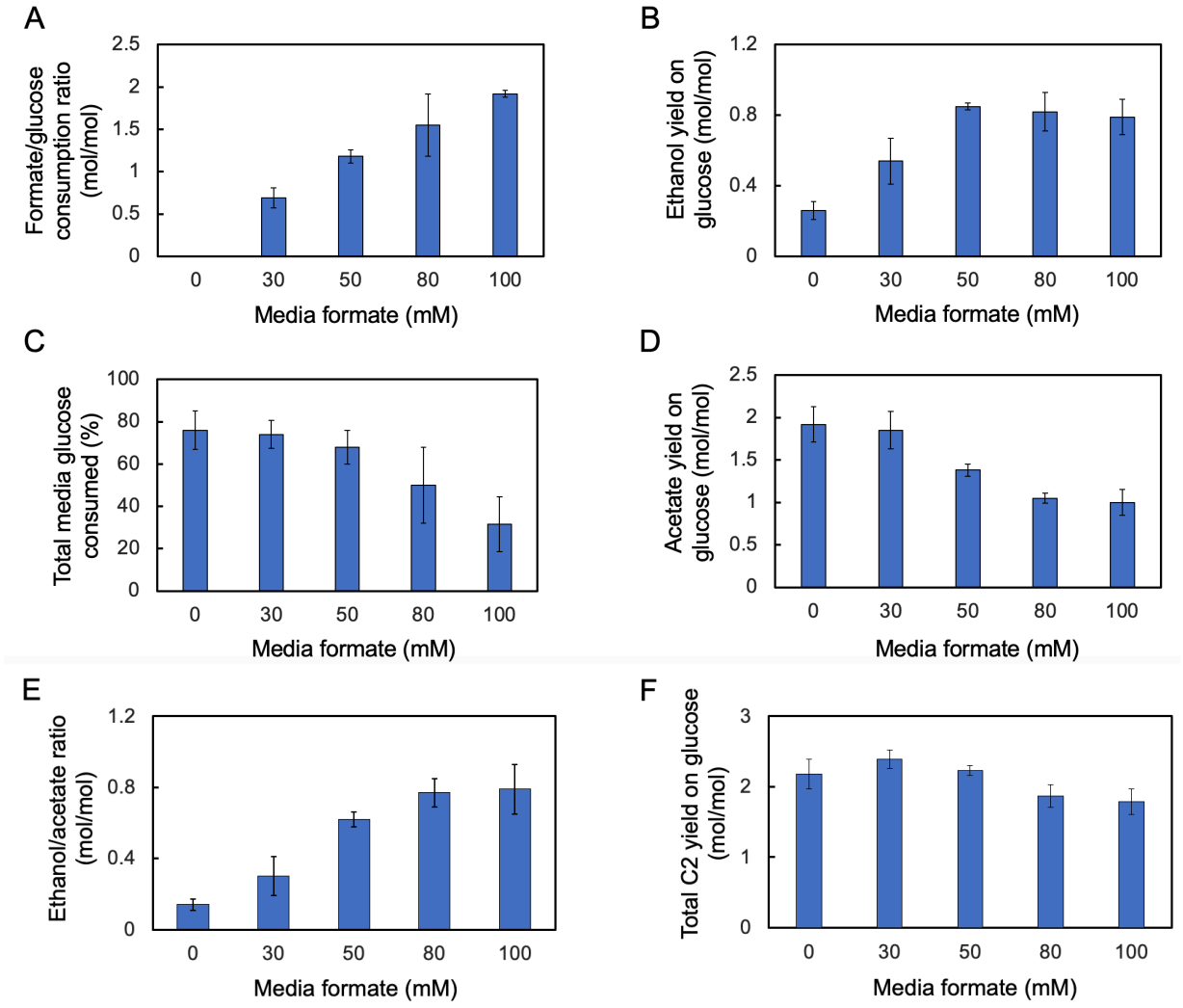

Figure 5-5: Production characterization in 50 mM glucose/10 mM nitrate media in NOG22/pJD437/pJD428* across different concentrations of media formate. All data are from time points taken 12 hr into production (A) Consumption ratio of formate to glucose (mol/mol) increases with increasing media formate concentration. (B) Ethanol yield on glucose (mol/mol) increases with increasing media formate concentration. (C) Total media glucose consumption decreases with increasing media formate concentration. (D) Acetate yield on glucose (mol/mol) decreases with increasing media formate. Acetate yield at 80 and 100 mM formate are approaching the minimum required to sustain sugar uptake. (E) Ratio of ethanol to acetate produced (mol/mol) increased with increasing media formate (F) Overall C2 (ethanol plus acetate) yield on glucose was decreased at 80 or 100 mM formate, indicating presence of competing pathways for NADH and/or loss of robustness in NOG pathway due to high stress redox/ATP conditions

5.4.10 Replacement of glucose with G6P to overcome ATP limitation

Production results in NOG22/pJD437/pJD428* suggested that a failure to maintain sufficient ATP production was limiting ethanol yields by capping the amount of formate than could be consumed. As the strain consumes more formate and diverted more carbon flux away from acetate, it is unable to regenerate the ATP required to phosphorylate glucose to G6P. Anaerobic molar acetate yields on glucose approached 1.0 mol acetate produced/mol glucose consumed in conditions where the cells ability to consume sugar was compromised, indicating the strain was approaching the minimum acceptable ATP yield to sustain glucose phosphorylation. In order to overcome this, we attempted to remove the requirement for ATP by directly feeding G6P to the strain and thus make the pathway ATP balanced. Is has been reported that *E. coli* is capable of directly transporting extracellular G6P using phosphate antiporter UhpT.[38]

To evaluate whether we could replace glucose with G6P to overcome ATP limitation and improve ethanol production, we replaced glucose with G6P in the high formate conditions where NOG22/pJD437/pJD428* had limitations consuming glucose, as well as a control condition without formate. We found the cell was able to consume >80% of media G6P in all conditions, supporting the hypothesis that ATP limitation was responsible for the impaired glucose consumption (Figure 5-6). While total glucose consumption over production decreased significantly from 0, to 80 mM to 100 mM formate, G6P consumption was not affected. However, in the high formate condition we also observed that both ethanol and overall C2 yield on G6P dropped dramatically relative to glucose (Figure 5-6). In the case with 10 mM nitrate and 100 mM formate, the ethanol yield dropped about 7 fold on G6P relative to glucose. We confirmed the decreased ethanol yield wasn't due to an inability to consume formate in G6P media, as the strain was able to consume formate on G6P (Figure 5-6). This indicated that there

was likely an alternative electron sink(s) that was manifesting more strongly on G6P media relative to glucose or that limitations in the ethanol pathway were occurring in G6P media. While the overall C2 yield on G6P in the condition without formate was also lower compared to glucose, the decrease wasn't as dramatic as it was with formate (Figure 5-6). Specifically, C2 yield on G6P dropped 23% in the 0 mM formate condition relative to glucose, while it dropped 30% with 100 mM formate. Removing nitrate from the media did not alter the low ethanol yield phenotype, indicating low ethanol yield was not from increased nitrate consumption. We checked the HPLC chromatogram for potential reduced products that could serve as alternative electrons sinks, such as glycerol or sugar alcohol, but did not observe any.

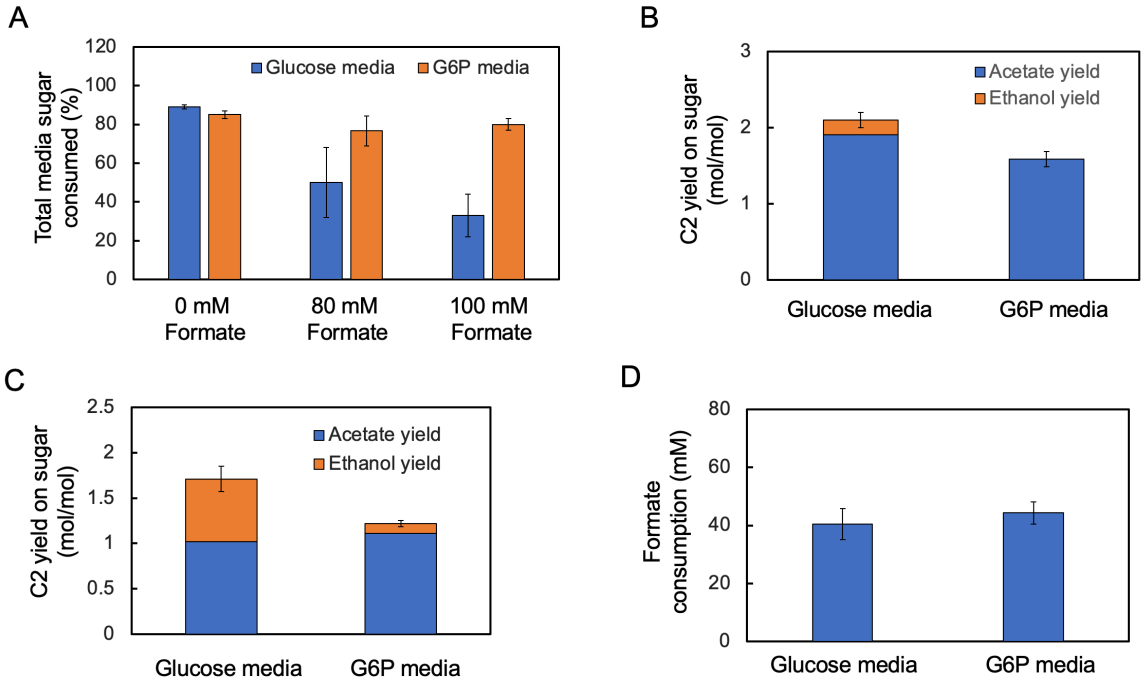

Figure 5-6: Production in G6P media in NOG22/pJD437/pJD428* to overcome ATP limitation. (A) Total glucose or G6P consumption over 24 hr production in media with 50 mM sugar, 10 mM nitrate, and 0, 80 or 100 mM formate. Impairment of sugar uptake by media formate was observed on glucose but not G6P, supporting the hypothesis the effect is due to ATP limitation (B) Molar yield of C2 (acetate and ethanol) on glucose or G6P in media containing 50 mM sugar, 0 mM formate and 10 mM nitrate. C2 yield was decreased on G6P media by 23% (C) Molar yield of C2 (acetate and ethanol) on glucose or G6P in media containing 50 mM sugar, 100 mM formate and 10 mM nitrate. Ethanol and overall C2 yield dropped significantly on G6P media (D) Total formate consumption over 24 hr in glucose or g6P in media containing 50 mM sugar, 100 mM formate, and 10 mM nitrate was similar.

5.4.11 Ethanol production in G6P media appears primarily limited by weak ethanol pathway

Although there appeared to be competing pathways for formate consumption G6P media, it is possible ethanol production could be increased through increasing the amount of formate consumption. Since the initial G6P production in Figure 5-6 was carried out in NOG22/pJD437/pJD428*, the strain with reduced Fdh activity, we evaluated whether we could improve ethanol production by switching back to the stronger, originally designed pJD428 construct, and increasing the formate in the media to serve as the driving force for ethanol production. However, when we tested production in NOG22/pPL274*/pJD428 in media containing 50 mM G6P and 200 mM formate, we found the strain was only able to consume about ~50 mM of the media formate and still produced limited ethanol titers. We reasoned the incomplete consumption of formate could be due to limitations in formate uptake/consumption or a lack of available electron acceptors to receive reducing equivalents from formate. To evaluate this, we retested the production with 200 mM formate in aerobic conditions to allow for excess supply of electron acceptors. We found that with oxygen, all 200 mM of media formate was consumed (Figure 5-7), suggesting that limited available electron acceptors were the limiting factor for formate consumption. However, it could be possible that formate-specific transport limitations occur only in anaerobic conditions. Further evidence supporting pathway limitation was demonstrated by the fact that we were able to see an increase in ethanol titer in 50 mM G6P and 200 mM formate media when using NOG22/pPL274*/pJD428, the strain expressing Fdh, PduP and AdhB, relative to NOG22/pPL274*/pJD225, the strain expressing Fdh only (Figure 5-7). This supported the hypothesis that the PduP/Adh expression was limiting for ethanol production. Based on the much lower ethanol yields/titers on G6P relative to glucose, it appears that ethanol pathway flux may be reduced on G6P media for an unknown reason. While

the low ethanol recovery from formate in G6P relative to glucose media suggest alternative electron sinks manifest on G6P, it is not certain whether these pathways occur because they become more favorable on G6P, or if they occur because flux through the ethanol pathway is significantly impaired. However, while production on G6P was not able to increase ethanol yield, we suggest this media could be an effective way to screen for improved ethanol pathway constructs. Unlike with glucose, in G6P media PduP overexpression leads to significantly increased ethanol production. In particular, it may be beneficial to screen variants of Pta and PduP from different organisms. However, since increased Pta is speculated to be detrimental for NOG-based growth however, any additional *pta* expression should be controlled such that it is only overexpressed during the production condition.

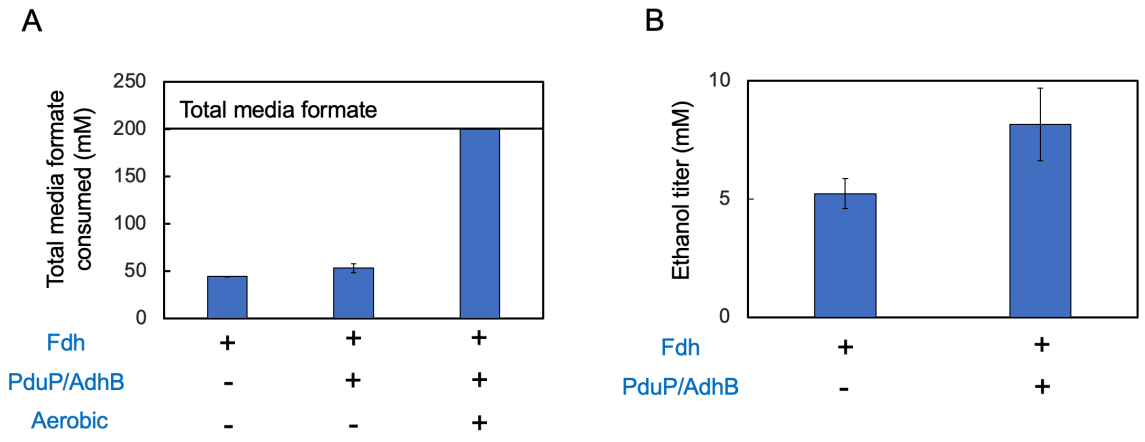

Figure 5-7: Pathway expression appears to be limiting factor for ethanol yields in 50 mM G6P/200 mM formate media in NOG22/pPL274*/pJD428 (A) Final formate consumption in NOG22/pPL274*/pJD225 (Fdh only) in anaerobic and NOG22/pPL274*/pJD428 (Fdh, PduP and AdhB) in aerobic and anerobic conditions. Media formate is completely consumed in aerobic conditions while only about ~25% is consumed in anaerobic conditions. This suggests lack of available electron acceptors is limiting for formate consumption. (B) Final ethanol titer in NOG22/pPL274*/pJD225 (Fdh only) and NOG22/pPL274*/pJD428 (Fdh, PduP and AdhB) in anaerobic conditions. PduP and AdhB overexpression increases ethanol titer from 5.23 to 8.16 mM. Since ethanol production is limited by PduP/AdhB, G6P plus formate can be used to screen for improved ethanol pathway constructs.

5.4.12 Metabolomics in G6P plus formate media to identify unknown electron sinks

Metabolomics is an emerging field that aims characterize the metabolome of cells, or the relative quantities of key intracellular metabolites. For the purpose of metabolomics, metabolites are considered to be products of cellular metabolism smaller than 1 kDa.[39] In order to identify the potential electron sinks that occur in G6P plus formate media, we applied metabolomics to compare the metabolome between the condition where the electron sink manifests (i.e. G6P plus formate media) vs. the control conditions (G6P no formate media). Since we did not observe notable reduced products such as sugar alcohol or glycerol on the HPLC, we wanted to see if we could determine potential pathway intermediates in the electron sink pathway that would be upregulated in the electron sink (i.e. G6P plus formate) condition. To maximize flux to the electron sink pathway, we carried out production in NOG22/pPL274*/pJD225, a strain expressing Fdh, but not PduP or AdhB. Anaerobic production was carried out in media containing 50 mM G6P with 100 mM formate to establish the electron sink condition. Intracellular metabolites were extracted at 6 hr and 24 hr, are samples were analyzed by LC-MS and the Tracefinder software. Sample detection and analysis was performed by the UCLA Metabolomics center at the California Nanosystems Institute (CNSI). From the metabolomics result, we found that the sugar alcohol sorbitol was upregulated almost 20 fold in the electron sink condition (Figure 5-8). Sugar alcohols, such as sorbitol and mannitol, can be obtained via the direct reduction of sugar phosphate by SrlD and MtlD respectively. Although we didn't observe either sugar alcohol on HPLC, *E. coli* does not have a known export system for sugar alcohol, and studies that investigated microbial production of sugar alcohol found that export is a limiting factor for production, due to observed high concentrations of intracellular product.[40,41] Thus, sorbitol could serve as a potential electron sink, but possible export limitations could

prevent it from being observed in significant quantites on HPLC. To investigate this, we compared production in NOG22/pPL274*/pJD428 and NOG22Δ*srlD*/pPL274*/pJD428, which had sorbitol dehydrogenase knocked out. We were able to observe a slight increase in ethanol titer of 17%, up to 9.84 mM from 8.15 mM (Fig5-8), following the knockout of SrlD. However, a more significant difference between the strains involved their relative formate consumption. Formate consumption in NOG22Δ*srlD*/pPL274*/pJD428 dropped about 40% relative to NOG22/pPL274*/pJD428, from 48.2 mM to 28.74 mM (Figure 5-8). These data further support the hypothesis that limitations in the ethanol pathway are a more direct factor causing the poor ethanol production in G6P plus formate media.

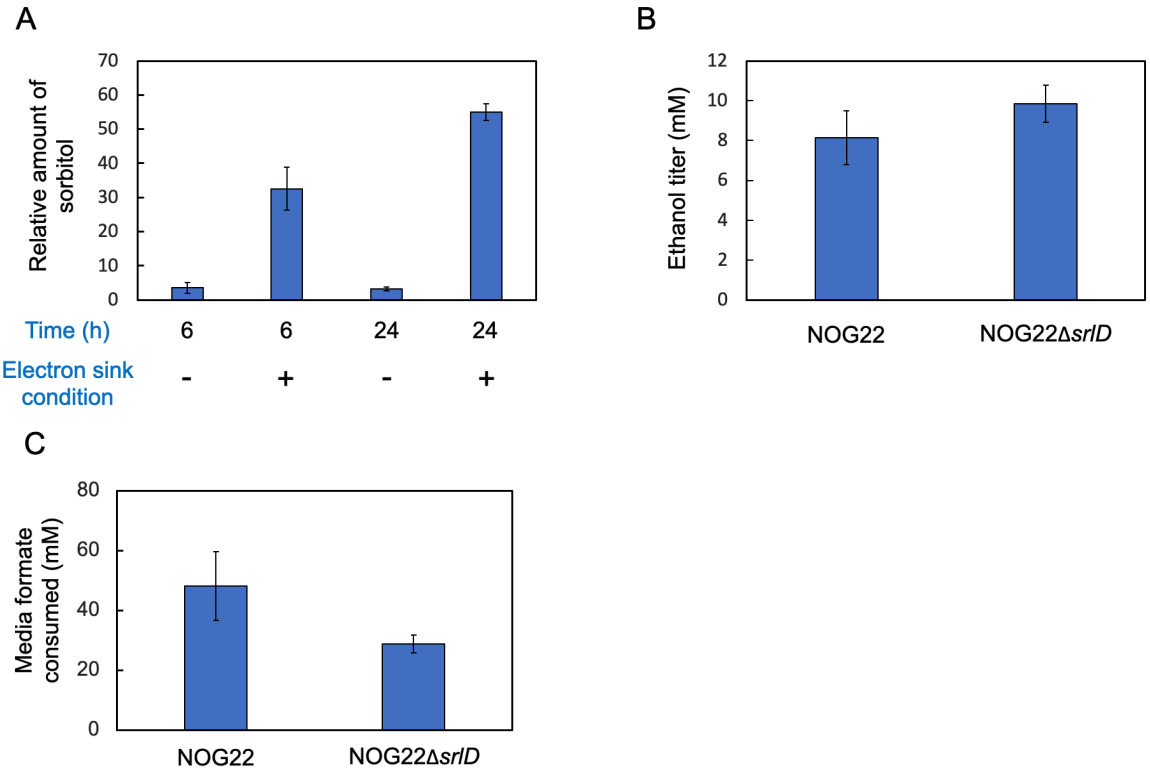

Figure 5-8: Metabolomics result in NOG22/pPL274*/pJD225 and comparison of production in NOG22 and NOG22Δ*srlD* containing pPL274* and pJD428 (A) Metabolomics result indicated intracellular sorbitol was upregulated ~20 fold is electron sink condition (+formate) Relative concentrations were normalized to the intracellular sorbitol concentration at T_0. (B) Ethanol titer was slightly upregulated following KO of s*rlD*. Both strains contained pPL274*/pJD428 (C) Total formate consumption over 24 hr production was reduced in the strain with s*rlD* knocked out. Both strains contained pPL274*/pJD428.

5.4.13 Metabolomics results suggest high formate conditions decreases robustness in NOG cycle

In the anaerobic ethanol production on glucose/formate/nitrate media, a drop in overall C2 yield was observed in conditions where sugar uptake began to be impaired by increased formate consumption. This specifically occurred at formate/glucose molar consumption ratios above 1.5. This problem could be significant for NOG-based alcohol production, since producing ethanol at theoretical yields requires a much higher glucose/formate consumption ratio of 6. This drop in C2 yield could be due to competing pathways that utilize NADH, and/or reductive stress decreasing robustness through the NOG pathway. If the NOG cycle loses robustness, this would likely lead to increases in intracellular sugar phosphate concentrations since the cell would be unable to effectively convert sugar phosphate into AcP. Such an event would likely lead to an accumulation of intracellular sugar phosphate. Since a similar drop in C2 yield caused by media formate was also observed in G6P media, we looked at how intracellular sugar phosphate concentration was affected by media formate in the metabolomics experiment in the previous section. In the condition with formate (i.e. electron sink condition), we observed sugar phosphates fructose bisphosphate (FBP) and glyceraldehyde 3-phosphate (G3P) were present at significantly (~10 fold) higher concentrations (Figure 5-9). However, other sugar phosphates, including ribose 5-phosphate (R5P), sedoheptulose 7-phosphate (S7P), hexose 6-phospahate were only slightly upregulated or present at similar levels. The concentration of other sugar phosphate intermediates in NOG, such as erythrose 4-phospahte (E4P), were not measured. An accumulation of FBP and G3P could be caused by a reduction in activity of Fbp, since this enzyme uses FBP as a substrate, and G3P is a precursor to FBP in NOG (Figure S5-7). Notably, reduced Fbp activity was previous predicted to have extremely detrimental effects on the

robustness of the NOG cycle.[42] Therefore, it could be possible reductive stress affects *in vivo* Fbp activity, leading to a loss of pathway robustness in NOG and thus reduced yields of C2.

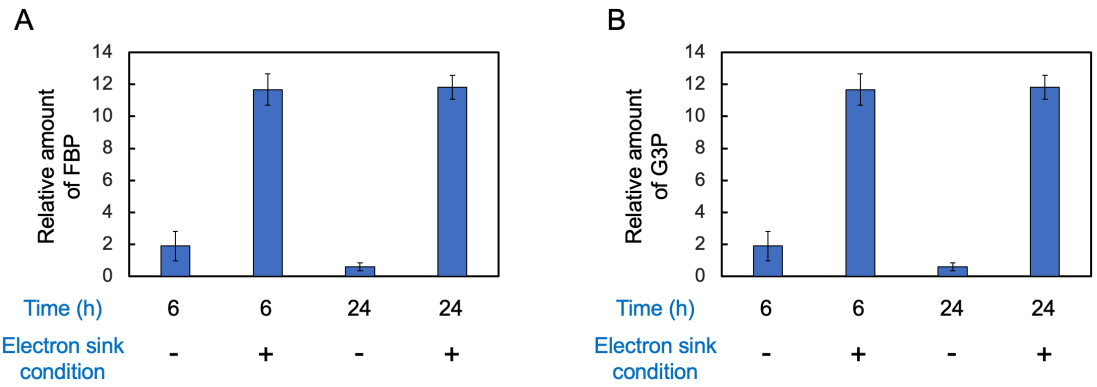

Figure 5-9: Relative concentrations of sugar phosphates in G6P media with 100 mM formate (electron sink condition) or without formate. Relative concentrations were normalized to concentrations at T_0 (A) The relative concentration of fructose bisphosphate (FBP) was increased about 10 fold in the electron sink (+ formate) condition. (B) Relative concentration of glyceraldehyde 3-phosphate (G3P) was increased about 10 fold in the electron sink (+ formate) condition.

5.4 Discussion and Conclusions

Here we were able to establish reductive fermentation for ethanol production in the NOG strain using formate as the electron donor. Initially relying on acetate production to supply ATP under anaerobic conditions, we were able to find that ethanol production was largely dependent on the overexpression of a heterologous *fdh*, and that increasing media formate could increase ethanol yield in media containing glucose, formate, and nitrate. These results demonstrated the feasibility of reductive fermentation to produce ethanol using the evolved NOG strain. As expected, ethanol production came at the expense of acetate production, and the results suggested that ultimately acetate yield dropped to a point where sugar uptake was impaired by

ATP limitation, preventing higher yields of ethanol from being attainable. To overcome ATP limitation, respiration must be upregulated in microaerobic conditions. When sugar uptake became impaired, overall C2 yields also became reduced, possibly due to the presence of competing pathways or a loss of robustness in the NOG cycle. Highly reductive conditions could potentially impair carbon flux through NOG, resulting in low C2 yields and thus exacerbating the reduction in acetate production. To further evaluate this, metabolomics could be applied on strains expressing Fdh in glucose plus formate conditions to confirm the results are consistent with the metabolomics result from G6P media, where G3P and FBP were significantly upregulated. Since media formate did not affect G6P consumption, replacing glucose with G6P as the carbon source was able to overcome ATP limitation. However, high yield ethanol production on G6P media was not obtained due to poor ethanol pathway flux and/or alternative electron sinks. While definitive evidence for the cause of this limitation does not exist, incomplete formate utilization in G6P media suggests poor ethanol pathway flux is a primary cause. Knocking out sorbitol dehydrogenase, a potential competing electron sink in G6P media identified by metabolomics, more significantly reduced formate consumption rather than increased ethanol production. However, since ethanol production in G6P media can be improved by the overexpression of PduP, this condition could represent a good background for screening different ethanol pathway constructs. In particular, it may be beneficial to evaluate different PduP enzymes aside from the *S. enterica* PduP used here, as well as Pta. More research also needs to be carried out to determine why C2 yields drop when the cell consumes high amounts of formate. Since intracellular FbP and G3P were highly upregulated in this condition, it is possible problems with Fbp lead to a loss of robustness, but more direct evidence to support that hypothesis needs to be obtained. If reductive stress is problematic, implementing respiration

could potentially mitigate both the ATP limitation and reductive stress by purging excess NADH. However, this could come at the expense of efficient utilization of reducing power, which is necessary for an economically viable NOG-based ethanol process. Therefore, if reductive stress is the cause of reduced C2 yields, it would be highly desirable to determine alternative ways to mitigate the detrimental effects.

5.5 Appendices

5.5.1 Strain list

Strain	Genotype	Comments	Reference
BW25113	*rrnB*$_{T14}$ Δ*lacZ*$_{w116}$*hsdR514* Δ*araBAD*$_{AH33}$ Δ*rhaBAD*$_{LD78}$	Wild Type	
JCL16	BW25113/F′[*tra*D36 *proAB*$^{+}$ lacI^{q}ZΔM15(Tet^{r})]	Wild Type	
PHL13	JCL16 Δ*gapA::FRT* Δ*mgsA::FRT* Δ(*pgk gapB)::FRT* Δ*pfkA::FRT* Δ*iclR::FRT* Δ*poxB::cat* Δ*zwf::FRT* Δ(*edd eda)::(*P$_{L}$*lacO*$_{1}$*::f/xpk*$_{BA}$) ΔP$_{pck}$::P$_{L}$*lacO*$_{1}$	Precursor to NOG strain that cannot grow on glucose	Lin, PP et. al
NOG21	Evolved from PHL13	PHL13 following evolution for glucose growth using NOG	Lin, PP et. al
NOG22	NOG21 with growth plasmids removed	NOG21 following removal of growth plasmids pPL274* and pTW371	This Study

5.5.2 Plasmid list

Plasmid	Description	Reference
pPL274	$P_L lacO_1$::*f/xpk*$_{BA}$ *glf*$_{ZM}$ *glk*$_{EC}$ tkt2$_{MB}$ *tal*$_{KP}$ *glpX*$_{EC}$ ColE *ori* Carb^r	Lin, PP et. al
pPL274*	$P_L lacO_1$::*f/xpk*$_{BA}$ (mutated by transposon insertion) *glf*$_{ZM}$ *glk*$_{EC}$ tkt2$_{MB}$ *tal*$_{KP}$ *glpX*$_{EC}$ ColE *ori* Carb^r	Lin, PP et. al
pTW371	$P_L lacO_1$:: *tkt2*$_{MB}$ *tkt1*$_{MB}$ CloDF13 *ori* Spec^r	Lin, PP et. al
pJD225	$P_L lacO_1$:: *tkt2*$_{MB}$ *tkt1*$_{MB}$ *fdh*$_{CB}$ CloDF13 *ori* Spec^r	This Study
pJD403	$P_L lacO_1$:: *fdh*$_{CB}$ *pduP*$_{SE}$ *adhB*$_{ZM}$ p15A *ori* Kan^r	This Study
pJD428	$P_L lacO_1$:: *tkt2*$_{MB}$ *tkt1*$_{MB}$ *fdh*$_{CB}$ *pduP*$_{SE}$ *adhB*$_{ZM}$ CloDF13 *ori* Spec^r	This Study
pJD428*	$P_L lacO_1$:: *tkt2*$_{MB}$ *tkt1*$_{MB}$ *fdh*$_{CB}$ *pduP*$_{SE}$ (contained insertion between *fdh* and *pduP)* *adhB*$_{ZM}$ CloDF13 *ori* Spec^r	This Study
pJD437	$P_L lacO_1$::*pduP*$_{SE}$ *glf*$_{ZM}$ *glk*$_{EC}$ tkt2$_{MB}$ *tal*$_{KP}$ *glpX*$_{EC}$ ColE *ori* Carb^r	This Study

5.5.3 Supplementary figures

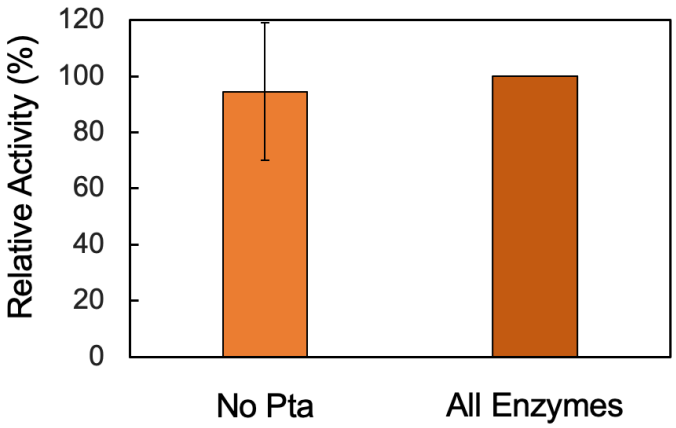

Figure S5-1: Test of Pta limitation. The data represent relative activities in the PduP assay in NOG22/pPL274*/pJD428 lysate. "All enzymes" contains both purified Pta and Adh as described in the methods. No Pta is the same assay except the purified Pta was left out of the reaction mix.

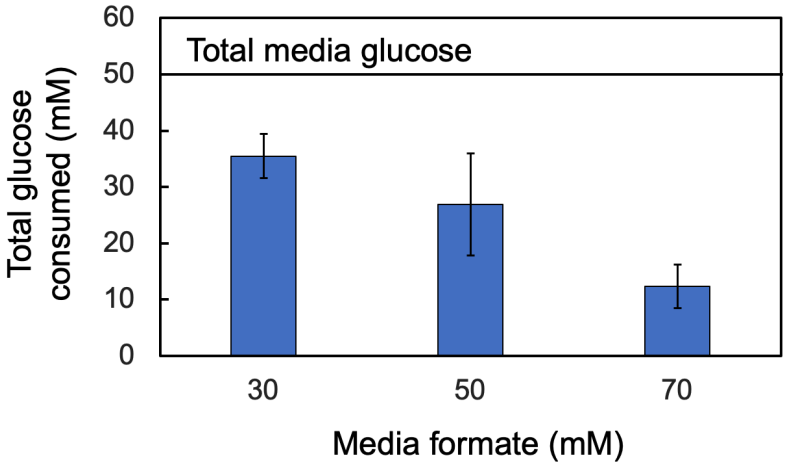

Figure S5-2: Total glucose consumption in NOG22/pPL274*/pJD428 over 24 hr production vs. formate concentration in media containing 50 mM glucose and 10 mM nitrate. The threshold for >50% media formate consumption was about 50 mM

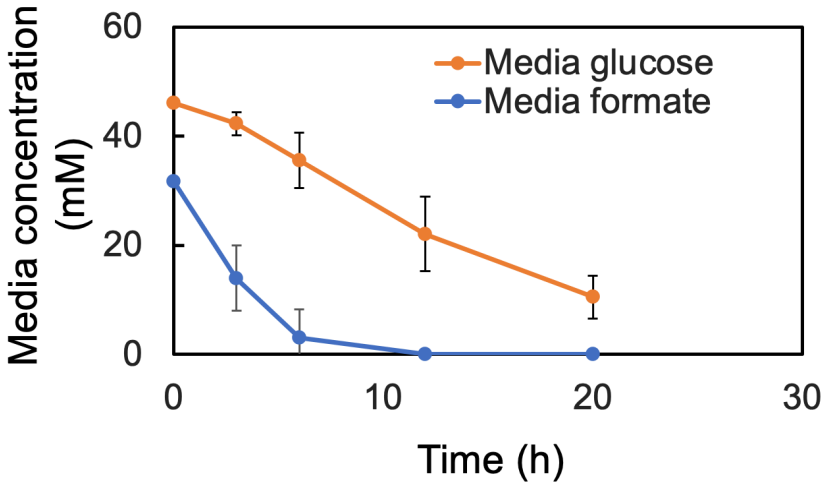

Figure S5-3: Time course of glucose and formate in NOG22/pPL274*/pJD428 in 50 mM glucose, 30 mM formate and 10 mM nitrate media

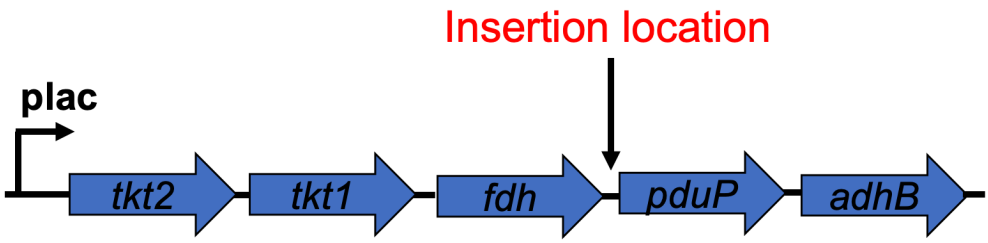

Figure S5-4: Location of insertion sequence in pJD428* was between *fdh* and *pduP* genes

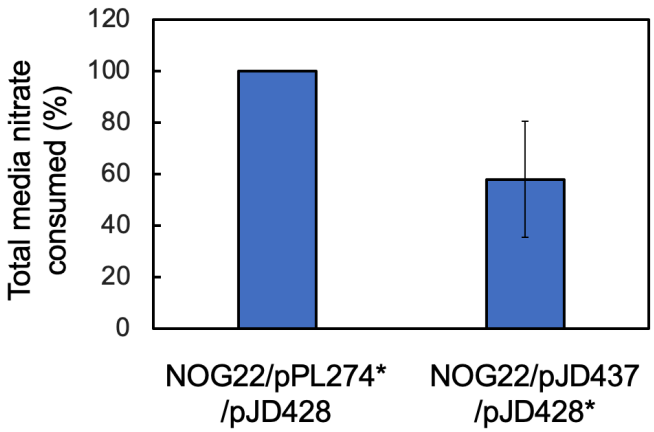

Figure S5-5: Total media nitrate consumption over 20 hr production in NOG22/pPL274*/pJD428 and NOG22/pJD437/pJD428* during anaerobic production in media containing 50 mM glucose, 50 mM formate and 10 mM nitrate. NOG22/pPL274*/pJD428 consumed all media nitrate.

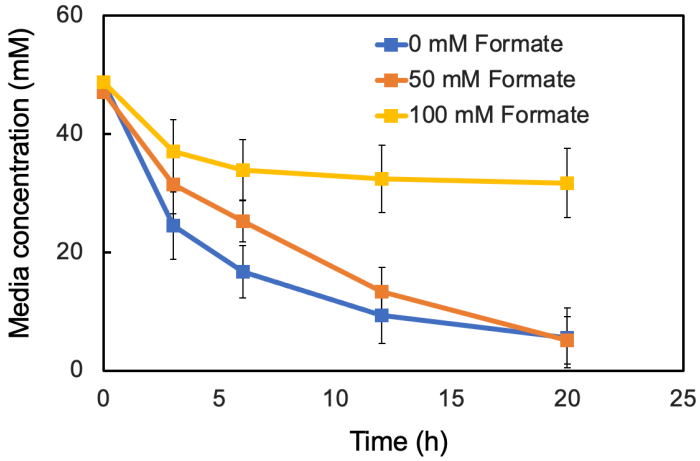

Figure S5-6: Time course of glucose consumption in NOG22/pJD437/pJD428* in production media containing 50 mM glucose and 10 mM nitrate media with 0 mM, 50 mM, or 100 mM formate. When the production media contained 100 mM formate, very little glucose consumption occurred after 6 hr. Since the condition with 100 mM formate a molar ethanol yield on glucose close to 1.0, ATP limitation was likely responsible for the lack of sugar uptake.

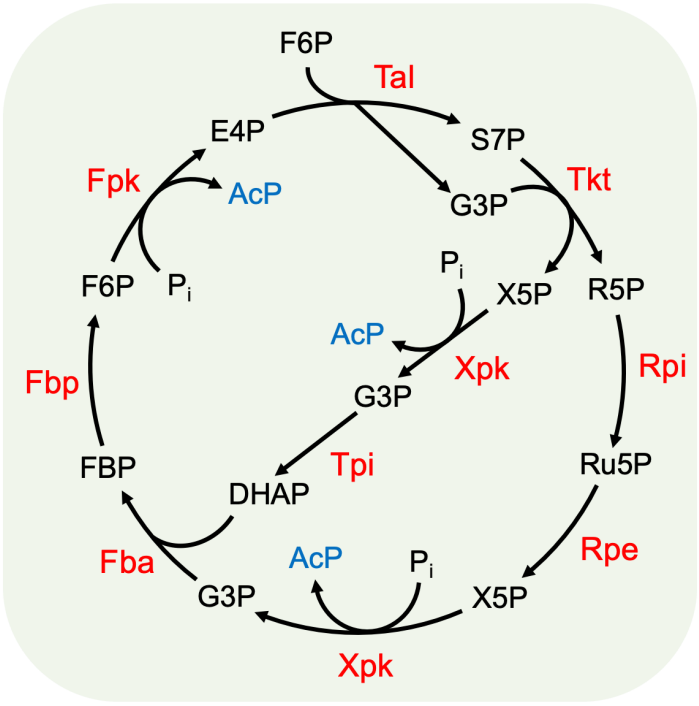

Figure S5-7: Core NOG cycle. Fructose bisphosphotase (FBP) is substrate for fructose bisphosphotase (Fbp). Since FBP accumulates intracellularly in the condition where C2 yields are decreased, it is possible a deficiency in Fbp activity causes a loss of pathway robustness. F6P (fructose 6-phosphate), S7P (sedoheptulose 7-phosphate), G3P (glyceraldehyde 3-phosphate), X5P xylulose 5-phosphate), R5P (ribose 5-phosphate), Ru5P (ribulose 5-phosphate), DHAP (dihydroxyacetone phosphate), E4P (erythrose 4-phosphate), AcP (acetyl-phosphate), P_i (inorganic phosphate). Fpk (F6P dependent phosphoketolase), Xpk (X5P dependent phosphoketolase), Tal (transaldolase), Tkt (transketolase), Rpi (ribose phosphate isomerase), Rpe (ribose phosphate epimerase), Fba (fructose bisphosphate aldolase).

5.6 References

1. Andres, R. J., Fielding, D. J., Marland, G., Boden, T. A., Kumar, N., & Kearney, A. T. (1999). Carbon dioxide emissions from fossil-fuel use, 1751–1950. *Tellus B*, *51*(4), 759-765.

2. Shaffer, G., Olsen, S. M., & Pedersen, J. O. P. (2009). Long-term ocean oxygen depletion in response to carbon dioxide emissions from fossil fuels. *Nature Geoscience*, *2*(2), 105-109.

3. Hashimoto, K. (2019). Global temperature and atmospheric carbon dioxide concentration. In *Global Carbon Dioxide Recycling* (pp. 5-17). Springer, Singapore.

4. Meng, Q. (2017). The impacts of fracking on the environment: A total environmental study paradigm. *Science of the Total Environment*, *580*, 953-957.

5. Mathews, J. A. (2008). Carbon-negative biofuels. *Energy policy*, *36*(3), 940-945.

6. Patil, V., Tran, K. Q., & Giselrød, H. R. (2008). Towards sustainable production of biofuels from microalgae. *International journal of molecular sciences*, *9*(7), 1188-1195.

7. Ingram, L. O., Conway, T., Clark, D. P., Sewell, G. W., & Preston, J. F. (1987). Genetic engineering of ethanol production in Escherichia coli. *Applied and Environmental Microbiology*, *53*(10), 2420-2425.

8. Atsumi, S., Cann, A. F., Connor, M. R., Shen, C. R., Smith, K. M., Brynildsen, M. P., ... & Liao, J. C. (2008). Metabolic engineering of Escherichia coli for 1-butanol production. *Metabolic engineering*, *10*(6), 305-311.

9. Generoso, W. C., Schadeweg, V., Oreb, M., & Boles, E. (2015). Metabolic engineering of Saccharomyces cerevisiae for production of butanol isomers. *Current opinion in biotechnology*, *33*, 1-7.

10. Atsumi, S., & Liao, J. C. (2008). Directed evolution of Methanococcus jannaschii citramalate synthase for biosynthesis of 1-propanol and 1-butanol by Escherichia coli. *Applied and environmental microbiology*, *74*(24), 7802-7808.

11. Atsumi, S., Hanai, T., & Liao, J. C. (2008). Non-fermentative pathways for synthesis of branched-chain higher alcohols as biofuels. *Nature*, *451*(7174), 86-89.

12. Avalos, J. L., Fink, G. R., & Stephanopoulos, G. (2013). Compartmentalization of metabolic pathways in yeast mitochondria improves the production of branched-chain alcohols. *Nature biotechnology*, *31*(4), 335-341.

13. Tao, L., Tan, E. C., McCormick, R., Zhang, M., Aden, A., He, X., & Zigler, B. T. (2014). Techno-economic analysis and life-cycle assessment of cellulosic isobutanol and comparison with cellulosic ethanol and n-butanol. *Biofuels, bioproducts and biorefining*, *8*(1), 30-48.

14. Wallner, T., Miers, S. A., & McConnell, S. (2009). A comparison of ethanol and butanol as oxygenates using a direct-injection, spark-ignition engine. *Journal of Engineering for Gas Turbines and Power*, *131*(3).

15. Robertson, G. P., Dale, V. H., Doering, O. C., Hamburg, S. P., Melillo, J. M., Wander, M. M., ... & Wilhlm, W. W. (2008). Agriculture. Sustainable biofuels redux. *Science (New York, NY)*, *322*(5898), 49.

16. Hamelinck, C. N., & Faaij, A. P. (2006). Outlook for advanced biofuels. *Energy policy*, *34*(17), 3268-3283.

17. Flamholz, A., Noor, E., Bar-Even, A., Liebermeister, W., & Milo, R. (2013). Glycolytic strategy as a tradeoff between energy yield and protein cost. *Proceedings of the National Academy of Sciences*, *110*(24), 10039-10044.

18. Bogorad, I. W., Lin, T. S., & Liao, J. C. (2013). Synthetic non-oxidative glycolysis enables complete carbon conservation. *Nature*, *502*(7473), 693-697.

19. Lin, P. P., Jaeger, A. J., Wu, T. Y., Xu, S. C., Lee, A. S., Gao, F., ... & Liao, J. C. (2018). Construction and evolution of an Escherichia coli strain relying on nonoxidative glycolysis for sugar catabolism. *Proceedings of the National Academy of Sciences*, *115*(14), 3538-3546.

20. Berrıos-Rivera, S. J., Bennett, G. N., & San, K. Y. (2002). Metabolic engineering of Escherichia coli: increase of NADH availability by overexpressing an NAD+-dependent formate dehydrogenase. *Metabolic engineering*, *4*(3), 217-229.

21. Ghosh, D., Bisaillon, A., & Hallenbeck, P. C. (2013). Increasing the metabolic capacity of Escherichia coli for hydrogen production through heterologous expression of the Ralstonia eutropha SH operon. *Biotechnology for biofuels*, *6*(1), 122.

22. Ikeda, S., Takagi, T., & Ito, K. (1987). Selective formation of formic acid, oxalic acid, and carbon monoxide by electrochemical reduction of carbon dioxide. *Bulletin of the Chemical Society of Japan*, *60*(7), 2517-2522.

23. Li, H., Opgenorth, P. H., Wernick, D. G., Rogers, S., Wu, T. Y., Higashide, W., ... & Liao, J. C. (2012). Integrated electromicrobial conversion of CO2 to higher alcohols. *Science*, *335*(6076), 1596-1596.

24. De Souza, R. F., Padilha, J. C., Gonçalves, R. S., De Souza, M. O., & Rault-Berthelot, J. (2007). Electrochemical hydrogen production from water electrolysis using ionic liquid as electrolytes: towards the best device. *Journal of Power Sources*, *164*(2), 792-798.

25. Unden, G., & Bongaerts, J. (1997). Alternative respiratory pathways of Escherichia coli: energetics and transcriptional regulation in response to electron acceptors. *Biochimica et Biophysica Acta (BBA)-Bioenergetics*, *1320*(3), 217-234.

26. Bogorad, I. W., Chen, C. T., Theisen, M. K., Wu, T. Y., Schlenz, A. R., Lam, A. T., & Liao, J. C. (2014). Building carbon–carbon bonds using a biocatalytic methanol condensation cycle. *Proceedings of the National Academy of Sciences*, *111*(45), 15928-15933.

27. Kato, N., Sahm, H., & Wagner, F. (1979). Steady-state kinetics of formaldehyde dehydrogenase and formate dehydrogenase from a methanol-utilizing yeast, Candida boidinii. *Biochimica et Biophysica Acta (BBA)-Enzymology*, *566*(1), 12-20.

28. Park, J. O., Rubin, S. A., Xu, Y. F., Amador-Noguez, D., Fan, J., Shlomi, T., & Rabinowitz, J. D. (2016). Metabolite concentrations, fluxes and free energies imply efficient enzyme usage. *Nature chemical biology*, *12*(7), 482-489.

29. Jiang, Y., Chen, B., Duan, C., Sun, B., Yang, J., & Yang, S. (2015). Multigene editing in the Escherichia coli genome via the CRISPR-Cas9 system. *Applied and environmental microbiology*, *81*(7), 2506-2514.

30. Chen, Y. M., & Lin, E. C. (1991). Regulation of the adhE gene, which encodes ethanol dehydrogenase in Escherichia coli. *Journal of bacteriology*, *173*(24), 8009-8013.

31. Lan, E. I., Ro, S. Y., & Liao, J. C. (2013). Oxygen-tolerant coenzyme A-acylating aldehyde dehydrogenase facilitates efficient photosynthetic n-butanol biosynthesis in cyanobacteria. *Energy & Environmental Science*, *6*(9), 2672-2681.

32. Bayer, T., Milker, S., Wiesinger, T., Rudroff, F., & Mihovilovic, M. D. (2015). Designer microorganisms for optimized redox cascade reactions–challenges and future perspectives. *Advanced Synthesis & Catalysis*, *357*(8), 1587-1618.

33. Rodriguez, G. M., & Atsumi, S. (2012). Isobutyraldehyde production from Escherichia coli by removing aldehyde reductase activity. *Microbial cell factories*, *11*(1), 90.

34. Farhana, A., Guidry, L., Srivastava, A., Singh, A., Hondalus, M. K., & Steyn, A. J. (2010). Reductive stress in microbes: implications for understanding Mycobacterium tuberculosis disease and persistence. *Advances in microbial physiology* (Vol. 57, pp. 43-117). Academic Press.

35. Shen, C. R., Lan, E. I., Dekishima, Y., Baez, A., Cho, K. M., & Liao, J. C. (2011). Driving forces enable high-titer anaerobic 1-butanol synthesis in Escherichia coli. *Applied and Environmental Microbiology*, *77*(9), 2905-2915.

36. Pontrelli, S., Fricke, R. C., Sakurai, S. S. M., Putri, S. P., Fitz-Gibbon, S., Chung, M., ... & Liao, J. C. (2018). Directed strain evolution restructures metabolism for 1-butanol production in minimal media. *Metabolic engineering*, *49*, 153-163.

37. Campos-Bermudez, V. A., Bologna, F. P., Andreo, C. S., & Drincovich, M. F. (2010). Functional dissection of Escherichia coli phosphotransacetylase structural domains and analysis of key compounds involved in activity regulation. *The FEBS journal*, *277*(8), 1957-1966.

38. Fann, M. C., & Maloney, P. C. (1998). Functional Symmetry of UhpT, the Sugar Phosphate Transporter of Escherichia coli. *Journal of Biological Chemistry*, *273*(50), 33735-33740.

39. Beale, D. J., Pinu, F. R., Kouremenos, K. A., Poojary, M. M., Narayana, V. K., Boughton, B. A., ... & Dias, D. A. (2018). Review of recent developments in GC–MS approaches to metabolomics-based research. *Metabolomics*, *14*(11), 152.

40. Heuser, F., Marin, K., Kaup, B., Bringer, S., & Sahm, H. (2009). Improving d-mannitol productivity of Escherichia coli: impact of NAD, CO2 and expression of a putative sugar permease from Leuconostoc pseudomesenteroides. *Metabolic engineering*, *11*(3), 178-183.

41. Chin, T., Okuda, Y., & Ikeuchi, M. (2018). Sorbitol production and optimization of photosynthetic supply in the cyanobacterium Synechocystis PCC 6803. *Journal of Biotechnology*, *276*, 25-33.

42. Lee, Y., Rivera, J. G. L., & Liao, J. C. (2014). Ensemble Modeling for Robustness Analysis in engineering non-native metabolic pathways. *Metabolic engineering*, *25*, 63-71.

6 Integration of NOG with microaerobic fermentation. Challenges and outlook

Synthetic non-oxidative glycolysis (NOG) has tremendous potential to lower costs in biorefining since it conserves feedstock carbon when forming two-carbon (C2) metabolites, which are precursors to numerous bioproducts. However, in order to use NOG to make reduced C2-derived products such as alcohol, new processing challenges will need to be addressed, most critically the external supply of electrons necessary to reduce acetyl-CoA and supply ATP through respiration. In order for NOG-based production of such products to be economically viable, the capital cost of the input reducing power must not exceed the cost savings on feedstock. Here, we outlined some potential strategies for efficient, robust production of reduced products in NOG under microaerobic conditions. While the overall yield of C2 product drops in microaerobic production, presumably due to excess oxidation in the TCA cycle, we suggest implementing a previously described method for gene knockdown in *E. coli* to knockdown these essential competing pathways following the transition to the production phase. This should allow for high yields of C2 products regardless of oxygen levels. In order to ensure efficient usage of reducing power while maintaining NAD(P)H) driving forces necessary for robust alcohol production, we recommend using different electron carriers to drive the ethanol pathway and respiration to avoid competition between the pathways. Finally, an economic analysis demonstrates the potential for an NOG-based ethanol process to reduce capital costs. With conventionally produced hydrogen as the reducing power, NOG can save over $1000 USD on input costs on a basis of 100 kmol ethanol. With renewable hydrogen produced from water electrolysis, savings are reduced to only $50 USD for 100 kmol ethanol. However, as research into improving the production of renewable hydrogen is ongoing, there is considerable potential for a completely renewable NOG-based process to have increased economic viability.

6.1 Introduction

Liquid fuels derived from renewable resources, sometimes defined as biofuel, are potential substitutes for nonrenewable fossil fuels such as petroleum and natural gas.[1,2] While biofuels such as ethanol[3] and butanol[4,5] can be produced at high titers using whole cell biocatalysts such as *E. coli* and yeast, these processes struggle to compete economically against petroleum. A major economic constraint for biofuel processes is high feedstock cost relative to market ethanol prices, which can also be produced using a petrochemical process.[6-7]
Ethanol and butanol are produced by microbial organisms such as *E. coli* and yeast using their endogenous metabolic pathways. Unfortunately, the maximum ethanol yields using endogenous metabolism, i.e. glycolysis, are only 67%, as one third of input carbon is lost to the environment as CO_2. This is due to the decarboxylation of pyruvate in native glycolytic pathways when generating precursors to ethanol. Since essentially all organisms use glycolysis to catabolize sugar, carbon loss is unavoidable unless the CO_2 is reincorporated by a carbon fixation pathway. The development of synthetic non-oxidative glycolysis (NOG), which bypasses pyruvate decarboxylation to generate stoichiometric amounts of two-carbon (C2) metabolites from sugar, represents a major breakthrough for metabolic engineering and opened the door to produce ethanol at 100% yield.[8] Moreover, an *E. coli* strain dependent on NOG for sugar catabolism was developed, and may be a promising host for biorefining.[9] While NOG does not produce reducing equivalents, reducing power can be added in the form of formate or hydrogen, both of which can be produced from potentially renewable electrochemical processes.[10,11] While reducing power addition can increase ethanol yields under the anaerobic fermentative conditions in which ethanol is normally produced, in the NOG-dependent *E. coli* strain the pathway must ultimately be integrated with respiration to overcome the inherent ATP deficit in the pathway. Here, we will

outline potential challenges and strategies for integrating NOG-dependent ethanol production in microaerobic conditions, allowing oxygen to be used as the electron acceptor for ATP production. To supply the electrons needed for respiration, excess reducing equivalents must be provided. Since the supply of reducing equivalents represents a capital cost, any NOG-based process must ensure the savings on carbohydrate feedstock exceeds the price of the reducing equivalents necessary for ethanol production. Here we will describe challenges and strategies for integrating NOG-based ethanol production in microaerobic conditions with efficient usage of reducing equivalents, overcoming carbon loss due to oxidation, and maintaining the NAD(P)H driving force to ensure high yields of ethanol production.

6.2 Materials and Methods

6.2.1 Medium and cultivation

All *E. coli* strains were cultured by rotary shaking (250 rpm, New Brunswick Scientific) at 37 degrees. All media ingredients were purchased through Fisher Scientific unless otherwise noted. Production media contained 50 mM glucose or Glucose 6-Phospahte (Sigma Aldrich), 1x m9 salts, 0.2 mM $CaCl_2$, 2 mM $MgSO_4$, (Sigma Aldrich), 100 mM MOPS buffer, and vitamin mix (0.02 g/L pyridoxamine dihydrochloride (Sigma Aldrich), 4-aminobenzoic acid (Sigma Aldrich), 0.002 g/L biotin, 0.002 g/L B12 and 0.01 g/L thiamin). Production media was titrated to ~pH 7 using NaOH.

6.2.2 Strains and plasmids

The evolved NOG strain, pPL274* and pTW371 were obtained from Lin, *et. al*.[9] All primers for the construction of ethanol production plasmids were purchased through Integrated DNA Technologies (idtdna.com). PCR fragments were amplified using KOD Xtreme Hot-Start DNA polymerase (EMD Milipore). *E. coli* DH10B (NEB) electrocompetent cells were used for cloning. For plasmid construction, each fragment contained 20-30 bp overlapping sequences and were mixed at equimolar amounts. Plasmids were assembled using HIFI Assembly Master (NEB). Fragments contained 20-30 bp overlaps and were mixed at equimolar amounts. Plasmids were verified by sequencing (Laragen, Culver City, CA). Strain and plasmid list are in Appendix I and Appendix II.

6.2.3 Anaerobic/microaerobic production

Strains were prepared for fermentation by cultivation in LB plus glucose media as previously described.[9] Cell culture was induced with 1 mM IPTG (Zymo scientific) at OD_{600} 0.7-1.0 for 14-17 hours. Induced cultures were centrifuged and washed once with production media containing no carbon source. Anaerobic cultures were concentrated in production media anaerobically to $OD_{600} \sim 20$. Microaerobic cultures were concentrated to $OD_{600} \sim 20$ aerobically in production media and placed in tightly capped tubes for 20-24 hours.

6.2.4 Quantification of production samples

Samples were analyzed using gas chromatography with flame ionization detection (Agilent) or HPLC (Thermo Scientific VWD and Refractomax detectors). The HPX-87H column (BioRad) was used for HPLC analysis.

6.2.5 CRISPR-Cas9 transformations for knockout of ackA

A previous described CRISPR-Cas9 protocol was adopted to perform genome edits in *E. coli*.[12] Linear donor DNA was constructed using SOE with 20 bp overlapping sequences. Cas9 was expressed on pCas9 and targeted to cut site by sgRNA containing 20 bp homology region and expressed on the pTarget plasmids. The removal of PAM sites was achieved by introducing a synonymous mutation to prevent further cutting. Recombination of the donor DNA was facilitated by expressing the lambda red recombinase on pCas9 under the arabinose promotor. Cultures were induced with 10 mM arabinose for ~3 hours prior to transformation. *E. coli* was made electrocompetent by washing twice with ice cold MQ water and twice with 10% glycerol. At least 100 ng pTarget and 500 ng donor DNA was transformed.

6.2.6 Economic analysis calculation

Prices of glucose ($0.5USD/kg) or hydrogen ($0.9 or $3USD/kg) were obtained from greentechmedia.com. A basis of 100 kmol ethanol was used for the production analysis. Six mols of hydrogen (2.02 g/mol) is required to convert one mol of glucose to 3 ethanol using NOG, and 0.33 mol glucose (180.16 g/mol) is saved using NOG. However, extra supply of hydrogen is required to supply ATP using respiration. Using O_2 as the electron acceptor will provide an H^+/e^- yield of 4.[13] Since the ATP/H^+ yield from E. coli's ATP synthase is about 4,[14] each mol of H_2 will generate about 2 mols of ATP. Since it can be obtained from air, the price of oxygen was considered to be negligible. Since the cell may require a positive ATP yield for cell maintenance, and hydrogen is unlikely to utilized with 100% efficiency, an ATP requirement of 1.5 mols/mol glucose was assumed.

6.3 Results

6.3.1 Microaerobic conditions reduce yield of C2 products

The previously developed *E. coli* strain dependent on NOG for sugar catabolism can produce yields of C2 derived products in excess of the theoretical maximum achievable using glycolytic metabolism.[9] On hexose, NOG can generate 3 C2 equivalents while glycolysis can only generate 2 equivalents. C2 products that can be produced in the NOG strain include acetate and ethanol. Since ethanol is a more valuable product and potential fuel source, it would be desirable to eliminate acetate production and make ethanol only. However, since the production of acetate in NOG is reduced balanced, this can only be achieved by supplying additional reducing power. In the NOG strain, reducing power under anerobic conditions is only produced in limited amounts by the oxidation of the small fraction of carbon that enters the TCA cycle. Therefore, under anaerobic conditions the NOG strain produces mostly acetate and only residual amounts of ethanol. Transitioning from acetate to ethanol production involves other challenges in addition to the supply of reducing power. Most notably, under anerobic conditions acetate production is the only way the NOG strain can produce ATP. Since ATP is required to phosphorylate sugar, eliminating acetate production would create an ATP deficit and make ethanol production infeasible. While the addition of reducing power could improve anaerobic ethanol yields in the NOG strain up to a certain level using acetate production to supply ATP, ultimately the cell will require another source of ATP if high ethanol yields are to be attained.

Thus, to produce ethanol at near theoretical yield, an alternate source of ATP production must be implemented. This can be achieved by supplying excess reducing equivalents to be used in respiration. Electrons from reducing equivalents are transferred to the electron acceptor using the electron transport chain (ETC), generating a proton gradient. This proton gradient is used by

ATP synthase to generate ATP. While *E. coli* can use a variety of electron acceptors, oxygen is the most promising due to its high proton yield and availability.

However, implementing respiration presents new challenges, which can threaten the strain's ability to produce C2 products at near theoretical yield. When electron acceptors are present, the cell can lose carbon to oxidation in the TCA cycle. Moreover, GltA, the entry point to the TCA cycle is upregulated under aerobic conditions and repressed under anaerobic conditions.[15] Therefore, introducing oxygen could potentially reduce C2 yields by increasing flux through the TCA cycle. To test this, we compared overall C2 yield in NOG22/pPL274*/pTW371, an isolated NOG dependent strain, in anaerobic and microaerobic conditions. Microaerobic conditions were obtained by resuspending cells in aerobic conditions before tightly capping the reaction vessel. Thus, the culture is able to access the oxygen available in the headspace of the reaction vessel, but the oxygen consumed can't be replaced by the outside environment.

We found that the overall C2 yields (acetate + ethanol) in NOG22/pPL274*/pTW371 dropped significantly in in microaerobic conditions, from 2.35 to 0.98 (Figure 6-1). Presumably, the carbon is mostly lost to oxidation in the TCA cycle through GltA.

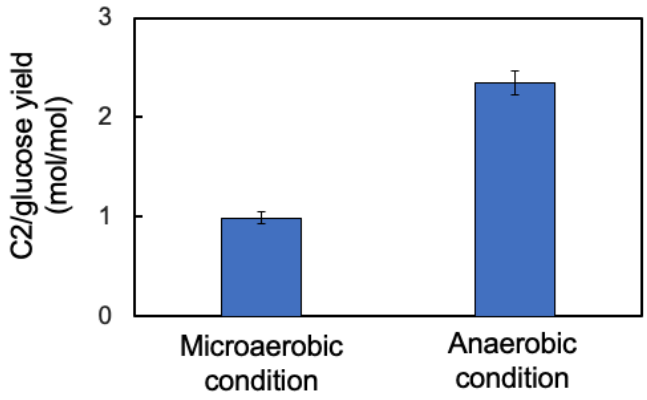

Figure 6-1: Combined C2 yield (ethanol plus acetate) in NOG22/pPL274*/pTW371 in production media under anaerobic or microaerobic conditions. Microaerobic conditions drop the molar C2 yield on glucose from 2.35 to 0.98.

6.3.2 Blocking TCA cycle flux using previously described system from protein knockdown in E. coli

In metabolic engineering, competing pathways are often knocked out to maximize yields of the desired product. Unfortunately, *gltA* cannot be deleted since it is essential for the strain to grow on minimal media. Therefore, to eliminate carbon loss to GltA without abolishing the cells ability to grow, this enzyme must be knocked down rather than knocked out. An effective system for protein knockdown should be able to quickly eliminate enzyme activity while also being tightly controllable. A previously described system for protein knockdown in *E. coli* that robustly degrades proteins with tight control has been developed and can be applied to the knockdown of GltA in the NOG strain.[16] This system is based on Lon protease and corresponding ssrA tag from *Mesoplasma florum*. The authors edited the ssrA tag to eliminate recognition from *E. coli's* native Lon protease, and the system was found to be able to degrade proteins of interest tagged at their C terminus within an hour while being completely dependent on Lon being induced.

Thus, *gltA* on the chromosome of the NOG strain could be similarly tagged, and its destruction could be induced following the transition from growth to production phase.

Theoretically, it could be possible to balance carbon and oxygen flux such that a knockdown of GltA activity is not necessary by manipulating the feed of oxygen. However, it may be quite difficult to achieve in practice.

6.3.3 Knockdown of other competing pathways such as AckA

A similar knockdown strategy can also be used to remove other competing pathways, particularly AckA, which was also found to be essential to growth in minimal media in the NOG strain. While increasing the supply of reducing power can lower yields of acetate, it may be difficult to completely eradicate acetate production without knocking down AckA. In addition to being necessary for growth, removing AckA also eliminates the NOG strain's ability to consume sugar anaerobically since it can no longer produce ATP. In order to ensure aerobic conditions could rescue sugar uptake in NOG22Δ*ackA* by supplying ATP through respiration, we tested production in NOG22Δ*ackA*/pPL274*/pJD428 and found that sugar consumption was indeed restored under microaerobic conditions (Figure 6-2). The plasmid pJD428 contained the ethanol pathway cloned onto the original growth plasmid pTW371.[9] This result validated the feasibility of replacing acetate production with respiration to supply ATP for NOG ethanol production.

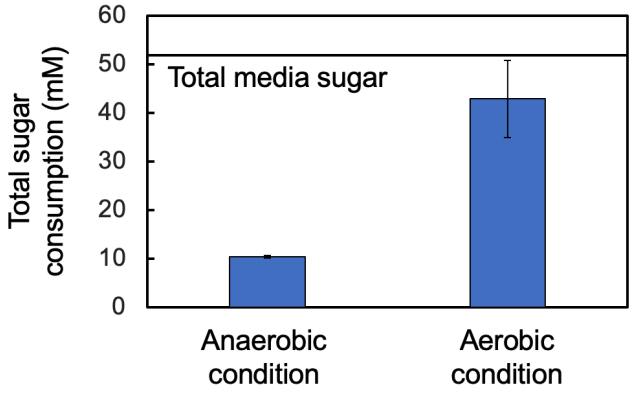

Figure 6-2: Total sugar consumption over 24 hr in NOG22Δ*ackA*/pPL274*/pJD428 in aerobic or anaerobic conditions. Sugar consumption is rescued in aerobic media, verifying respiration can replace acetate production to generate ATP during production in the NOG strain.

6.3.4 Overview of scalable NOG based ethanol production

Achieving the scalable production of ethanol production in the NOG strain is likely best achieved using two phases. Initially, a growth phase to prioritize biomass production, followed by ethanol production as the strain approaches stationary phase. While growth and production sometime occur simultaneously, numerous studies have reported that microbial chemical production is best achieved by decoupling growth and production.[17-20]

For NOG-based ethanol production, cells can be cultured under aerobic conditions to maximize biomass formation, since the NOG strain cannot grow anaerobically. Following the growth phase, there will be a transition to microaerobic conditions along with the addition of reducing power. The induction of GltA and AckA knockdown can be achieved at this time by expressing Lon under promotors where transcription is induced at stationary phase. Although many promotors in *E. coli* that are upregulated at stationary phase are controlled by RpoS, which was

mutated in the evolved NOG strain, some promotors are still upregulated by stationary phase even in the absence of RpoS.[21]

6.3.5 Economic analysis of NOG-based ethanol production using hydrogen as electron donor demonstrates potential economic advantage

Although NOG can potentially improve the economics of C2 derived biofuels such as ethanol, this can only be achieved if the savings on feedstock costs does not exceed the capital cost of reducing power supply. To evaluate this, an economic analysis of NOG-based ethanol production using hydrogen as reducing was performed. Industrially, there are several important processes for hydrogen production. One method, known as green hydrogen, is renewable and is produced from the hydrolysis of water using electricity.[22] The price of green hydrogen is around $3 USD/kg. Hydrogen produced from natural gas or coal is cheaper, with prices as low as $0.90/kg, but it is not renewable. Hydrogenase oxidizes one mol of H_2 to generate one mol of NADH.[23] Two mols of NADH are required to produce one mol of ethanol from one mol of acetyl-phosphate (AcP), the output of NOG. An economic analysis was performed contrasting EMP vs. NOG based ethanol production to compare the savings on carbon feedstock using NOG vs. the input cost of hydrogen. A basis of 100 kmol ethanol produced was used and the extra hydrogen necessary for ATP production in NOG-based production was accounted for. Enough hydrogen to provide 1.5 mols ATP per mol of glucose was used to account for the fact hydrogen would likely not be used at 100% efficiency. Bulk liquid glucose ($ 0.5 USD/kg) was used as the feedstock. The savings on feedstock and cost of input reducing power are shown in Table 6-I and Table 6-II for conventional and green hydrogen respectively.

Table 6-I: Capital cost savings using NOG with conventionally produced hydrogen

Feedstock savings (USD)	Reducing power input cost (USD)	Total Savings (USD)
1538.5	448.5	1090

Table 6-II: Capital cost savings using NOG with renewable (green) hydrogen

Feedstock savings (USD)	Reducing power input cost (USD)	Total Savings (USD)
1538.5	1494.5	44

For 100 kmol ethanol, NOG saves 16.7 kmol glucose which amounts to a savings of $1538.5 USD. Two hundred mols of hydrogen are required as reducing power for ethanol production and about another fifty are required for use as ATP. The cost of 225 kmol hydrogen is $1363.5 USD for green hydrogen, and $410 USD for conventional hydrogen. Thus, NOG-based ethanol production has economic viability in both cases. Moreover, the completely renewable process may become more profitable in the near future as the price of green hydrogen is expected to drop. However, even though NOG can be more profitable on a per mol basis, to truly compete with EMP dependent organisms any NOG-dependent process will need to achieve similar productivities and titers. Thus, constructing robust yet efficient ethanol production is necessary to achieve the full potential of NOG.

6.3.6 Cofactor engineering to alleviate competition between respiration and ethanol pathway

As seen from the economic analysis, efficient utilization of reducing power is a key factor affecting the economic viability for NOG-based ethanol production. High ratios of reducing

equivalents serve as the driving force for ethanol productivities and yields. In NOG-based ethanol production, reducing power is necessary to both reduce C2 metabolic precursors to ethanol as well as supply ATP through respiration. Both potential sources of reducing power, hydrogen and formate, are oxidized by NADH dependent enzymes.[23-24] The resulting NADH is then directly used as an electron donor both by ethanol pathway enzymes PduP and Adh, and for the ETC, through *E. coli*'s endogenous NADH reductases Ndh1 and Ndh2.[13] The competition between these two pathways can be problematic for multiple reasons. First, the direct competition for NADH would require strict balance between the pathways. If the ethanol pathway is too strong, ATP supply could be limiting resulting in slow sugar consumption and decreased productivity. If respiration is too strong, there would not be enough NADH available to drive the ethanol pathway and as a result ethanol yield could be comprised. While it may be possible to control the rate of respiration by manipulating the rate of oxygen supply this may be difficult to achieve in practice.

Therefore, it may be desirable to create a system where both pathways utilize different electron donors to avoid direct competition. NADPH is an alternate electron donor from NADH which contains an extra phosphate. NADPH is used in fatty acid synthesis and other biosynthetic pathways.[25] Unlike NADH, NADPH does not donate electrons to the electron transport chain. Thus, it may be possible to decouple respiration from the ethanol pathway by making the ethanol pathway NADPH dependent and avoiding having the pathways compete for the same cofactor. In this system, the strain will express two formate dehydrogenases or two hydrogenases, one generating NADH for respiration, the other generating NADPH for ethanol production. While most PduP, Fdh and SH utilize NADH, a general methodology for changing the cofactor requirement from NAD^+/NADH to $NADP^+$/NADPH for oxidoreductase enzymes has been

established.[26] This system has already been applied to create an $NADP^+$/NADPH dependent PduP.[27] Ideally, this system could allow for a robust supply of oxygen without compromising the driving force for ethanol production. The rate of oxygen supply would still need to be optimized to maximize the efficiency of reducing power usage, but the need to maintain extremely strict control to maintain desirable ethanol yields and/or productivities could be avoided.

6.4 Discussion and conclusion

Synthetic non-oxidative glycolysis (NOG) has been demonstrated to produce C2 derived products at yields exceeding the theoretical maximum with glycolysis. In order to fully realize the potential of NOG, it is desirable to apply it for the production of reduced products such as alcohol, which serve as potential liquid fuel and petroleum substitutes. However, establishing an economically viable process using NOG for the production of reduced products would require robust titers, yields and productivities along with the efficient utilization of the external electron supply. Since external reducing power is required for both the ethanol pathway and respiration, we propose decoupling the respiratory pathways from the ethanol pathway as much as possible. Changing the cofactor dependence of the ethanol pathway from NADH to NADPH, can avoid competition with respiration and maintain high NAD(P)H driving forces to move carbon through the ethanol pathway along even while the cell is generating a lot of ATP through respiration. In order to prevent competing pathways from AckA or GltA, the latter of which manifests more strongly under aerobic conditions, a targeted knockdown of these proteins can be achieved after the growth phase is complete. By significantly eliminating flux through these pathways, the cell may have no choice but to move carbon through the ethanol pathway if no other competing pathways exist. Although these strategies could potentially allow for high ethanol yields through the blockage of competing pathways, the reducing power supply would likely need optimization

in order to be economically viable. Fast supply of O_2 could lead to high productivities due to the fast regeneration of ATP but could lead to a waste of excess reducing power. On the other hand, a slow supply of O_2 could lead to more efficient conservation of reducing power but worse productivities. Therefore, O_2 supply should be manipulated in order to create the most optimal system.

6.4 Appendices

6.4.1 Strain list

Strain	Genotype	Comments	Reference
BW25113	*rrnB*$_{T14}$ Δ*lacZ*$_{w116}$*hsdR514* Δ*araBAD*$_{AH33}$ Δ*rhaBAD*$_{LD78}$	Wild Type	
JCL16	BW25113/F′[*tra*D36 *proAB*$^{+}$ lacI^{q}ZΔM15(Tet^{r})]	Wild Type	
PHL13	JCL16 Δ*gapA::FRT* Δ*mgsA::FRT* Δ(*pgk gapB)::FRT* Δ*pfkA::FRT* Δ*iclR::FRT* Δ*poxB::cat* Δ*zwf::FRT* Δ(*edd eda)::*(P$_{L}$*lacO*$_{1}$*::f/xpk*$_{BA}$) ΔP$_{pck}$::P$_{L}$*lacO*$_{1}$	Precursor to NOG strain that cannot grow on glucose	Lin, PP et. al
NOG21	Evolved from PHL13	PHL13 following evolution for glucose growth using NOG	Lin, PP et. al
NOG22	NOG21 with growth plasmids removed	NOG21 following removal of growth plasmids pPL274* and pTW371	This Study

6.4.2 Plasmid list

Plasmid	Description	Reference
pPL274	P$_{L}$*lacO*$_{1}$*::f/xpk*$_{BA}$ *glf*$_{ZM}$ *glk*$_{EC}$ tkt2$_{MB}$ *tal*$_{KP}$ *glpX*$_{EC}$ ColE *ori* Carb^{r}	Lin, PP et. al
pPL274*	P$_{L}$*lacO*$_{1}$*::f/xpk*$_{BA}$ (mutated by transposon insertion) *glf*$_{ZM}$ *glk*$_{EC}$ tkt2$_{MB}$ *tal*$_{KP}$ *glpX*$_{EC}$ ColE *ori* Carb^{r}	Lin, PP et. al
pTW371	P$_{L}$*lacO*$_{1}$*:: tkt2*$_{MB}$ *tkt1*$_{MB}$ CloDF13 *ori* Spec^{r}	Lin, PP et. al
pJD428	P$_{L}$*lacO*$_{1}$*:: tkt2*$_{MB}$ *tkt1*$_{MB}$ *fdh*$_{CB}$ *pduP*$_{SE}$ *adhB*$_{ZM}$ CloDF13 *ori* Spec^{r}	This Study

6.5 References

1. Wander, M. M., Parton, W. J., Adler, P. R., Barney, J. N., Cruse, R. M., Duke, C. S., ... & Mladenoff, D. J. (2008). Sustainable biofuels redux. *Science*, *322*(5898), 4950.

2. Stephanopoulos, G. (2007). Challenges in engineering microbes for biofuels production. *Science*, *315*(5813), 801-804.

3. Ingram, L. O., Conway, T., Clark, D. P., Sewell, G. W., & Preston, J. F. (1987). Genetic engineering of ethanol production in Escherichia coli. *Applied and Environmental Microbiology*, *53*(10), 2420-2425.

4. Atsumi, S., Cann, A. F., Connor, M. R., Shen, C. R., Smith, K. M., Brynildsen, M. P., ... & Liao, J. C. (2008). Metabolic engineering of Escherichia coli for 1-butanol production. *Metabolic engineering*, *10*(6), 305-311.

5. Generoso, W. C., Schadeweg, V., Oreb, M., & Boles, E. (2015). Metabolic engineering of Saccharomyces cerevisiae for production of butanol isomers. *Current opinion in biotechnology*, *33*, 1-7.

6. Alonso, D. M., Hakim, S. H., Zhou, S., Won, W., Hosseinaei, O., Tao, J., ... & Houtman, C. J. (2017). Increasing the revenue from lignocellulosic biomass: Maximizing feedstock utilization. *Science advances*, *3*(5), e1603301.

7. Hamelinck, C. N., & Faaij, A. P. (2006). Outlook for advanced biofuels. *Energy policy*, *34*(17), 3268-3283.

8. Bogorad, I. W., Lin, T. S., & Liao, J. C. (2013). Synthetic non-oxidative glycolysis enables complete carbon conservation. *Nature*, *502*(7473), 693-697.

9. Lin, P. P., Jaeger, A. J., Wu, T. Y., Xu, S. C., Lee, A. S., Gao, F., ... & Liao, J. C. (2018). Construction and evolution of an Escherichia coli strain relying on nonoxidative glycolysis for sugar catabolism. *Proceedings of the National Academy of Sciences*, *115*(14), 3538-3546.

10. Ikeda, S., Takagi, T., & Ito, K. (1987). Selective formation of formic acid, oxalic acid, and carbon monoxide by electrochemical reduction of carbon dioxide. *Bulletin of the Chemical Society of Japan*, *60*(7), 2517-2522.

11. De Souza, R. F., Padilha, J. C., Gonçalves, R. S., De Souza, M. O., & Rault-Berthelot, J. (2007). Electrochemical hydrogen production from water electrolysis using ionic liquid as electrolytes: towards the best device. *Journal of Power Sources*, *164*(2), 792-798.

12. Jiang, Y., Chen, B., Duan, C., Sun, B., Yang, J., & Yang, S. (2015). Multigene editing in the Escherichia coli genome via the CRISPR-Cas9 system. *Applied and environmental microbiology*, *81*(7), 2506-2514.

f

13. Unden, G., & Bongaerts, J. (1997). Alternative respiratory pathways of Escherichia coli: energetics and transcriptional regulation in response to electron acceptors. *Biochimica et Biophysica Acta (BBA)-Bioenergetics*, *1320*(3), 217-234.

14. Steigmiller, S., Turina, P., & Gräber, P. (2008). The thermodynamic H+/ATP ratios of the H+-ATPsynthases from chloroplasts and Escherichia coli. *Proceedings of the National Academy of Sciences*, *105*(10), 3745-3750.

15. Park, S. J., McCabe, J., Turna, J., & Gunsalus, R. P. (1994). Regulation of the citrate synthase (gltA) gene of Escherichia coli in response to anaerobiosis and carbon supply: role of the arcA gene product. *Journal of bacteriology*, *176*(16), 5086-5092.

16. Cameron, D. E., & Collins, J. J. (2014). Tunable protein degradation in bacteria. *Nature biotechnology*, *32*(12), 1276-1281.

17. Li, S., Jendresen, C. B., Landberg, J., Pedersen, L. E., Sonnenschein, N., Jensen, S. I., & Nielsen, A. T. (2020). Genome-Wide CRISPRi-Based Identification of Targets for Decoupling Growth from Production. *ACS Synthetic Biology*, *9*(5), 1030-1040.

18. Lo, T. M., Chng, S. H., Teo, W. S., Cho, H. S., & Chang, M. W. (2016). A two-layer gene circuit for decoupling cell growth from metabolite production. *Cell systems*, *3*(2), 133-143.

19. Soma, Y., Tsuruno, K., Wada, M., Yokota, A., & Hanai, T. (2014). Metabolic flux redirection from a central metabolic pathway toward a synthetic pathway using a metabolic toggle switch. *Metabolic engineering*, *23*, 175-184.

20. Brockman, I. M., & Prather, K. L. (2015). Dynamic knockdown of E. coli central metabolism for redirecting fluxes of primary metabolites. *Metabolic engineering*, *28*, 104-113.

21. Shimada, T., Makinoshima, H., Ogawa, Y., Miki, T., Maeda, M., & Ishihama, A. (2004). Classification and strength measurement of stationary-phase promoters by use of a newly developed promoter cloning vector. *Journal of bacteriology*, *186*(21), 7112-7122.

22. Zeng, K., & Zhang, D. (2010). Recent progress in alkaline water electrolysis for hydrogen production and applications. *Progress in energy and combustion science*, *36*(3), 307-326.

23. Burgdorf, T., van der Linden, E., Bernhard, M., Yin, Q. Y., Back, J. W., Hartog, A. F., ... & Friedrich, B. (2005). The soluble NAD+-reducing [NiFe]-hydrogenase from Ralstonia

eutropha H16 consists of six subunits and can be specifically activated by NADPH. *Journal of bacteriology*, *187*(9), 3122-3132.

24. Schütte, H., Flossdorf, J., Sahm, H., & KULA, M. R. (1976). Purification and properties of formaldehyde dehydrogenase and formate dehydrogenase from Candida boidinii. *European Journal of Biochemistry*, *62*(1), 151-160.

25. Olavarría, K., Valdés, D., & Cabrera, R. (2012). The cofactor preference of glucose-6-phosphate dehydrogenase from Escherichia coli–modeling the physiological production of reduced cofactors. *The FEBS journal*, *279*(13), 2296-2309.

26. Cahn, J. K., Werlang, C. A., Baumschlager, A., Brinkmann-Chen, S., Mayo, S. L., & Arnold, F. H. (2017). A general tool for engineering the NAD/NADP cofactor preference of oxidoreductases. *ACS synthetic biology*, *6*(2), 326-333.

27. Trudeau, D. L., Edlich-Muth, C., Zarzycki, J., Scheffen, M., Goldsmith, M., Khersonsky, O., ... & Tawfik, D. S. (2018). Design and in vitro realization of carbon-conserving photorespiration. *Proceedings of the National Academy of Sciences*, *115*(49), E11455-E11464.